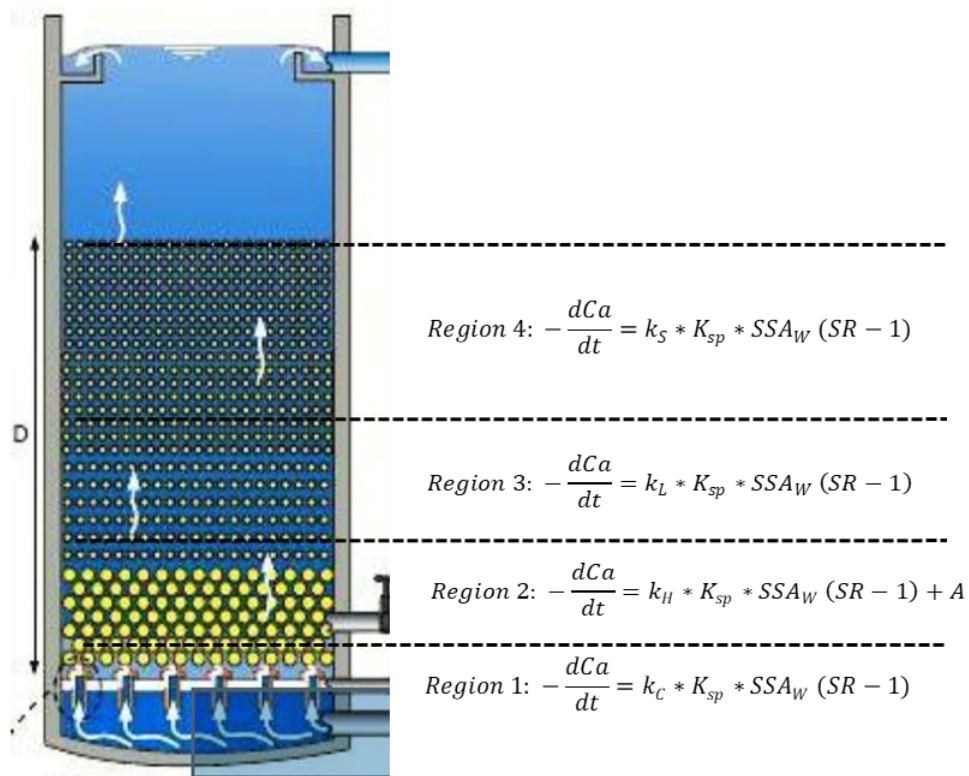


# An improved kinetic model and optimized configurations for pellet softening

Modeling and optimization of pellet softening process in drinking water treatment



# Colophon

## Author

Rubayat Sobhan  
Email: [r.sobhan@tudelft.student.nl](mailto:r.sobhan@tudelft.student.nl)

## Education

Delft University of Technology  
Faculty Of Civil Engineering and Geosciences  
Water management  
Stevinweg 1, 2628 CN

## Company

Waternet  
Waternet, Drinking Water Sector, Production Department  
Water Quality and Process Support Team  
Location Weesperkarspel  
1108 AJ Amsterdam, Southeast  
Tel. 020 - 608 7000

## Daily supervisors

Ing. Eric. T. Baars  
E-mail: [eric.baars@waternet.nl](mailto:eric.baars@waternet.nl)

Ir. Peter. J. De Moel  
E-mail: [peter.de.moel@waternet.nl](mailto:peter.de.moel@waternet.nl)

PhD candidate Ir. Onno J. I. Kramer  
E-mail: [onno.kramer@waternet.nl](mailto:onno.kramer@waternet.nl)

## Chairman

Prof.dr.ir. Jan Peter van der Hoek MBA  
Delft University of Technology  
Department of Water management  
Section of Sanitary engineering  
E-mail: [j.p.vanderhoek@tudelft.nl](mailto:j.p.vanderhoek@tudelft.nl)  
Executive Officer, Strategic Centre, Waternet  
E-mail: [jan.peter.van.der.hoek@waternet.nl](mailto:jan.peter.van.der.hoek@waternet.nl)

## Supervisor

Prof. dr. ir. H.J.M. Kramer  
Delft University of Technology  
Department of Process and Energy  
E-mail: [h.j.m.kramer@tudelft.nl](mailto:h.j.m.kramer@tudelft.nl)

## Date of Defense

26 July, 2019

# Acknowledgement

This thesis contains the graduation research of my master in civil engineering, department of water management at Delft University of Technology. The successful completion of the thesis is a collective effort of a number of extraordinary persons.

I always wanted to do my graduation project on a topic which is interesting yet challenging and related to drinking water. For this reason I cannot thank enough Prof. Jan Peter van der Hoek for providing me the opportunity to do a master thesis on my desired topic. He was the bridge for me to apply my academic knowledge in the water industry and excel it further by research. He always helped me with his important feedback when it was needed. In addition, I would like to thank the entire team Water Quality and Process support, specially Mr. Leon Kors for allowing me to be a part of the research.

I would like to show my gratitude to Eric Baars for his constant support and guidance. He was the first person to whom I could go and seek for help in any sort of challenges during my tenure.

It wouldn't have been possible to finish my thesis without the support of Peter de Moel. He helped me with his technical knowledge and supported my research in every possible ways. I have learned from him how to think like a practitioner engineer from an academic lens.

I would like to thank Prof. Herman Kramer for his advice in his field of expertise and the support required for the research at TU Delft industrial crystallization laboratory.

I would also like to show my gratitude to Onno Kramer for his guidance. His technicality and critical thinking about documentation helped me in my report writing.

During my tenure at Waternet it was really delightful with my wonderful colleagues Tim and Pablo.

I would like to thank my parents for their support and love. Finally yet importantly, Avi for keeping me close while I am on the other side of the world.

Rubayat Sobhan

Amsterdam, 2019



# Summary

In the last decade, several process modifications took place in the Loenderveen (LDV)-Weesperkarspel (WPK) Water Treatment Plant (WTP) of Waternet. There are four process modifications initiated over time: first, a shift from garnet sand to calcite pellets as seeding materials for pellet softening process. Second, the elimination of acid dosing in the pretreatment plant at Loenderveen (LVN). Third, a set point adjustment in total hardness level to 1.4 mmol/L from 1.5 mmol/L. Finally, a switch from the acid (HCl) dosing to CO<sub>2</sub> dosing for conditioning of softened water for further treatment process. The existing pellet softening models with linear calcium carbonate crystallization kinetic (Rietveld, 2005, van Schagen et al., 2008a) describing calcium and pH profile over the height of the bed and the supersaturated calcium concentration after bypass mixed water, are not capable to cope with these process modifications. Therefore, an improved prediction model for softening process and a set of optimal operational configurations is needed. Recent researches (Chiou, 2018, Seepma, 2018) showed the first improvement path by using a prediction model based on bi-linear kinetics and hydraulics (Hout, 2016, Kramer, 2016). Hence, in this research a model is developed on the basis of new knowledge on kinetics on 4 regions depending on saturation ratio and hydraulics in the reactor and proposed optimal operational configurations.

The proposed new prediction model is based on experimental data from Continuous Stirred Batch Reactor (CSTR) and Plug Flow Reactor (PFR). The chemical model is described in 4 regions depending on the level of supersaturation. The kinetic rate constants for calcium carbonate crystallization on seeding material for these 4 regions are taken from CSTR and PFR experiments. The model is calibrated and validated based on previous experimental data from WPK and full-scale treatment plant (Schooten, 1985, Seepma, 2018, Schetters, 2013). Finally, the calibrated and validated results from studied model were compared with model outcomes proposed by Rietveld., 2005.

Calcium Carbonate Crystallization Potential (CCCP) is the amount of supersaturated calcium in the effluent and determines the efficiency of the entire pellet softening process. A scenario analysis is performed for summer and winter based on bypass, linear velocity and fluidized bed height, aiming for the lowest CCCP, high reliability, minimum cost and sustainability. CCCP determines the amount of chemicals used and principal cost of pellet softening process. The high reliability of the process comes from the full-scale plant operations over 30 years. The cost minimizations takes into account the chemical cost of NaOH and CO<sub>2</sub> (dosing chemical). Ultimately, an optimal operational configuration will lead to a sustainable operational approach for pellet softening by using as little chemicals as possible. The outcomes from the scenario analysis provided an operational window of 15-25% bypass and linear flow velocity of 69-85 m/h for pellet reactors depending on temperature (0-24°C). This choice of optimal configuration comes with a cost reduction between 3-4% both in winter and summer. Previous optimum configurations suggested a bypass of 50% with linear velocity of 60-70 m/h (Rietveld, 2005) and a cost reduction of 10%. This reduction of cost is less pronounced because of process modifications, improved prediction model with 4 regional kinetics and the set of operational windows. Therefore, the process modifications induced a different set of operational criteria for optimum outcome in the pellet softening process at WPK.

# Table of contents

<b>1</b>	<b>INTRODUCTION .....</b>	<b>1</b>
1.1	BACKGROUND OF THE THESIS .....	1
1.2	SOFTENING PRACTICES IN DRINKING WATER TREATMENT .....	1
1.3	OVERVIEW OF DRINKING WATER TREATMENT AT WEESPERKARSPEL .....	1
1.3.1	<i>Pretreatment at Loenderveen .....</i>	<i>2</i>
1.3.2	<i>Drinking water treatment at Weesperkarspel .....</i>	<i>2</i>
1.4	DRINKING WATER SOFTENING AT WEESPERKARSPEL.....	3
1.5	PROBLEM STATEMENT .....	5
1.6	KNOWLEDGE GAP .....	5
1.7	OBJECTIVE AND GOAL .....	5
1.8	RESEARCH QUESTIONS .....	6
1.9	THESIS OUTLINE .....	6
<b>2</b>	<b>THEORETICAL BASIS FOR HARDNESS REDUCTION.....</b>	<b>7</b>
2.1	AQUATIC CHEMISTRY RELATED TO CARBONIC EQUILIBRIUM .....	7
2.2	HYDRAULICS OF FLUIDIZATION.....	9
2.2.1	<i>Superficial Velocity.....</i>	<i>9</i>
2.2.2	<i>Temperature .....</i>	<i>10</i>
2.2.3	<i>Density and size of pellets .....</i>	<i>10</i>
2.2.4	<i>Pressure drop.....</i>	<i>11</i>
2.3	PREVIOUS MODELS ON PELLETT SOFTENING.....	11
2.3.1	<i>Ergun-Huisman approach .....</i>	<i>11</i>
2.3.2	<i>Richardson-Zaki approach .....</i>	<i>12</i>
<b>3</b>	<b>DEVELOPMENT OF THE PREDICTION MODEL.....</b>	<b>14</b>
3.1	CHEMICAL EQUILIBRIUM MODEL .....	16
3.1.1	<i>Development of calcium carbonate crystallization model .....</i>	<i>16</i>
3.1.2	<i>Final kinetic equations for chemical model.....</i>	<i>20</i>
3.1.3	<i>Chemical modeling in PRHEEQXCEL.....</i>	<i>22</i>

3.2	PARTICLE BED MODEL .....	23
3.2.1	<i>Choice of initial diameter per layer</i> .....	23
3.2.2	<i>Total number of particles in a fluid bed</i> .....	24
3.2.3	<i>Contact time</i> .....	24
3.2.4	<i>Change of diameter in each layer</i> .....	26
3.3	HYDRAULIC FLUIDIZATION MODEL.....	28
<b>4</b>	<b>CALIBRATION</b> .....	<b>29</b>
4.1	PILOT-SCALE EXPERIMENTS.....	29
4.1.1	<i>CSTR Experiments</i> .....	29
4.1.2	<i>PFR experiments</i> .....	29
4.1.3	<i>Method of parameter calculation with PHREEQCXCEL</i> .....	31
4.2	CALIBRATION.....	31
4.2.1	<i>Selection of experiments for calibration</i> .....	32
4.2.2	<i>Calibration with Seepma's experimental data</i> .....	33
4.2.3	<i>Calibration with Schooten's experiments</i> .....	34
4.2.4	<i>Calibration with Schetters's experiments</i> .....	35
4.2.5	<i>Re-calibration with full-scale for winter</i> .....	35
<b>5</b>	<b>VALIDATION</b> .....	<b>37</b>
5.1	METHOD OF VALIDATION.....	37
5.2	VALIDATION ON THE TOTAL HARDNESS .....	37
5.3	VALIDATION ON PH .....	38
5.4	ABSOLUTE RELATIVE ERROR IN MODEL PREDICTIONS.....	39
<b>6</b>	<b>OPTIMAL OPERATION FOR PELLET SOFTENING PROCESS</b> .....	<b>41</b>
6.1	CHOICE OF RAW WATER QUALITY.....	41
6.2	CHOICE OF OPERATIONAL PARAMETERS FOR SCENARIO ANALYSIS.....	42
6.3	OUTCOME OF SCENARIO ANALYSIS .....	43
6.3.1	<i>Operational windows</i> .....	43
6.3.1.1	<i>Reliability on number of the reactors in operation</i> .....	43
6.3.1.2	<i>Reliability on overdose</i> .....	43

6.3.1.3	Switching on and off reactors .....	45
6.3.1.4	Reliability on minimal velocity.....	45
6.3.2	<i>Optimum operation based on fluid bed height</i> .....	47
6.4	OPTIMAL CONFIGURATIONS.....	48
6.4.1	<i>Comparison optimal configurations</i> .....	51
<b>7</b>	<b>DISCUSSION</b> .....	<b>54</b>
7.1	MODEL .....	54
7.2	OPERATIONAL CONFIGURATIONS .....	54
7.3	CRITICAL THOUGHTS ON THE RESEARCH.....	55
<b>8</b>	<b>CONCLUSIONS AND RECOMMENDATIONS</b> .....	<b>57</b>
8.1	CONCLUSIONS .....	57
8.2	RECOMMENDATIONS .....	58
<b>BIBLIOGRAPHY</b> .....		<b>60</b>
<b>APPENDIX 1</b>	<b>RELATIVE NUMBER FOR EACH LAYER IN PARTICLE BED MODEL</b> .....	<b>63</b>
<b>APPENDIX 2</b>	<b>ADOPTED INITIAL DIAMETER PROFILE AND PROFILE AFTER 60 ITERATIONS</b> .....	<b>64</b>
<b>APPENDIX 3</b>	<b>HYDRAULIC MODEL USED FOR POROSITY ESTIMATION</b> .....	<b>65</b>
<b>APPENDIX 4</b>	<b>RELATIONSHIP BETWEEN THE MERCK POWDER AND SSA<sub>w</sub> (SEEPMA, 2018)</b> .....	<b>68</b>
<b>APPENDIX 5</b>	<b>CODING FOR CHEMICAL MODEL</b> .....	<b>69</b>
<b>APPENDIX 6</b>	<b>DCA/DT VS (SR-1) PLOT OF THE SELECTED EXPERIMENT</b> .....	<b>72</b>
<b>APPENDIX 7</b>	<b>EXPERIMENTAL DETAILS (SCHOOTEN, 1985)</b> .....	<b>74</b>
<b>APPENDIX 8</b>	<b>CALIBRATION GRAPHS (SCHOOTEN, 1985)</b> .....	<b>75</b>
<b>APPENDIX 9</b>	<b>EXPERIMENTAL DATA (SCHETTERS, 2013)</b> .....	<b>78</b>
<b>APPENDIX 10</b>	<b>CALIBRATION GRAPHS (SCHETTERS, 2013)</b> .....	<b>81</b>
<b>APPENDIX 11</b>	<b>DOSING OF NAOH IN JANUARY AND JULY, 2018</b> .....	<b>83</b>

# List of figures

Figure 1 Pre-treatment scheme at Loenderveen (LDN) (Van der Helm et al., 2015). .....	2
Figure 2 Process scheme of drinking water treatment plant at Weesperkarspel of Waternet (Van der Helm et al., 2015).....	3
Figure 3 Partial process flow diagram of Weesperkarspel (WPK) treatment plant.....	3
Figure 4 Schematic view of a pellet reactor (Left), where water flows in at (A), NaOH influent (B), insert/extraction point of seeding material (C), classification of CP in a fluidized bed (D) and reactor-effluent (E). Schematic view of a dosing head (Right). NaOH is flowing horizontally between two false plates and the 'to-be-treated'-water flows vertically for optimal mixing conditions (Van Dijk Hans et al., 2006).....	4
Figure 5 Relation between pH, $CO_2$ and $HCO_3^-$ – and $CO_3^{2-}$ -- lime-carbonic balance .....	8
Figure 6 stages of fluidization with increasing different flow velocity (Jobse, 2013) .....	10
Figure 7 Schematic diagram of modeled layers of fluidized bed.....	14
Figure 8 Schematic representation of the 3 sub-models and their relation in the prediction model of the pellet softening process. ....	16
Figure 9 Schematic description of bi-linear calcium carbonate crystallization kinetics. The data points are based on experiment 1.1.....	19
Figure 10 Schematic description of 4 regional calcium carbonate crystallization kinetics. ....	20
Figure 11 Four kinetic regions in the pellet reactor.....	22
Figure 12 Schematic overview of the simulations carried out in PHREEQCXCEL.....	22
Figure 13 Profiles of initial diameter per layer (left) and initial diameter in different iteration (right).....	24
Figure 14 Fluid bed height in m (left) and reaction time in seconds in each layer (right) for a simulation with $C_{ain}= 1.9$ mmol/L, $T= 20$ °C, $v= 80$ mh <sup>-1</sup> , $L= 4$ m and NaOH dosing=1.3 mmol/L for 20 layers.....	26
Figure 15 Experimental setup of the CSTR. The agitator's generator (1) is connected onto the top of the CSTR, which is attached to the RVS agitator (4). The pH and EC probes are then held by arms (2) into the solution. Finally NaOH is added through one of the holes present (3) in the lid and the holes are sealed off accordingly (Seepma, 2018) .....	30
Figure 16 Displays the used PFR. Hard water flows in (1) as the valve (2) is turned to a certain discharge, which is read at an venturi meter (5). NaOH is mixed with incoming hard water (7) and goes through a static mixer (4). Finally it is brought via a mixing h (3) into the 1 m column (6) (Seepma, 2018) .....	30

Figure 17 $dCa_{tot}/dt$ plotted against (SR-1) of calcite to calculate model parameters from experiment 1.1 (Table 1).....	31
Figure 18 Experimental and model pH profile for experiment 1.1 (left) and experiment 1.5 (right). .....	33
Figure 19 Experimental and modeled calcium content over fluid bed height. Operational conditions: $Ca_{in}$ = 1.99 mmol/L, temperature = 13.5-15.8°C, Flow= 20-25 m <sup>3</sup> /h, NaOH dosing =1.55 mmol/L (Left figure) and 0.57 mmol/L (Right figure).....	34
Figure 20 Experimental and modeled pH profile of Marc Schettters's experiments. Operational conditions: $Ca_{in}$ = 1.94 mmol/L, temperature = 1.5-3°C, Flow= 5.7 m <sup>3</sup> /h, NaOH dosing =1.76 mmol/L (Left figure) and 1.75 mmol/L (Right figure). ....	35
Figure 21 Average HCl dose from WebQuery for full-scale and modeled CCCP with different CP and SP value.....	36
Figure 22 Modeled and full-scale total hardness measurements for the month of January in 2018. Temperature range 4-6°C. ....	38
Figure 23 Modeled and full-scale total hardness measurements for the month of July in 2018. Temperature range at 18-23°C.....	38
Figure 24 Modeled and full-scale pH measurements for the month of January in 2018. Temperature range at 4-6°C. ....	39
Figure 25 Modeled and full-scale pH measurements for the month of July in 2018. Temperature range at 18-23°C. ....	39
Figure 26 Outcome of scenario analysis with prediction model for softening at WPK in winter and summer.....	43
Figure 27 Sides of the reactor on the top where crystallization occurs due to uneven mixing of NaOH on the left and schematic of internal bypass on the right.....	44
Figure 28 Operational window for dosing in winter after restrictions on the overdose of NaOH. .....	45
Figure 29 Operational window for dosing in summer after restrictions on the overdose of NaOH .....	45
Figure 30 Operational window for velocity in winter after restrictions on porosity/velocity....	46
Figure 31 Operational window for velocity in summer after restrictions on porosity/velocity.	47
Figure 32 Calcium collection profile over the bed height. Winter scenario (left) and Summer scenario (right) operational conditions: $Ca_{in}$ = 1.8-1.9 mmol/L, $v$ =71 m/h, caustic dose =0.84 mmol/L, total flow per reactor =375 m <sup>3</sup> /h, bypass =0%, and particle diameter= 1mm. The dosing in summer is 0.54 mmol/L and in winter 1.05 mmol/L.....	47
Figure 33 Optimal configuration for the operation of pellet softening in winter.....	49

Figure 34 Optimal configuration for the operation of pellet softening in summer. ....	50
Figure 35 Operation scenarios for softening at WPK, flow 3500 m <sup>3</sup> /h, 10°C (left figure) and 1.2°C (right figure)(HCO <sub>3</sub> <sup>-</sup> = 204 mg/L, Ca <sup>2+</sup> =80 mg/L, pH=7.61, EC=53 mS/m, Mg <sup>2+</sup> =6.6 mg/L) (Rietveld, 2005). ....	51
Figure 36 Operation scenarios for softening at WPK in winter, flow 3000 m <sup>3</sup> /h, 6°C (HCO <sub>3</sub> <sup>-</sup> = 211 mg/L Ca <sup>2+</sup> =76 mg/L, pH=7.6 (left) and pH=7.8 (right), EC=47 mS/m, Mg <sup>2+</sup> =6.48 mg/L). ....	52
Figure 37 Operation scenarios for softening at WPK in summer, flow 3000 m <sup>3</sup> /h, 20°C (HCO <sub>3</sub> <sup>-</sup> = 204 mg/L, Ca <sup>2+</sup> =71 mg/L, pH=7.44 (left) and pH=7.6 (right), EC=47 mS/m, Mg <sup>2+</sup> =6.48 mg/L)..	52
Figure 38 Relation of CO <sub>2</sub> dose and CCCP with bypass and Correlation of CCCP and CO <sub>2</sub> for WPK water quality. ....	58
Figure 39 Porosity as a function of linear velocity and temperature for sieve fraction 0.8-0.9 mm. ....	66
Figure 40 Fourth-order polynomials of the measured points on the sieve fraction 0.8-0.9 mm.	66
Figure 41 Kinematic viscosity against the porosity, with the trend line function for sieve fraction 0.8-0.9 mm.....	67
Figure 42 Particle diameter is against the porosity with a fourth-degree polynomial at T = 4.6°C and v = 73 m/h .....	67
Figure 43 Experiment no 1.1, temperature 8.5°C.....	72
Figure 44 Experiment no 50, temperature 5.6°C.....	72
Figure 45 Experiment no 1.5, temperature 22°C.....	73
Figure 46 Experiment no 29, temperature 20°C.....	73
Figure 47 Experimental and modeled calcium content over bed height. Operational conditions: Cain= 1.99 mmol/L, temperature = 13.5°C, Flow= 20 m <sup>3</sup> /h, NaOH dosing =0.88 mmol/L.....	75
Figure 48 Experimental and modeled calcium content over bed height. Operational conditions: Cain= 1.99 mmol/L, temperature = 13.8°C, Flow= 20 m <sup>3</sup> /h, NaOH dosing =0.76 mmol/L.....	75
Figure 49 Experimental and modeled calcium content over bed height. Operational conditions: Cain= 1.87 mmol/L, temperature = 14.3°C, Flow= 35 m <sup>3</sup> /h, NaOH dosing =1.09 mmol/L.....	76
Figure 50 Experimental and modeled calcium content over bed height. Operational conditions: Cain= 1.88 mmol/L, temperature = 15.3°C, Flow= 15 m <sup>3</sup> /h, NaOH dosing =1.43 mmol/L.....	76
Figure 51 Experimental and modeled calcium content over bed height. Operational conditions: Cain= 1.88 mmol/L, temperature = 15.8°C, Flow= 25 m <sup>3</sup> /h, NaOH dosing =0.7 mmol/L.....	77
Figure 52 Experimental and modeled calcium content over bed height. Operational conditions: Cain= 1.91 mmol/L, temperature = 15.8°C, Flow= 25 m <sup>3</sup> /h, NaOH dosing =1.19 mmol/L.....	77

## List of tables

Table 1 PFR experiments used for calibration .....	32
Table 2 CSTR experiments used for calibration .....	32
Table 3 Parameters obtained from the experiments (Seepma, 2018).....	32
Table 4 Initial kinetic parameters used in the prediction model. ....	33
Table 5 Experimental conditions for experiment no 1.1 and experiment no 1.5 .....	33
Table 6 Parameters after first calibration.....	34
Table 7 Calibrated parameters for prediction model in summer.....	34
Table 8 Calibrated parameters for prediction model in winter .....	35
Table 9 Final calibrated parameters for prediction model of summer and winter. ....	36
Table 10 Average Relative Error (ARE) of model results .....	40
Table 11 Influent water quality used in scenario analysis for summer and winter .....	42
Table 12 Choice of operation parameters for scenario analysis.....	42
Table 13 Operational boundary proposed by (Maduro, 2015) on physical parameters.....	46
Table 14 Multi criteria analysis for optimal scenario in winter.....	48
Table 15 Multi criteria analysis for optimal scenario in summer .....	49
Table 16 Optimal configurations for summer and winter.....	50
Table 17 Cost reduction.....	50

# List of Abbreviations

WPK	Weesperkarspel
LVN	Loenderveen
WTP	Water Treatment Plant
HMF	Hydraulic Fluidized Model
LDN	Leiduin
CSTR	Continuous Batch Stirred Reactor
PFR	Plug Flow Reactor
SSA	Specific Surface Area
CP	Changing Point
SP	Sleeping point
EBCT	Empty Bed Contact Time
SI	Saturation Index
SR	Saturation Ratio
$SSA_w$	Specific Surface area in water phase
$SSA_r$	Specific Surface area
ARE	Average Relative Error
EC	Electrical Conductivity
KPI	Key Performance Indicator

# List of Symbols

$K_s$	Equilibrium constant	$M_C$	Mass of calcium carbonate
$f$	Activity factor	$k_{W,T}$	Rate constant
$IS$	Ionic strength	$k_T$	Rate Constant
$K_1$	Reaction constants	$K_{sp}$	Solubility Product
$K_2$	Reaction constants	$k_f$	Transport coefficient
$K_w$	Reaction constants	$S_h$	Sherwood number
$SI$	Saturation index	$D_f$	diffusion coefficient
$SR$	Saturation ratio	$k_i$	Rate constant
$\nu$	Kinematic viscosity	$SR_{CH}$	Changing point in Saturation ratio
$\mu$	Dynamic viscosity	$A_H$	Intercept
$\rho_w$	Density of water	$k_H$	High rate constant
$v_b$	Settling velocity	$k_L$	Low rate constant
$\rho_p$	Density of pellets	$\frac{dCa}{dt}$	Rate of calcium crystallization
$d_p$	Diameter of pellets	$A_r$	Area of reactor
$\Delta P$	Pressure drop	$MW_{CaCO_3}$	Molecular weight of calcium carbonate
$\Delta L$	Bed thickness	$k_C$	Rate constant at CSTR zone
$p$	Porosity	$k_S$	Rate constant at sleeping zone
$v_s$	Superficial velocity	$N_p$	Number of particles
$T$	Temperature	$N_T$	Total number of particles
$H$	Head loss	$V_p$	Total volume of particles
$L_{b0}$	Height of expanded bed	$V_{W+P}$	The total volume of water and pellets
$Re$	Reynolds Number	$H$	Layer thickness in particle bed model
$\phi$	Shape factor	$V_W$	Volume of water
$v_0$	Terminal velocity	$A_T$	Total area of pellets
$g$	Gravitational acceleration	$d_{Ca}$	Change in the amount of calcium
$C_{w2}$	Drag coefficient	$t_{real}$	Real contact time
$n$	Exponent	$V_{Pout}$	Volume of pellets out from reactor
$X_W$	Upward water flow	$V_{Pin}$	Volume of pellets input to reactor
$v_p$	Downward volume of pellet transport	$d_{pbal}$	Diameter of pellet
$M_p$	Mass of pellets	$y_{model}$	Model predicted value
$A$	Intercept of high rate line	$y_{meas}$	Experimental data

# 1 Introduction

*The chapter starts with the background of the research and a process description of softening practices in the drinking water treatment. Afterwards, a short overview of the drinking water treatment plant at Weesperkarspel (WPK), one of the two drinking water treatment facilities of Waternet is presented. It includes a summary describing the softening process at WPK. It also focuses on the challenges on how to translate the new acquired knowledge on kinetics and hydraulics into an innovative process design. Furthermore, it specifies the goals and objectives of the research by establishing the research questions. Finally, an outline for the thesis is provided.*

## 1.1 Background of the thesis

Waternet (formerly known as Amsterdam Water Supply) is currently the only water cycle company in the Netherlands (Rietveld et al., 2009). Water cycle activities include drinking water treatment and distribution, wastewater collection and treatment and water system management and control (van der Hoek, 2012). The company has the ambition of becoming climate neutral in 2020 by saving energy, process optimization with respect to water quality guidelines (valorization to raw materials re-use and efficient use of chemicals), shifting to renewable energy and compensation measures for CO<sub>2</sub> emissions. Among the activities, the process optimization step is crucial for drinking water treatment as a bulk amount of chemicals are exploited in this process.

## 1.2 Softening practices in drinking water treatment

Calcium is one of the divalent ions that contribute to the hardness of water (Harms Jr and Robinson, 1990). Hardness removal from water primarily helps to reduce the dissolution of certain heavy metals such as lead, copper. Furthermore, it also helps reducing scaling in heating equipment's and appliances, improves the taste of water and reduces the use of detergents (De Moel et al., 2007). Pellet reactor with an internal fluidized bed is an enticing process for water softening. In general, in this process, a cylindrical tank is filled with sand, or broken pellets as seeding materials having a diameter of 0.15 to 0.5 mm. Water is pumped upward with a constant velocity of 60-100 m/h (Maeng et al., 2016). The size of the seeding materials will increase in this process due to the crystallization of Calcium Carbonate (CaCO<sub>3</sub>) on it. Crystallization of CaCO<sub>3</sub> is induced by increasing pH to approximately 9.0 – 10.0 by dosing Caustic Soda (NaOH) or lime. Instantaneous crystallization causes gradual stratification of the seeding materials, larger pellets at the bottom and smaller ones on the upper level of the reactor. Periodically the bottom pellets are withdrawn and the same amount of fresh pellets are introduced from the top of the reactor (Maeng et al., 2016). Waste pellets are often reused in agricultural, glass, paper, carpet and steel industries (Van der Bruggen et al., 2009).

## 1.3 Overview of drinking water treatment at Weesperkarspel

The drinking water treatment plant at WPK consists of two step treatment process: pretreatment at Loenderveen (LVN) and the main drinking water treatment at Weesperkarspel (WPK).

### 1.3.1 Pretreatment at Loenderveen

As surface water is treated at WPK, a series of pretreatment is necessary to make impeccable drinking water. Figure 1 shows the pre-treatment at LVN. The raw water is the collected seepage water from Bethune polder and Amsterdam-Rhine canal. After, it is transported to LVN pre-treatment plant. A series of treatment scheme of coagulation, sedimentation, self-purification in a lake water reservoir and rapid sand filtration takes place (Van der Helm et al., 2015). The pre-treated water is transported over a 14-kilometer pipeline to the treatment plant WPK without chlorination.

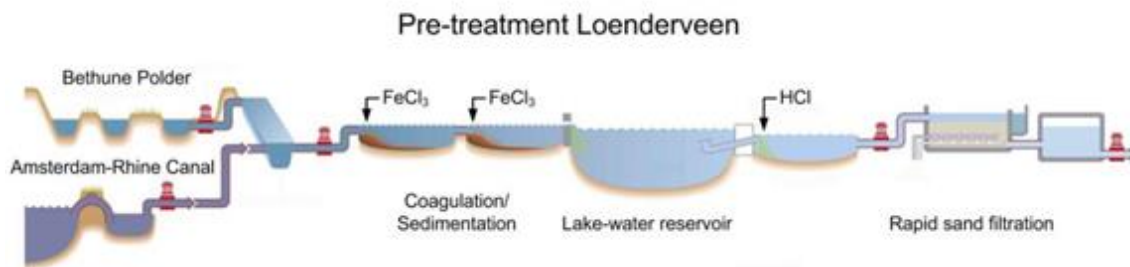


Figure 1 Pre-treatment scheme at Loenderveen (LDN) (Van der Helm et al., 2015).

### 1.3.2 Drinking water treatment at Weesperkarspel

The first process at WPK is the disinfection and oxidation of the organic material by ozonation. After that, the pellet reactors are used for the reduction of hardness from water. There are eight softener reactors at WPK and two main streets: South and North. Water from reactors transported to the next treatment process through the two streets. Each street carries softened water from four reactors mixed with bypass water (Figure 3). The mixed effluent<sup>1</sup> generally still has the potential to form CaCO<sub>3</sub> crystals so it can further crystallize or precipitate on activated carbon bed. So, conditioning of mixed effluent is done by lowering the pH to 7.5 (saturation index = ± 0.05) by dosing CO<sub>2</sub> in each street. Then the water is transported to the biological activated carbon filtration to remove pesticides and micropollutants either by adsorption or removal by biological activity. The last step in the treatment is slow sand filtration to remove any remaining organic or inorganic particles (Chiou, 2018, Van der Helm et al., 2015). Figure 2 shows the scheme of the treatment scheme WPK.

<sup>1</sup> In this report mixed effluent refers to the softened water mixed with non-softened bypass water

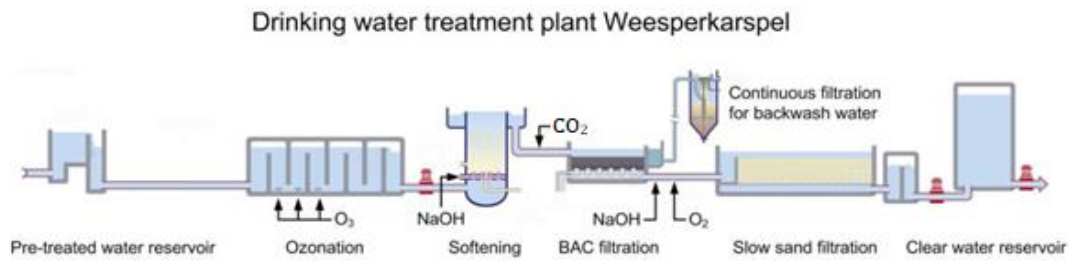


Figure 2 Process scheme of drinking water treatment plant at Weesperkarspel of Waternet (Van der Helm et al., 2015).

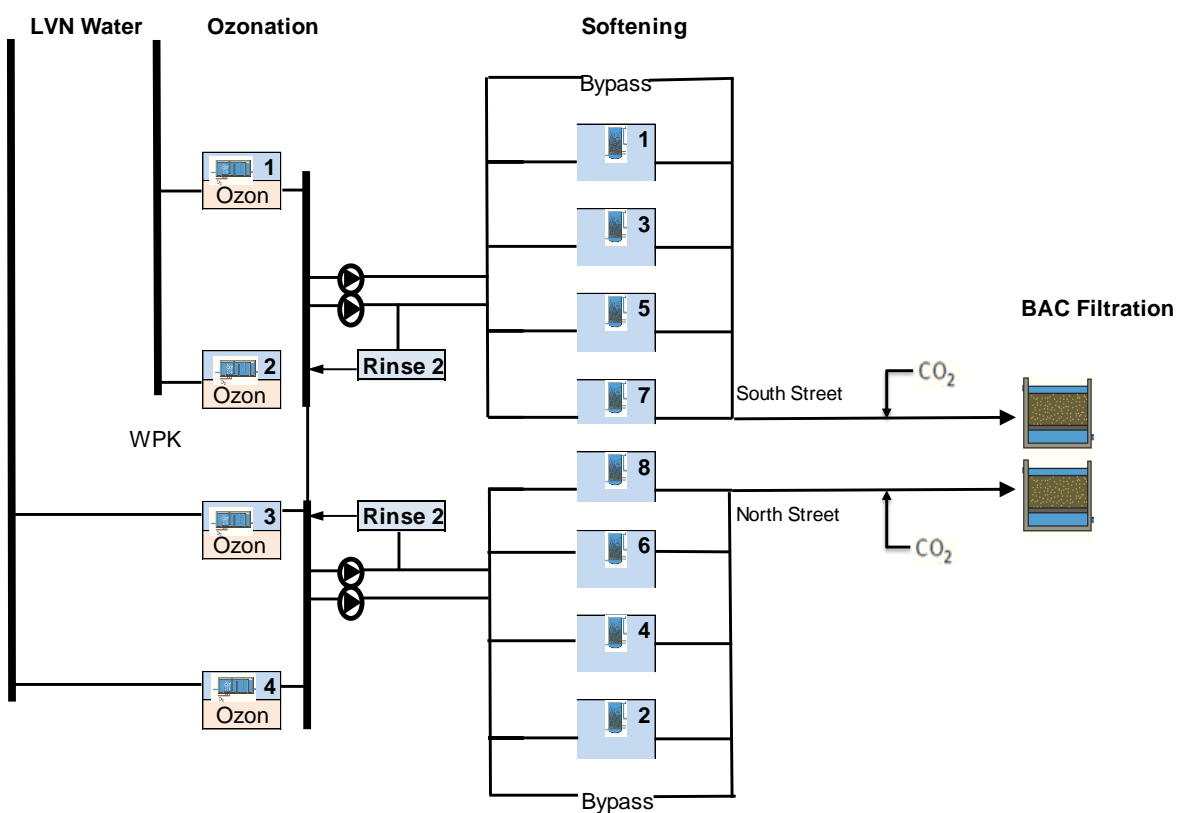


Figure 3 Partial process flow diagram of Weesperkarspel (WPK) treatment plant.

### 1.4 Drinking water softening at Weesperkarspel

Each of the eight pellet softening reactors have a diameter of 2.6 m and a height of 5.5. The maximum fluid bed height and capacity of each pellet reactors are 4.5 m and 4800 m<sup>3</sup>/h. The influent has a calcium content of 1.8-2.2 mmol/L varying around the year and magnesium content of 0.28 mmol/L. The target hardness is 1.4 mmol/L after the addition of NaOH. An amount of 0.8-1.5 mmol/L of NaOH (25% w/w) is added to achieve a pH around 9.8 at the bottom of each pellet

reactors. As the calcium is taken out from the water in this process, the reactor-effluent<sup>2</sup> has a lower pH varying between 8.5-9.2. Softening in the pellet reactors is normally deeper than the target value of 1.4 mmol/L. Therefore, a part of ozonated water is bypassed and mixed with the reactor-effluent (Rietveld, 2005).

The pellet reactors are cylindrical vessels and about two-thirds of their volume is filled with seeding materials in fluidized state. As seeding materials, Dutch calcite pellets are used having a diameter around 0.5 mm. Ozonated water is pumped upward with a superficial velocity of 60-95 m/h. This upward flow causes the fluidization of seeding materials in the reactor. The bottom of the reactor has a distinct plate containing 35 dosing points per m<sup>2</sup> which separate water and NaOH at the bottom (Figure 4). The dosing point and incoming water jet create turbulence at the bottom of the reactor which causes rapid mixing. After that, NaOH flows upward through small channels and also the water streams are vertical due to upward pumping. So, in the upper part of the reactor axial mixing takes place. Ultimately the solubility product of CaCO<sub>3</sub> is exceeded and it starts to crystallize on calcite pellets. Due to fluidization of calcite pellets, a high amount of Specific Surface Area ( $SSA_{H_2O}$ ) around 5000 m<sup>2</sup>/m<sup>3</sup> is available for crystallization.

The crystallization of CaCO<sub>3</sub> on calcite pellet causes an increase of their diameter by crystals growth and the area to volume ratio reduces. Due to fluidization, classification of calcite pellets takes place by orienting larger pellets at the bottom and the smaller pellets at top of the reactor. So, it makes easy to extract the large pellet of (0.8-1.5 mm) from the bottom. Crushed calcite pellets (0.5 mm) are introduced from the top of the reactor at 1 meter height of the reactor. The insertion and extraction of calcite pellets are regulated by pressure. If the pressure at a height of 0.5 m at the bottom of the reactors exceeds 3.5-4.0 kPa, the oversized pellets are automatically taken out from the system and new pellets are introduced. Figure 4 shows the schematic view of pellet reactor and dosing nozzles of NaOH.

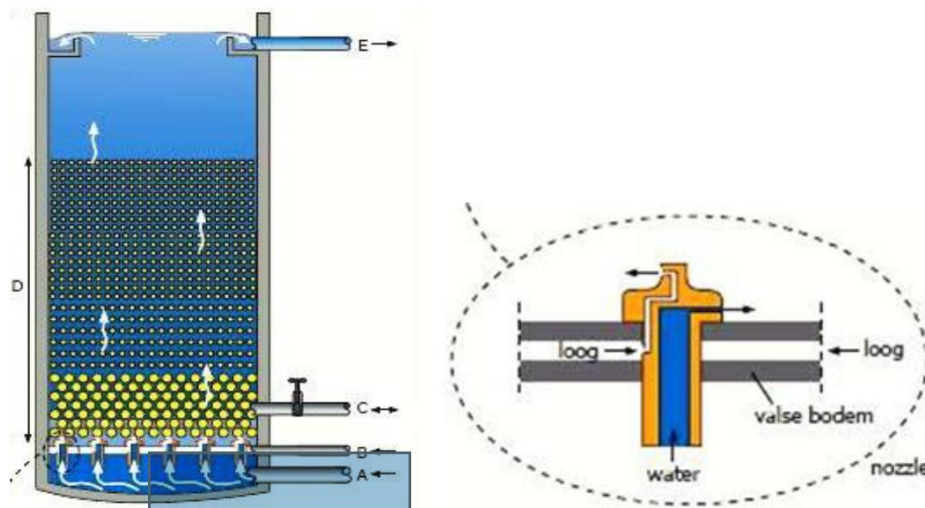


Figure 4 Schematic view of a pellet reactor (Left), where water flows in at (A), NaOH influent (B), insert/extraction point of seeding material (C), classification of CP in a fluidized bed (D) and reactor-effluent (E). Schematic view of a dosing head (Right). NaOH is flowing horizontally between two false plates and the 'to-be-treated'-water flows vertically for optimal mixing conditions (Van Dijk Hans et al., 2006).

<sup>2</sup> Reactor-effluent refers to the softened water from the reactor without bypass water mixing.

A new system of dosing point is established in the pellet reactors recently. The NaOH is dosed in seven dosing heads in a cross like metal armature and placed near the bottom.

## 1.5 Problem statement

In the last decade, several process modifications took place in the big line of the water treatment process at the plant WPK.

Previously garnet sand having a diameter of 0.25 mm offering a large specific surface area was used as seeding materials in the softening reactors. Comprehending the importance of the circular economy, Waternet decided to replace garnet sand to Dutch Calcite (Schetters et al., 2015). Further important process modifications are the elimination of acid dosing in the pretreatment plant at LDN in 2010 and for conditioning of softened water, in 2017 hydrochloric acid was replaced by CO<sub>2</sub>. In addition, the water quality requirement at Waternet has shifted to a more conservative side by setting a total hardness from 1.5 to 1.4 mmol/L. lastly, additional dosing points are established in the softening reactors (dosing cross) for process improvement. Due to these outset changes, the existing model for pellet softening needs to be improved for better prediction of the softening process. Several pieces of research took place in the last few years to endure optimal water quality, reduction of cost and to increase sustainability. Therefore, it is imperative to upgrade the existing model with the gained knowledge from previous researches for a better control of the softening process.

The existing chemical modeling describing seeded crystallization of CaCO<sub>3</sub> on calcite grains in a fluidized bed is based on the mono-linear kinetics model of Wiechers (Wiechers et al., 1975). In contrary, Eleftheria Chiou and Seepma came up with new bi-linear kinetics for seeded crystallization (Chiou, 2018, Seepma, 2018) which provides a better prediction of CaCO<sub>3</sub> crystallization process in the pellet reactors. Moreover, the hydraulics describing the expansion of fluid bed can be better predicted by data driven model rather than traditional fluid-bed expansion approaches (Richardson et al., 1971, Ergun, 1952).

## 1.6 Knowledge gap

The knowledge gap for this research is that whether **the acquired new knowledge on CaCO<sub>3</sub> kinetics and hydraulic improvements can address the process modifications in the new improved softening prediction model and provide an optimized configuration of the softening process in the drinking water treatment plant at Waternet.**

## 1.7 Objective and goal

The objective of this thesis is to develop an improved prediction model based on recent findings in the pellet softening process.

The goal of the development of the new prediction model is to execute a scenario study and suggest optimal configurations for pellet softening in the full-scale plant at (WPK). The optimal configuration is based on quality of softened water, reliability of operational processes, and minimization of cost. A sustainable operational configuration can be achieved by exploiting fewer chemicals.

## **1.8 Research questions**

The research questions of this thesis are:

- I. What are the components needed to develop a model that can translate the acquired knowledge on seeded crystallization to optimize the configuration of the softening process?
- II. Is the knowledge about the kinetics of seeded crystallization accurate to design the model?
- III. Is the current experimental data set being accurate enough to calibrate and validate the model?
- IV. Which criteria are important to choose the optimal operational configuration?

## **1.9 Thesis Outline**

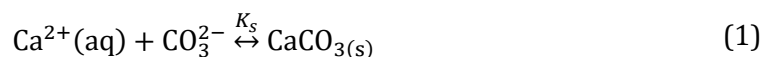
The report is divided into 8 chapters. In the first chapter, the background and the knowledge gap is presented along with the goal and objective of the research. The second chapter deals with the theoretical basis for the hardness reduction process. Third, fourth and fifth chapter describes the prediction model development, calibration, and validation of the it. The optimum configurations and the main outcomes of the research are presented in chapter six. Chapter seven discusses the overall outcomes and the limitations if the research. Finally, chapter eight presents the concluding remarks and recommendations for the future.

## 2 Theoretical basis for hardness reduction

The process of hardness reduction from water is described chemically and physically. The chemical part mainly focuses on the aquatic chemistry related to carbonic equilibrium. The physical part deals with the hydraulics of fluidization. Finally, an overview is presented of the existing models of pellet softening that describes both the chemical and hydraulic part.

### 2.1 Aquatic chemistry related to carbonic equilibrium

Crystallization of calcium carbonate occurs in two processes: nucleation and growth. In seeded crystallization the growth on the pellets is the dominant process which is known as heterogeneous crystallization (van Dijk and Wilms, 1991). For any crystallization process a driving force is needed, hence in this case the driving force is supersaturation of carbonate which can be determined by calcium carbonic equilibrium (Van Schagen et al., 2008b). Wiechers et al. in 1975 experimentally found the rate of the crystallization by the following equation (Wiechers et al., 1975).

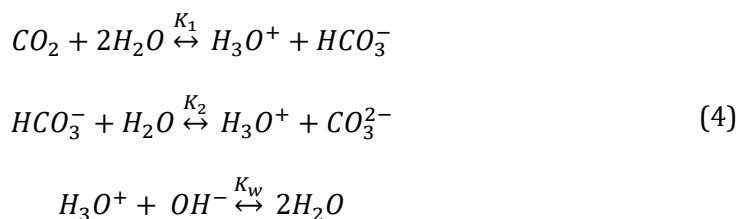


$$K_s = f^8[\text{Ca}^{2+}][\text{CO}_3^{2-}] \quad (2)$$

Where  $K_s$  is the equilibrium constant that depends on the water temperature. The activity factor  $f$  is based on the ionic strength of water and proposed by Schock (Schock, 1984).

$$\log(f) = \frac{-0.5\sqrt{IS}}{\sqrt{1000 + \sqrt{IS}}} + 0.00015IS \quad (3)$$

Here  $IS$  is the ionic strength of the water. To determine the carbonate concentration in the water carbonic equilibrium must be taken into account. Carbonic equilibrium occurs by the balance of these three fractions  $\text{CO}_2$ ,  $\text{HCO}_3^-$  and  $\text{CO}_3^{2-}$ . The ratio between these fractions has a strong influence on the pH of the water (Stumm and Morgan, 2012). The following equations describes the equilibrium:



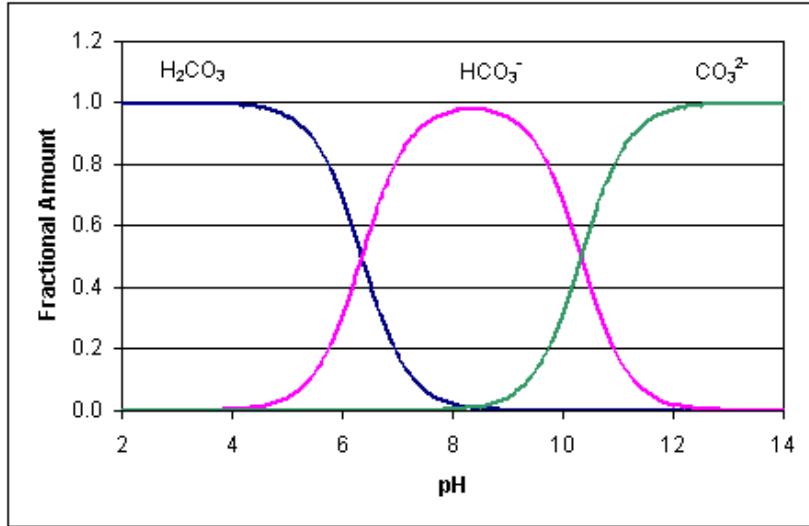


Figure 5 Relation between pH,  $CO_2$  and  $HCO_3^-$  and  $CO_3^{2-}$  - lime-carbonic balance

By the definition of m-alkalinity (M) and p-alkalinity (P):

$$\begin{aligned}
 M &= 2[CO_3^{2-}] + [HCO_3^-] + [OH^-] - [H_3O^+] \\
 P &= [CO_3^{2-}] - [CO_2] + [OH^-] - [H_3O^+] \\
 K_1 &= f^2[HCO_3^-][H_3O^+][CO_2]^{-1} \\
 K_2 &= f^4[CO_3^{2-}][H_3O^+][HCO_3^-]^{-1} \\
 K_w &= f^2[H_3O^+][OH^-]
 \end{aligned} \tag{5}$$

The reaction constants  $K_1$ ,  $K_2$  and  $K_w$  are temperature depended and can be determined also experimentally (Plummer and Busenberg, 1982). By solving equation set 5, the carbonic group concentrations can be known. There are seven unknowns ( $M$ ,  $P$ ,  $CO_2$ ,  $HCO_3^-$ ,  $CO_3^{2-}$ ,  $H_3O^+$  and  $OH^-$ ) in the equation set 5, two of these concentrations must be known in order to determine the others. In the softening reactors the raw water concentrations of  $H_3O^+$  and  $HCO_3^-$  are known by the continuous measurements. The  $H_3O^+$  concentration is given by the pH.

$$pH = -\log(f[H_3O^+]) \tag{6}$$

By solving equation 5 and 6, the concentration of carbonate throughout the crystallization process can be determined. First, the with raw water pH and  $HCO_3^-$  concentration give the value of M and P alkalinity. The NaOH dosing increases the M and P alkalinities as it introduces  $OH^-$  ions to the system. With this new alkalinity,  $CO_3^{2-}$  concentrations are determined. The crystallization of calcium carbonate on the pellets begins which is the removal of carbonate from the water, causes lowering of M and P alkalinity. The equilibrium is set and based on M and P alkalinities, again new  $CO_3^{2-}$  concentration is determined.

To describe the supersaturation of calcium carbonate in the water, there exists two parameters, Saturation index (SI) which is the driving force for crystallization and CCCP<sup>3</sup> (Calcium Carbonate Crystallization Potential). SI of calcium carbonate is defined as follows:

$$SI = \log \left( \frac{[Ca^{2+}][CO_3^{2-}]}{K_s} \right) \quad (7)$$

CCCP (mmol/L) is the amount of calcium carbonate or supersaturated calcium in the system yet to precipitate or crystallize to achieve chemical equilibrium (saturation index zero). These two indices are strongly inter-dependent, but both are used as quality check for crystallization process. In this research, Saturation Ratio (SR) is used to quantify the driving force which is derived from SI. The expression for saturation ratio:

$$SR = 10^{SI} \quad (8)$$

## 2.2 Hydraulics of fluidization

The basics hydraulics involved in fluidization is a function of superficial velocity, temperature, pressure drop and size and density of particles (pellets). The porosity of the bed is a function of all these element. In this section a brief description of the hydraulic components of fluidization is presented.

### 2.2.1 Superficial Velocity

Superficial velocity is the hypothetical fluid velocity through porous media that considers that only one type fluid flowing in a given cross sectional area. With an increase of upward superficial flow, the bed calcite pellets undergo several distinct stages (Figure 4). It starts with a fixed bed where the fluid does not have enough power to make the pellets in motion (Figure 6, stage 1).

With the increasing upward superficial velocity, a point reach where the bed gets the minimum homogeneous fluidization. (Figure 6, stage 2).

The fluid flows through the empty spaces of the packed bed with a higher speed that the particles are separated from each other by moving the fluid greatly and benefits the behavior of the expanded bed (Figure 6, stage 3).

At higher speeds, the empty spaces are between the particles (porosity) and the height of the bed increases. Expansion is measured by the height of the bed. A ratio between the bed in a fluidized state and in the fixed-bed state is called the degree of expansion and this is expressed in porosity.

When the velocity reaches a state where its greater than the combined rate of settling of the pellets are entrained with the flow. This is known as washout of pellets (Figure 6, stage 4). So the

---

<sup>3</sup> Calcium Carbonate Crystallization Potential (CCCP) is also called as TCCP (Theoretical Calcium Carbonate Crystallization potential) or Theoretisch Afzetbaar Calcium Carbonaat (TACC) in Dutch.

degree of fluidization of bed is primarily depended on the superficial velocity. Although the expansion is also depended on temperature, viscosity, the density of pellets and pellet size.

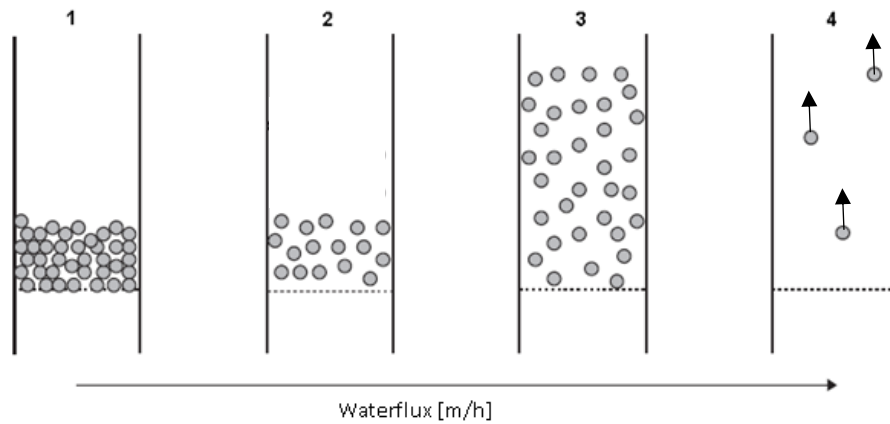


Figure 6 Four stages of fluidization with increasing different flow velocity (Jobse, 2013)

## 2.2.2 Temperature

The temperature is an important parameter in case of fluidization. The density also determines the expansion of the bed. With increasing temperature, the density of the water decreases, so the dynamic viscosity also decreases. The dynamic viscosity and the kinematic viscosity is related by the following relation:

$$\nu = \frac{\mu}{\rho_w} \quad (9)$$

Here,  $\nu$  is the kinematic viscosity and  $\mu$  is the dynamic viscosity.  $\rho_w$  is the density of water.

## 2.2.3 Density and size of pellets

Density and pellet size play an important role in the fluidization. It helps the classification of the pellets in the fluidized bed. The classification of pellets causes a non-stationary state of the fluid bed. Particles with the highest density ( $\rho_p$ ) and largest diameter are located at the bottom of the reactor after classification. In contrast, pellets having the smallest diameter and lowest density ( $\rho_p$ ) stays in the upper part of the reactor. The settling velocity of a pellet is a function of density and diameter (Kramer, 1991).

$$v_b \propto \rho_p * d_p^2 \quad (10)$$

Here,  $v_b$  is the settling velocity.

## 2.2.4 Pressure drop

When the fluid flows through the packed bed of pellets, it experiences pressure loss within the bed due to frictional resistance. When the upward drag force exerted by the fluid on the pellets is equal to the apparent weight of the pellets in the bed, at this point the pellets are lifted by fluid and separation of particles increases and thus it gets fluidized. The force balance dictates the pressure drop in the pellet bed which is equal to the apparent weight of pellets per unit area of bed (Rhodes and Rhodes, 2008).

$$\Delta P = \frac{\text{Weight of pellets} - \text{upthrust on pellets}}{\text{bed cross sectional area}} \quad (11)$$

Here  $\Delta P$  is the pressure drop across fluid bed. If the particle density is  $\rho_p$  fluidized by a fluid density of  $\rho_w$  to form a bed depth of  $\Delta L$  and the porosity is  $p$ . Then the pressure drop can be expressed as:

$$\frac{\Delta P}{\Delta L} = (\rho_p - \rho_w) g (1 - p) \quad (12)$$

Therefore, to maintain optimal process conditions in pellet softening fluidized bed reactor, it is important to determine the porosity of fluidized bed. Porosity is an crucial parameter determining  $SSA_w$ , minimum fluidization and flushing conditions and the residence time of water particle. The degree of expansion is also depended on temperature, viscosity, the density of the pellets density and size. So the porosity can be expressed as a function of:

$$p = f\{v_s, T, \rho_p, d_p, \Delta P\} \quad (13)$$

Here,  $v_s$  is the upward velocity,  $T$  is the temperature of water,  $\rho_p$  is the density of pellets,  $d_p$  is the diameter of the pellets and  $\Delta P$  is the pressure drop across the bed.

## 2.3 Previous models on pellet softening

There are numerous models for expansion of fluidized bed exists. Two approaches (Richardson et al., 1971) are widely use. Ergun approach (Ergun, 1952) based on the forces acting on the particles and Richardson Zaki (Richardson and Zaki, 1954) approach which is based on expansion formula . The formula for expansion of uniform pellets is then used in pellet-softening bed reactor. For the chemical model, so far Wiechers (Wiechers et al., 1975) proposed linear kinetics.

### 2.3.1 Ergun-Huisman approach

To determine the rate of crystallization in an unit element specific surface area of the pellets (a) diameter of the pellets ( $d_p$ ) and the porosity ( $p$ ) over the height of the reactor must be known. During fluidization the head loss over the bed can be calculated by the following empirical

formula of Carman-Kozeny (van Dijk and Wilms, 1991). The head loss over in the fluid bed for spherical pellets:

$$H = \frac{260 L_{b0} (1-p) v_s^2}{Re^{0.8} d_p p^3 2g} \quad (14)$$

Here,

$H$  = Head loss, pa

$L_{b0}$  = height of expanded bed, m

$p$  = Porosity (-)

$Re$  = Reynolds Number (-),  $Re = \frac{1}{1-p} \frac{v_s d_p}{\nu}$

$\nu$  = kinematic viscosity, m<sup>2</sup>/s.

Submerged weight of the pellet bed are given by

$$\text{submerged bed weight} = (1-p)L_{b0} \frac{\rho_P - \rho_w}{\rho_w} \quad (15)$$

Therefore, fluidization will occur when the head loss in the pellet bed (equation 14) is equal to the submerged weight of the pellet (equation 15). So, the porosity can be determined by solving the following equation:

$$\frac{p^3}{(1-p)^{0.8}} = 130 \frac{v^{0.8} v_s^{1.2} \rho_w}{(\phi d_p)^{1.8} g \rho_P - \rho_w} \quad (16)$$

Here  $\phi$  is a shape factor for taking into account the non-spherical pellets.

### 2.3.2 Richardson-Zaki approach

In Richardson and Zaki (1954) approach the porosity in fluidized bed is given by:

$$p = \left( \frac{v_s}{v_0} \right)^{\frac{1}{n}} \quad (17)$$

Here terminal velocity  $v_0$  and the exponent  $n$  is experimentally determined properties for single particle. For perfectly round particles  $v_0$  can be determined by Newtons-Stokes equation (Bird et al., 1960).

$$v_0^2 = \frac{4 d_p (\rho_P - \rho_w) g}{3 C_{w2} \rho_w} \quad (18)$$

$C_{w2}$  is the drag coefficient given by (Schiller and Naumann, 1933):

$$C_{w2} = \frac{24}{Re} (1 + 0.15Re^{0.687}) \quad (19)$$

The empirical relationship between  $n$  and  $Re$  is given by following set of equation

$$n = \begin{pmatrix} 4.6 & \text{for } Re < 0.2 \\ 4.4Re^{-0.03} & \text{for } 0.2 < Re < 1 \\ 4.4Re^{-0.1} & \text{for } 1 \leq Re < 500 \\ 2.4 & \text{for } Re > 500 \end{pmatrix} \quad (20)$$

Both models (Ergun and Richardson-Zaki) assume perfectly round, uniform and smooth pellets.

Previously, two models were proposed for describing pellet softening process at WPK : Rietveld (2005) and Van Schagan (2009). In the model of Rietveld (2005), Ergun approach is (van Dijk and Wilms, 1991) is used in combination with Wiechers linear kinetic chemical model. In the model of Van Scahgen (2009), Richardson-Zaki approach is used in combination with improved Wiechers chemical model with an additional parameter for diffusion (van Schagen et al., 2008c).

### 3 Development of the prediction model

*This chapter provides an explanation of the structure of the prediction model and the principles on which it is based. The prediction model has three inter-connected sub-models: chemical equilibrium model based on kinetics, Hydraulic Fluidization Model (HFM) for porosity estimation and particle bed model describing the entire fluid bed in layers. First, the main lines are sketched, the hardness reduction process with the corresponding dosages. After this, the incorporation of new kinetics is elaborated. Then it zooms in on the fluidized bed and finally the particle bed model is described. Towards the end of the chapter a schematic representation of these three sub-models is presented. Here lies the heart of the modeling and combined chemical and physical aspects of hardness reduction.*

For a better prediction of seeded crystallization for current process conditions and efficiency of the softening process, an improved model needs to be developed. The previous models (Rietveld, 2005, van Schagen et al., 2008c) was based on linear kinetics for seeded crystallization. Recent researches (Chiou, 2018, Seepma, 2018) showed that a bilinear kinetics can define the rate of seeded crystallization more accurately.

The prediction model consists of three parts, a chemical model, a particle bed model and a porosity determination model which is based on an ongoing research on Hydraulic modeling of liquid-solid fluidization (HMF) (Kramer, 2016). As the prediction model is developed in layers, in this research it is also called layers model interchangeably.

In the full-scale treatment plant at Weesperkarspel, the softening process consists of fluidized bed reactors with a single bypass. All the chemical reaction occurs within the reactors and mixing is modelled as instantaneous mixing without kinetics.

Layers model (Hout, 2016) is perceived as the division of the entire fluidized bed into smaller layers with uniform pellets as shown in Figure 7.

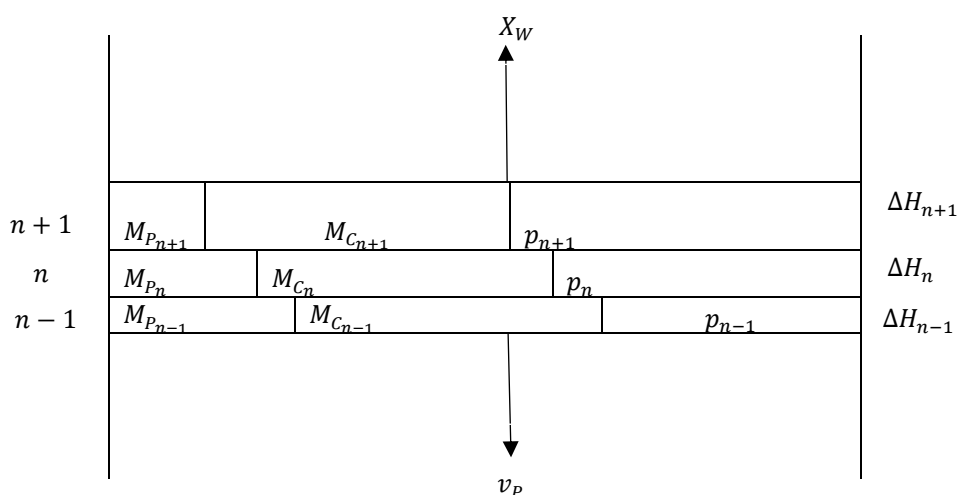


Figure 7 Schematic diagram of modeled layers of fluidized bed.

In Figure 7,  $M_p$ ,  $M_C$  and  $p$  denotes mass of pellets or seeding materials, mass of calcium carbonate and porosity in each layer.  $\Delta H$  is the thickness of the layers. The water is flowing ( $X_w$ ) only in the upward direction and the pellets are transported ( $v_p$ ) in the downward direction. In the hydraulic model, the state variables are the mass of calcium carbonate and the mass of pellets.

There are three contributing fractions in each layer: the mass of the pellets or seeding materials, the mass of precipitated calcium carbonate and the volume of water which is determined by the porosity (Van Schagen et al., 2008b). Though the calcium carbonate precipitates on the pellets, but in this model this is considered as separate entity. As in the chemical model the precipitation of calcium carbonate in each layer is calculated by the pre-defined kinetics, so, it does not calculate the growth of pellets. The growth of the pellets is calculated in particle bed model by adding the precipitated amount of calcium carbonate to the pellets of that layer and calculates the new diameter of the pellets. Thickness ( $\Delta H$ ) of each layer is determined by the total mass of pellets including calcium carbonate and seeding materials and the porosity of the bed. The basic principle of the mass balance is the shift of equal number of pellets from one layer to another. When a pellet will gain mass in the softening process, due to stratification it tends to come to a lower position of the reactor. Similarly, another pellet from upper part of the reactor after gaining enough mass will come to the same position of the first pellet. So, if a small strip of fluid bed is considered, there is always equal number of pellets coming in and going out. The total number of pellets in that small strip depend on the size of pellet. Lower it goes in the reactor, less numbers of pellet can be accommodated as pellets gets bigger in the softening process.. For example, in Figure 7, if  $x$  numbers of particle are transported from  $n^{\text{th}}$  layer to  $(n-1)^{\text{th}}$  layer, then the same amount of pellets will be transported from  $(n+1)^{\text{th}}$  layer to  $n^{\text{th}}$  layer. Furthermore, with increasing numbers of layers,  $\Delta L$  increases due to stratification. The smaller the pellets are, more space for water is available which makes the porosity higher in that region. A higher porosity will give higher thickness of layer.

Therefore, the change in mass of pellets in each layer is calculated by using chemical model. The changing mass of pellets changes the thickness of each layer and the number of pellets in each layer which is calculated in particle bed model. Due to change in pellet size the porosity changes which is described in Hydraulic Fluidization Model (HFM). Figure 8 shows schematic diagram three sub-models and depicts the interrelation of them.

Finally prediction model provides the mixed-effluent CCCP and  $\text{CO}_2$  dose which are the Key Performance Indicators (KPI) for quality check of softening process.

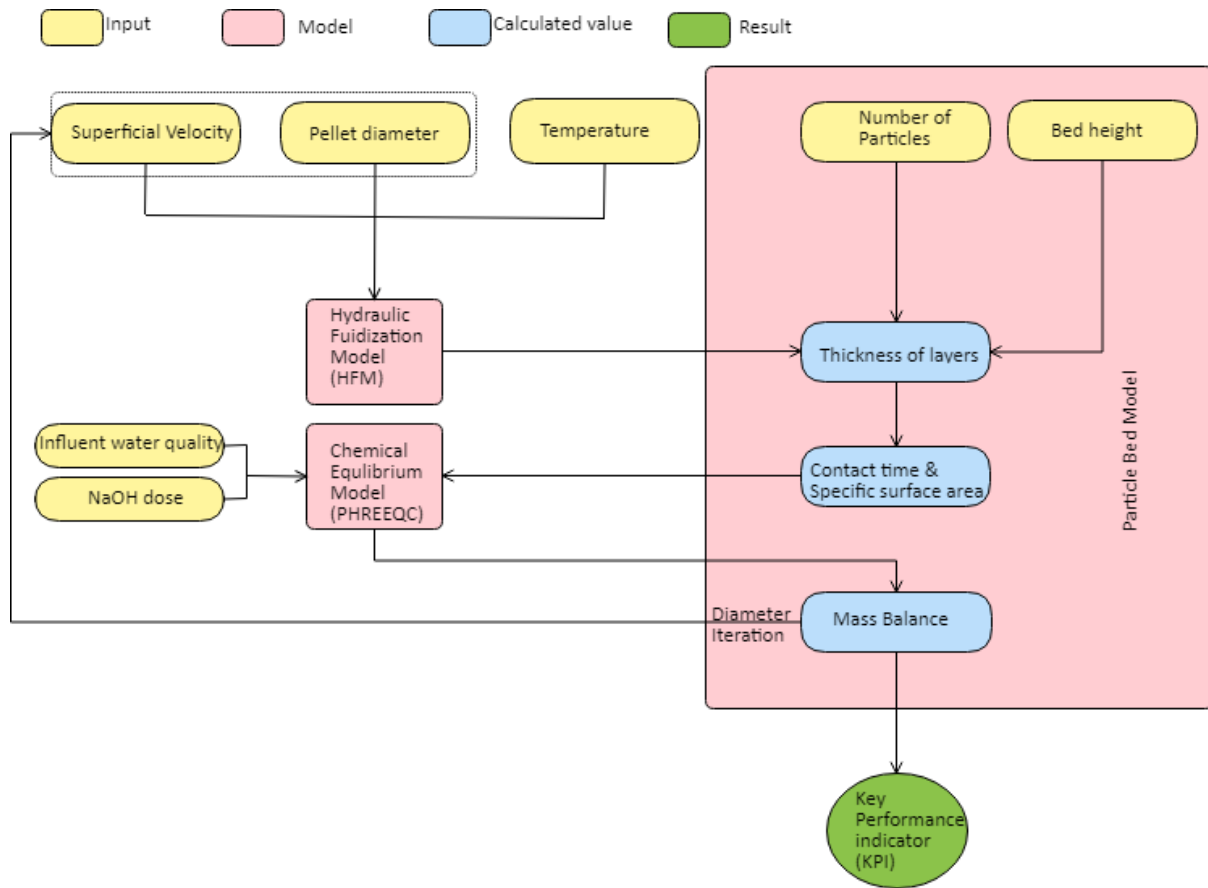


Figure 8 Schematic representation of the 3 sub-models and their relation in the prediction model of the pellet softening process.

In the following sections the components of the prediction model are described.

### 3.1 Chemical equilibrium model

The chemical modeling involves the process of calcium carbonate crystallization which is based on the supersaturation of the calcium carbonate in the water, available crystallization surface and the porosity of the fluidized bed. The chemical model describes the kinetics of the crystallization of calcium carbonate on the pellets in the fluid bed.

#### 3.1.1 Development of calcium carbonate crystallization model

The previous models of pellet softening (van Schagen et al., 2008a, Rietveld, 2005) was based on the mono linear kinetics proposed by Wiechers (Wiechers et al., 1975) where the rate constant is only depended on the temperature.

$$-\frac{dCa}{dt} = k_{w,T} * C * [(Ca^{2+})(CO_3^{2-}) - K_{sp}] \quad (21)$$

$$k_{w,T} = 0.0255 * 1,053^{(T-20)} \quad (22)$$

Here,  $dCa/dt$  is the rate of total calcium concentration reduction ( $\text{mol L}^{-1} \text{s}^{-1}$ ).  $k_{w,T}$  is a temperature dependent constant ( $\text{L mol}^{-1} \text{s}^{-1} \text{L mg}^{-1}$ ),  $C$  is the concentration of the seeding material in  $\text{mg/L}$ ,  $T$  is the temperature in  $^{\circ}\text{C}$ ,  $(\text{Ca}^{2+})$  and  $(\text{CO}_3^{2-})$  are the activities of calcium and carbonate ions in  $\text{mol L}^{-1}$ ,  $K_{sp}$  is the solubility product.

Van Dijk and Wilms used similar kinetics of Wiechers to model crystallization of calcium carbonate inside a pellet softening bed reactor (van Dijk and Wilms, 1991). The kinetic equation used in this research is as follows:

$$-\frac{dCa}{dt} = k_T * SSA_r * [(\text{Ca}^{2+})(\text{CO}_3^{2-}) - K_{sp}] \quad (23)$$

Where  $dCa/dt$  is the calcium carbonate crystallization rate ( $\text{mol L}^{-1} \text{s}^{-1}$ ),  $k_T$  is a temperature dependent constant ( $\text{L mol}^{-1} \text{L m s}^{-1}$ ),  $SSA_r$  is the specific surface area  $\text{m}^2/\text{m}^3$ ,  $(\text{Ca}^{2+})$  and  $(\text{CO}_3^{2-})$  are the activities of calcium ( $\text{mol/L}$ ) and carbonate ions and  $K_{sp}$  is the solubility product. Unlike Wiechers, Dijk and Wilms used specific surface area  $SSA_r$  instead of concentration of seeding material. The equation for  $SSA_r$  is:

$$SSA_r = \left( \frac{6(1-p)}{d_p} \right) \quad (24)$$

Here,  $p$  is porosity of fluid bed and  $d_p$  is the diameter of the pellets.

In 2008, Van Schagen also used similar yet modified equation as Wiechers model to predict calcium carbonate crystallization rate taking into account the diffusion transport (van Schagen et al., 2008a, Van Schagen et al., 2008b). The equation he used:

$$-\frac{dCa}{dt} = \frac{k_{w,T} * k_f}{k_{w,T} + k_f} * SSA_r * [(\text{Ca}^{2+})(\text{CO}_3^{2-}) - K_{sp}] \quad (25)$$

Where the  $dCa/dt$  the calcium carbonate crystallization ( $\text{mol L}^{-1} \text{s}^{-1}$ ),  $k_{w,T}$  is a temperature dependent constant ( $\text{L mol}^{-1} \text{L m s}^{-1}$ ),  $k_f$  is the transportation coefficient which is defined by the equation:

$$k_f = \frac{S_h * D_f}{d_p} \quad (26)$$

Where  $S_h$  was the Sherwood number,  $D_f$  is the diffusion coefficient and  $d_p$  is the diameter of the pellets. Coefficient  $k_f$  is used to anticipate the flow conditions inside the reactor. This is the existing model used in both Water treatment plant WPK and LDN.

Later on, Eleftheria Chiou (2017) and Sergej Seepma (2018) came up with bilinear kinetics which describes the rate of calcium carbonate crystallization better. The bilinear kinetics depends on

two rate constants ( $k$  values) for different supersaturation level. For higher supersaturation, there exists a high rate constant ( $k_H$ ). When the supersaturation is lowered the rate of calcium carbonate crystallization follows a different rate constant which is designated as low rate constant ( $k_L$ ). The changing point (CP) from high rate constant to low rate constant also depends on temperature. For higher temperature, changing point is lower than for lower temperature.

The proposed equation (Chiou, 2018):

$$-\frac{dCa}{dt} = k_i * K_{sp} * SSA_w (SR - A_i) \quad (27)$$

$dCa/dt$  is the calcium carbonate crystallization rate ( $\text{mmol L}^{-1} \text{s}^{-1}$ ),  $SR$  is the calcite saturation ratio,  $SSA_w$  is the specific surface area ( $\text{m}^2/\text{m}^3$ ,  $k_i$  is the rate constants depending on the region of high or low crystallization rate.  $A_i$  is the intercept of high rate and low rate constant line. For low rate constant line is  $A_L = 1$ . The shift from high rate constant to low rate constant is the changing point in saturation ratio which is given by the intersection of the two line and calculated by the following equation:

$$SR_{CH} = -\frac{k_L - A_H * k_H}{k_L - k_H} \quad (28)$$

$A_H$  is the intercept of the high rate constant line.

The specific surface area ( $SSA_w$ ) per volume of water is calculated by the given equation:

$$SSA_w = \frac{\left(\frac{6(1-p)}{d_p}\right)}{p} \quad (29)$$

Where  $p$  is the porosity of the fluid bed and  $d_p$  is the diameter of the pellet. In order to compare the  $SSA_r$  in a pellet reactor with the surface area in other types of reactors or under different fluidization conditions the specific surface is per volume of water is calculated by dividing  $SSA_r$  with porosity (Eleftheria, 2018).

The equations used in this research for modeling calcium carbonate crystallization are modified from Chiou's proposed one in 2017. The following equations are used for the improved prediction model.

$$-\frac{dCa}{dt} = k_H * K_{sp} * SSA_w (SR - 1) + A \quad (30)$$

$$-\frac{dCa}{dt} = k_L * K_{sp} * SSA_w (SR - 1) \quad (31)$$

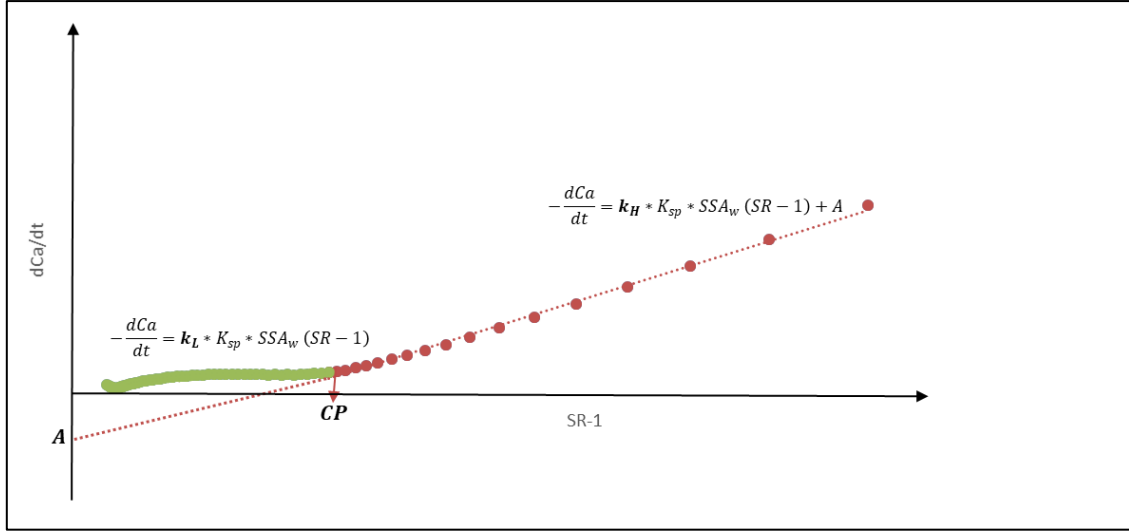


Figure 9 Schematic description of bi-linear calcium carbonate crystallization kinetics. The data points are based on experiment 1.1.

$dCa/dt$  is the calcium carbonate crystallization rate ( $\text{mmol L}^{-1} \text{s}^{-1}$ ),  $SR$  is the saturation ratio of calcite,  $SSA_w$  is the specific surface area per volume of water ( $\text{m}^2/\text{m}^3$ ),  $k_H$  and  $k_L$  are the high and low rate constants respectively and  $A$  is the intercept of the high rate constant line. Equation 30 describes the kinetics for high rate constant which occurs in the high saturation ratio and equation 31 describes the kinetics in low supersaturation. Eleftheria defined the intercept as a function of  $k_H$ ,  $k_L$  and  $SR_{CH}$ . Unlike Eleftheria, the intercept ( $A$ ) of high rate constant line is regarded as an independent parameter which is not a function of  $k_H$ ,  $k_L$  and  $SR_{CH}$  instead, a geometrical value which helps better prediction of the slope of the high rate line. For the low rate line, the interception is excluded as it is assumed that eventually it will go to zero saturation if enough time is allowed for water to stay in the reactor. In Figure 9 the red and green line shows the high and low crystallization rate line respectively. The changing point in saturation ratio (CP) from high rate to low rate is chosen based on the experimental values as its highly depended on the temperature and influent water quality.

In each layer, the change of M-alkalinity, ionic strength and accumulated calcium on pellets is given by the combination of one directional water flow ( $X_w$ ) (Figure 7) through reactors and crystallization of calcium carbonate (van Schagen et al., 2008a). The mass balance over one layer is given as follows:

$$\begin{aligned}
 p_n A_r \Delta L_n \frac{d[Ca^{2+}]_n}{dt} &= X_w ([Ca^{2+}]_{n-1} - [Ca^{2+}]_n) - A_r \Delta L_n \frac{dCa}{dt} \\
 p_n A_r \Delta L_n \frac{dM_n}{dt} &= X_w (M_{n-1} - M_n) - 2A_r \Delta L_n \frac{dCa}{dt} \\
 p_n A_r \Delta L_n \frac{dP_n}{dt} &= X_w (P_{n-1} - P_n) - A_r \Delta L_n \frac{dCa}{dt} \\
 p_n A_r \Delta L_n \frac{dIS_n}{dt} &= X_w (IS_{n-1} - IS_n) - 2A_r \Delta L_n \frac{dCa}{dt}
 \end{aligned} \tag{32}$$

When caustic soda is dosed with a flow of  $X_{NaOH}$  at the bottom of the reactor, the M and P alkalinity and ionic strength are calculated by given mass balance equation.

$$\begin{aligned}
 M_{Bottom} &= (M_{raw}X_w + [OH^-]X_{NaOH}) / (X_w + X_{NaOH}) \\
 P_{Bottom} &= (P_{raw}X_w + [OH^-]X_{NaOH}) / (X_w + X_{NaOH}) \\
 IS_{Bottom} &= (IS_{raw}X_w + 0.5[OH^-]X_{NaOH}) / (X_w + X_{NaOH})
 \end{aligned}
 \tag{33}$$

The amount of crystallized material in a layer is given by

$$\frac{dM_{C,n}}{dt} = A\Delta L_n MW_{CaCO_3} \frac{dCa}{dt}
 \tag{34}$$

Here,  $MW_{CaCO_3}$  is the molecular weight of calcium carbonate and  $A_r$  is the are of reactor

### 3.1.2 Final kinetic equations for chemical model

To describe the rate kinetics, the entire chemical reactions are defined in four regions based on saturation ratio and height of the reactor. The previous experiments show that there exists two more region of kinetics in addition to Eleftheria's bi-linear kinetics. In the first 10 centimeter of the reactor, due to rapid mixing, there exists a high crystallization rate zone, even higher than  $k_H$  and after low crystallization rate zone there even exists an extremely slow crystallization rate lower than  $k_L$ .

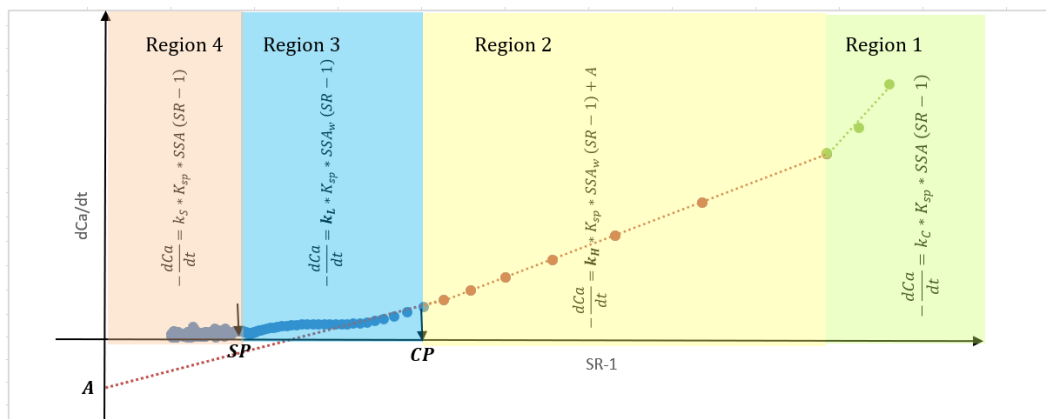


Figure 10 Schematic description of 4 regional calcium carbonate crystallization kinetics.

**Region 1:** At the bottom 10 centimeters of the reactor the NaOH and the incoming raw water jet mix properly due to the turbulence. Therefore it is considered as the CSTR and the rate constant ( $k_C$ ) used in this region is taken from the CSTR experiments (Table 2). In Figure 10, the green zone designates the region 1 with higher rate constant.

**Region 2:** After approximately 10 centimeters of rapid mixing a region (0.1-0.5 m of the reactor), the reactor acts as a PFR. But the driving force is still high in this region. Therefore a higher rate constant ( $k_H$ ) is considered.  $k_H$  and intercept A are taken from PFR experiments (Table 1). In Figure 10 the yellow zone shows region 2.

**Region 3:** In this region (between 0.5-2 m of the reactor) the reactor is considered PFR with a lower driving force. So, a low rate constant ( $k_L$ ) is used to describe the kinetics in this region. In Figure 10 CP designates the saturation ratio border between high and low rate region. The rate constants used here are also based on PFR experiments (Table 1). This region continues until there a dead-end slow zone occurs. The border between low rate zone and dead-end slow zone is called Sleeping point (SP). SP and CP both depend on the temperature of the water and incoming raw water quality. In Figure 10, blue zone is region 3.

**Region 4:** Finally, a region (2-4 m) with dead-end slow zone or metastable zone ( $k_S$ ) is considered where basically no change in saturation ratio occurs with time. If the water in the reactor has a higher residence time, the saturation ratio will eventually go to one. To incorporate this region in the model, a rate constant is considered which is  $1 \times 10^3 - 2 \times 10^3$  times smaller than the low rate constant ( $k_L$ ). This dead-end slow rate is taken into account to describe the entire kinetics in the reactor as experiments evidently show that there is a dead-end slow zone at very low supersaturation level. Pink zone in Figure 10 shows region 4.

In the chemical kinetics model, the height of the regions is established precisely by the level of supersaturation, temperature and contact time. Experimental data used to determine the rate constants ( $k_C, k_H, k_L$  and  $k_S$ ) for these four-regions (Seepma, 2018).

The rate equations used in the prediction model for this research are as follows:

$$\begin{aligned}
 \text{Region 1: } & -\frac{dCa}{dt} = k_C * K_{sp} * SSA_W (SR - 1) \\
 \text{Region 2: } & -\frac{dCa}{dt} = k_H * K_{sp} * SSA_W (SR - 1) + A \\
 \text{Region 3: } & -\frac{dCa}{dt} = k_L * K_{sp} * SSA_W (SR - 1) \\
 \text{Region 4: } & -\frac{dCa}{dt} = k_S * K_{sp} * SSA_W (SR - 1)
 \end{aligned} \tag{35}$$

Figure 11 shows the schematic of these four region of kinetics in a pellet reactor.

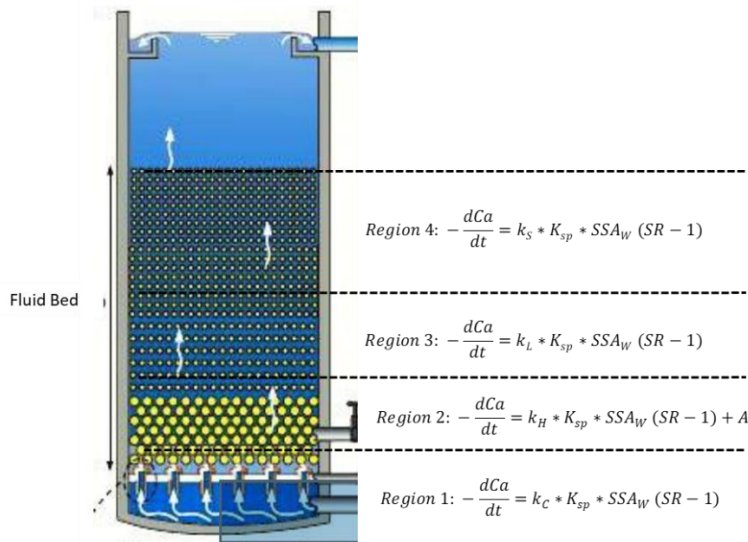


Figure 11 Four kinetic regions in the pellet reactor

### 3.1.3 Chemical modeling in PHREEQCXCEL

The chemical equilibrium model is developed in PHREEQCXCEL, is a computer program to perform a wide variety of aqueous geochemical calculations (Parkhurst and Appelo, 2013). The database used in PHREEQCXCEL is stimela.dat which is established on PHREEQC.dat database (de Moel et al., 2013)

The following steps in the model are carried out with the aid of PHREEQCXCEL and comprise all the chemistry in the previous section. The prediction model is divided into 20 layers and in total 29 simulations are done estimate CCCP after bypass water mixing and required CO<sub>2</sub> dose for conditioning of softened water. Figure 12 gives a schematic representation of the steps performed in PHREEQCXCEL followed by a short description of each simulation step.

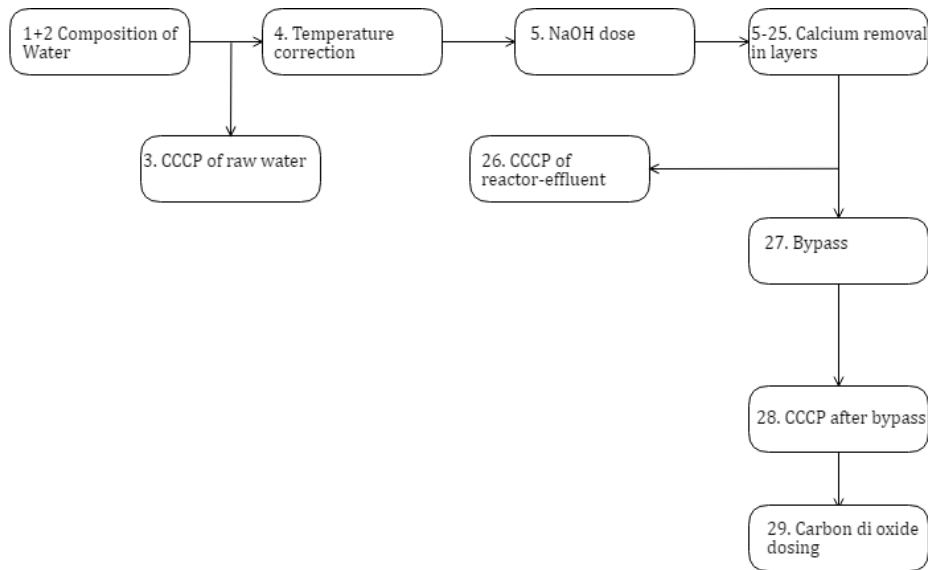


Figure 12 Schematic overview of the simulations carried out in PHREEQCXCEL.

First of all, in simulation 1, the incoming water quality is defined. In Appendix 5, the raw water quality input tab is shown. Next, in simulation 2 – reduction potential (pe) is calculated using redox equilibrium.

In the next step, the CCCP of raw water is determined by describing the equilibrium state in simulation 3. The same equilibrium simulation is carried out also in simulation 26 and 28 in order to determine the CCCP reactor-effluent (CCCP after 20 layers) and after bypass water mixing. The model assumes a theoretically precipitated calcium carbonate in the crystal form of calcite.

In simulation step 4, the temperature correction is done. This step is important if the raw water and experimental temperature is not same. In that case, PHREEQCXEL recalculates all the SI, chemical compositions of all the ions and pH at the experimental temperature.

In the next step, simulation is carried out for the dosing of NaOH solution. The composition of the water after dose is the starting point for the hardness reduction in the reactor. Subsequently, the 20 layers are addressed by simulation 6-24. In these 20 steps kinetics of CaCO<sub>3</sub> crystallization is described by 3.1.2. The porosity, particle diameter and contact time between water and seeding material need to be known which are given by the HFM and particle bed model.

In this model, it is assumed that all of the calcium carbonate is crystallized to the calcite pellets only, and that there is no spontaneous precipitation takes place in the water phase. In each layer the calculation shows the decrease in calcium content and at the end the overall decrease in calcium known.

In simulation 27, the composition is calculated after bypass. The softened water is mixed with a fraction ranging from 0 to 40% of the non-softened raw water.

In simulation 29, the CO<sub>2</sub> dose is calculated for conditioning of softened water to bring the SI to zero.

## **3.2 Particle bed model**

The particle bed model is based on the number and size of particles in each layer. The entire particle bed is based on 20 layers as after 7 layers the effects of diffusion is independent of the number of layers, so the reactor acts like a PFR (Van Schagen et al., 2008b). Stepwise development of the particle bed model can be found from sections 3.2.1 to 3.2.4.

### **3.2.1 Choice of initial diameter per layer**

The starting point of the particle bed model is to define the initial particle diameter for each layer. There are three choices for initial diameter. In Figure 13 (left), three initial diameter profiles in 20 layers are shown. Due to using NaOH as dosing chemical, the adopted profile (red line in Figure 13) has a preference as the initial diameter profile in the particle bed model. Linear initial diameter profile (blue line) is not achievable as due to high supersaturation at the bottom of the reactor, the bottom layers are the most kinetically active layers and there will be high rate of CaCO<sub>3</sub> precipitation. Therefore the initial diameters of pellets at the bottom layers will be much larger than the top layers. So, the initial diameters will not follow a linear trend from bottom to the top of the reactor. The third profile (red line) more likely occurs when the dosing chemical is lime (Ca(OH)<sub>2</sub>), as first lime will dissolve in the water and then will react with present calcium in

the water. So, in that case, the initial diameters will be similar in the first 5-7 layers. Then the size of pellets will reduce.

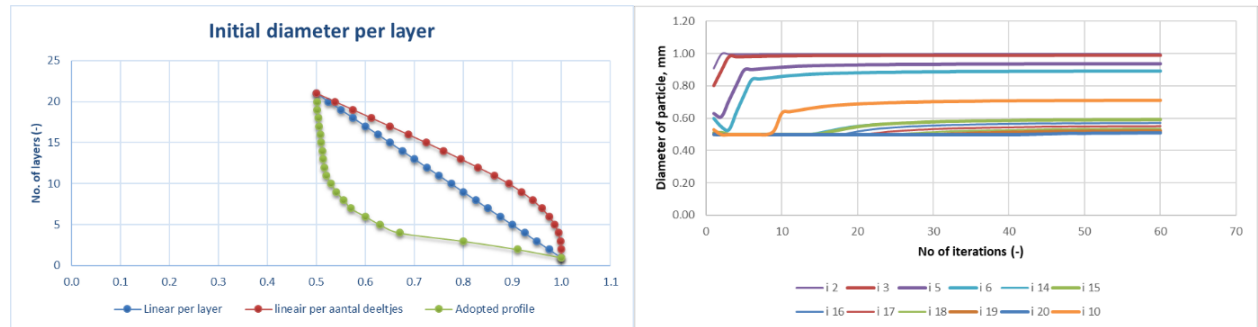


Figure 13 Profiles of initial diameter per layer (left) and initial diameter in different iteration (right).

To have a stable profile for diameters in each layer, 60 iterations are chosen. Figure 13 (right) it is evident that mostly after 30 iterations, the profiles are quite stable. Choosing 60 iterations is a conservative approach.

### 3.2.2 Total number of particles in a fluid bed

A total number of particles ( $N_T$ ) in the fluidized bed depends on the initial particle diameter in each layer and fluidized bed height. Porosity is a function of fluidized bed height. After each iteration, with a new porosity in each layer coming from HFM (section 3.3) and chemical model (section 3.1), the initial number of particles will change to have a mass balance of zero. The change in porosity is derived from the chemical model that describes the kinetics in four regions of the reactor and a data-driven porosity model.

### 3.2.3 Contact time

Contact time between water (mixed with NaOH) and seeding material is the important parameter in the model because it connects the chemical and hydraulic model. In order to materialize the chemical reactions between  $\text{Ca}^{2+}$  and  $\text{CO}_3^{2-}$  in each layer, contact time needs to be defined in PHREEQCXCEL. As the total number of particles after each iteration is calculated as mentioned in section 3.2.2, a relative number is incorporated in each layer classifying how kinetically active that layer is. For example, the bottom layers are more kinetically active, as the supersaturation level in those layers is higher. In addition, the diameter of the seeding materials are larger due stratification of the fluidized bed and causes a smaller preferential flow path. So, a lower relative number would represent that layer distinctly. Furthermore, if the relative numbers are not mentioned in each layer, higher contact time will be incorporated in the bottom layers which is not representative. In Appendix 1 relative number used in each layer is presented.

The Number of particles for each layer  $N_p$  is calculated by multiplying the relative number in each layer by the total number of particles  $N_T$ .

$$N_p = \text{Relative number} * N_T \quad (36)$$

The total volume of particles in each layer ( $V_p$ ) is calculated by the following equation:

$$V_P = \frac{\pi * d_p^3}{6} * N_P \quad (37)$$

Here  $d_p$  denotes the diameter of pellets in each layer.

The total volume of water and pellets ( $V_{W+P}$ ) in each layer is calculated dividing  $V_P$  by  $(1-p)$ . Here  $p$  denotes porosity in each layer (section 3.1.2.2).

$$V_{W+P} = \frac{V_P}{(1-p)} \quad (38)$$

As the entire model is based on per unit square meter of water volume, so  $V_{W+P}$  is also the thickness of each layer ( $H$ ).

Only water volume per layer is calculated as follows:

$$V_W = V_{W+P} - V_P \quad (39)$$

Empty Bed Contact Time ( $EBCT$ ) is the time during water to be treated is in contact with the treatment medium in a reactor. It is assumed all liquids pass through the reactor at the same velocity. Calculated by using the following equation:

$$EBCT = \frac{H}{v_s} \quad (40)$$

Here  $v_s$  represents the flow velocity of water in the reactor in  $\text{ms}^{-1}$

Therefore, the real contact time ( $t_{real}$ ) in seconds between water and calcite pellets is given by

$$t_{real} = \frac{EBCT}{p} \quad (41)$$

The thickness,  $H$  of each layer is a function of porosity,  $p$ , equation (40). Contact time, equation (41), is estimated depending on the thickness of each layer. So basically, thickness and contact time of each layer changes proportionately based on porosity in different scale of reference. That can be seen in Figure 14.

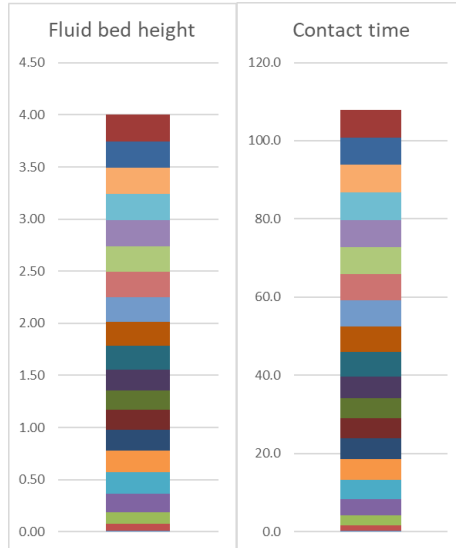


Figure 14 Fluid bed height in m (left) and reaction time in seconds in each layer (right) for a simulation with  $C_{ain}= 1.9 \text{ mmol/L}$ ,  $T= 20 \text{ }^\circ\text{C}$ ,  $v= 80 \text{ mh}^{-1}$ ,  $L= 4\text{m}$  and  $\text{NaOH dosing}=1.3 \text{ mmol/L}$  for 20 layers.

So, the contact time in each layer changes proportionately with the thickness in the fluid bed. The thickness of the fluid bed in each layer is depended on the porosity of that layer. Figure 14 the different color defines the thickness of each layer. The thickness of the first layer is the smallest, and that is defined by assigning a lower relative number to that layer. Correspondingly, the contact time of that layer is also the shortest. So the kinetic reaction in that first layer will occur in a very short period of time (1-5 seconds). This represents the full-scale reactor scenario. As at the bottom of the reactor, due to higher supersaturation, the reaction rates are higher than in the higher region of the reactor. Therefore, the contact time is the link in the prediction model that connects the chemical equilibrium model (PHREEQCXEL), particle bed model and the HFM. This is also described schematically in Figure 8.

### 3.2.4 Change of diameter in each layer

In this section, the process of estimating the change in diameter in each layer is described.

At first, Specific Surface Area ( $SSA_w$ ) is calculated using equation (29) and a total area of pellets ( $A_T$ ) are calculated as follows:

$$A_T = N_p * A_p \quad (42)$$

Here  $A_p$  is the available crystallization area of one pellet in a layer assuming a spherical shape and  $N_p$  is the number of pellets in each layer.

After each iteration, the total amount of calcium in each layer changes which is calculated by PHREEQC. So, the change in the amount of calcium ( $d_{Ca}$ ) in consecutive two layers is determined by the following equation.

$$d_{Ca} = Ca_n - Ca_{n+1} \quad (43)$$

Here,  $n$  and  $n + 1$  are two consecutive layers.

After that, the amount of precipitated calcium or velocity of transportation ( $v_p$ ) in  $\text{kgs}^{-1}$  in each layer is calculated by the following equation:

$$v_p = d_{Ca} * MW_{CaCO_3} * v * \rho_W * t_{real} \quad (44)$$

Here  $\rho_W$  is the density of water.

The volume of precipitated calcium in each layer can be calculated dividing  $v_p$  by density of the calcium carbonate pellets and contact time in that layer.

$$\text{Volume of deposited calcite} = v_p / \rho_C * t_{real} \quad (45)$$

Here  $\rho_C$  is the density of the calcite pellets and  $t_{real}$  is in days.

So, the discharge of pellets per day can be estimated by the following equation:

$$\text{Discharge of number of pellets per day} = \frac{\sum \text{Volume of deposited calcite}}{V_{Pout} - V_{Pin}} \quad (46)$$

Here,  $V_{Pin}$  and  $V_{Pout}$  are the volume of seeding material at top of the reactor and volume of the particle at the bottom layer respectively. So, the number of input and discharged particles remain the same within the reactor, only pellets gain volume due to the softening process. Therefore, the same number of particles are transferring from one layer to another and at the end taken out from the reactors.

Discharge of calcite in volumetric basis per day can be calculated by employing mass balance in consecutive layers.

$$\begin{aligned} \text{Discharge of volume per day} \\ = \text{Discharge of number of pellets per layer} * (V_{P_n} - V_{P_{n+1}}) \end{aligned} \quad (47)$$

Here,  $V_{P_n}$  and  $V_{P_{n+1}}$  denotes the volume of the particles in layer  $n$  and  $n + 1$ .

So, the net pellet volume increase in each layer can be calculated as follows:

$$\text{Net pellet volume increase} = \text{Volume of deposited calcite} - \text{Discharge of volume} \quad (48)$$

Therefore, the volume of individual pellet ( $V_{P_{bal}}$ ) derived from the mass balance in each layer can be calculated as:

$$V_{p_{bal}} = \text{Net pellet volume increase} / \text{Discharge of number of pellets} \quad (49)$$

And finally, pellet diameter can also be calculated.

$$d_{p_{bal}} = \sqrt[3]{6 * V_{p_{bal}} / \Pi} \quad (50)$$

The above equation could also be used as a check for the model. In Appendix 2, the initially adopted diameter profile, profile after 60 iterations and profile calculated based on the mass balance in each layer is presented.

### 3.3 Hydraulic fluidization model

The aim of the Hydraulic Fluidized bed Modeling (HFM) model is to determine the relationship of porosity (bed expansion), pellet diameter, water flow velocity and viscosity of water.

The HFM used in this research is a data-driven model based on experiments conducted in the pilot plant of WPK (Hout, 2016). The input values of the porosity model are the particle diameter, temperature, and water flow velocity. It is assumed that in each layer the particle has the same size. There is still research going on to get a perfect hydraulics model that describes porosity (Kramer, 2016). A proper porosity model lies beyond the scope of the thesis. In Appendix 3, a detailed description of the data-driven porosity model is described.

*To sum up, the improved prediction model has 20 layers describing the entire fluid bed of pellet softening reactor. It has three part: chemical model, particle bed model, and porosity estimation model and these three parts are interconnected in each layer of the model.*

## 4 Calibration

*This chapter describes the calibration of the parameters for the improved prediction model.*

To determine the parameters of the prediction model, it is calibrated with the data available from experiments performed with raw water from drinking water treatment plant at Weesperkarspel (WPK) and at Leiduin (LDN) of Waternet. Afterward, the calibrated model parameters are validated with previous experiments (Schooten, 1985, Schetters, 2013) and data from full-scale plant at WPK. The objective is to calibrate the crystallization rate constant ( $k_T$ ) and changing point ( $CP$ ) in saturation ratio ( $SR$ ) from high rate constant to the low rate constant. A third temperature dependent parameter is also calibrated which is called the sleeping point ( $SP$ ), a point where the change in saturation ratio with time is almost zero. Only the chemical part of the model is calibrated. The hydraulic part is adapted from ongoing research on Hydraulic fluidization model (HFM) (Kramer, 2016).

### 4.1 Pilot-Scale experiments

The first model calibration is done with the data from CSTR and PFR experiments. In the CSTR experiments homogeneous mixing eliminates the effect of diffusion. Whereas, in the PFR experiments there is no mixing in the axial direction. The experimental data used in this research are taken from previous research (Seepma, 2018). Data from the CSTR and PFR experiments, were processed in PHREEQXCEL in order to get the values of  $k_T$ ,  $CP$  and  $SP$ . In the following section, the materials and method for this research are described.

#### 4.1.1 CSTR Experiments

CSTR experiments were done with WPK raw water before ozonation. 1 L of water and weighted amount of  $\text{CaCO}_3$  Merck powder<sup>4</sup> depending on the experiment's specific conditions were added to the CSTR reactor. CSTR contains RVS agitator<sup>5</sup> attached to RVS lid. Continuous measurement for every second of pH was done using a pH probe<sup>6</sup> connected to the multimeter<sup>7</sup>. The pH probe also measures temperature (accuracy;  $\pm 0.1$  °C). The stirrer was set at about 1000 rpm and 5 mL of 1.46 w/w NaOH was added to the solution. The reactor was sealed in every possible way accepts the ones containing probes in order to minimize the influence of  $\text{CO}_2$ . The time duration for the experiments continued from several minutes to an hour depending upon the amount of Merck powder used for the experiment. The experiments were done at 5°C and 20°C. Relationship between the amount of  $\text{CaCO}_3$  Merck powder and available specific surface area ( $SSA_w$ ) is presented in Appendix 4. The experimental setup is showed in Figure 15.

#### 4.1.2 PFR experiments

PFR experiments were carried out with WPK ozonated raw water in 1- 2 m height transparent PVC columns. A static Kenics mixer was placed to make sure well mixing NaOH and water. The experiments were carried out with WPK water and calcite pellets extracted from full-scale. To represent the first two meters of the real pellet reactor, the calcite pellets were sieved, either 1.00-1.12 mm or 0.80-0.90 mm and weighted each time before adding to the columns.

---

<sup>4</sup> VWR/Boom - calcium carbonate precipitated for analysis EMSURE® Reag. Ph Eur, prod. nr. 1.02066.0250

<sup>5</sup> AVSH - IKA Work Janke & Kunkel blender/mixer type RW 18, serial nr. 21517

<sup>6</sup> WTW - SensoLyt® 900-P, serial nr. C180307013;  $\pm 0.001$  pH-unit

<sup>7</sup> WTW - portable pH meter MultiLine® Multi 3630 IDS

Approximately 1000 L water was kept in a cubic container and flowed with a discharge rate of  $420 \text{ Lh}^{-1}$  resembling a velocity of  $80 \text{ mh}^{-1}$ . With a heater and refrigerator, the temperature of the water in the cubic container could be conditioned from  $0^\circ\text{C}$  to  $40^\circ\text{C}$ . NaOH was dosed with a peristaltic dosing and metering pump<sup>8</sup> having at a certain frequency and volume in a way that the pH at the bottom of the reactor could be established to 10.0. During the experiment, a continuous pH measurement above the bed of fluidized pellets, with an interval of five seconds was logged. Duration of the experiments ranges from 10 to 15 minutes as it is assumed this duration was enough to have a stable fluidized bed to form after calcite pellets addition (Seepma, 2018). The experimental setup is shown in Figure 16.



Figure 15 Experimental setup of the CSTR. The agitator's generator (1) is connected onto the top of the CSTR, which is attached to the RVS agitator (4). The pH and EC probes are then held by arms (2) into the solution. Finally NaOH is added through one of the holes present (3) in the lid and the holes are sealed off accordingly (Seepma, 2018)



Figure 16 Displays the used PFR. Hard water flows in (1) as the valve (2) is turned to a certain discharge, which is read at an venturi meter (5). NaOH is mixed with incoming hard water (7) and goes through a static mixer (4). Finally it is brought via a mixing h (3) into the 1 m column (6) (Seepma, 2018)

<sup>8</sup> IWAKI, EH-B10VC-230PR2

### 4.1.3 Method of parameter calculation with PHREEQCXCEL

The pH data from CSTR and PFR experiments were transferred with PHREEQCXCEL via PHREEQC environment. The raw water qualities (temperature, pH, EC alkalinity, etc.) were obtained from the web-queries which is linked to inline measurements for the specific date and time of the experiments. After that, the obtained parameters were recalculated with PHREEQCXCEL with experimental temperatures (such as 5, 20 and 40°C) as it could lead to slight changes in solubility products, saturation indices and concentrations of different species.

The NaOH was added in the dosing step in the model. There was a time lag of pH measurements with the probe, therefore the initial pH calculated by PHREEQC never matches with logged pH value during the experiments with the same amount of NaOH dosing. So, the first couple of points on pH were not consistent with the experimental value. In that case, a polynomial function (5<sup>th</sup>/6<sup>th</sup> order) was used for those points in a way that the real measurements match smoothly to the polynomial curve. After adjusting the pH, again PHREEQC was run to get the parameters such as Saturation index (SI), Saturation Ratio (SR) of calcite, amount of total calcium in the system ( $Ca_{TOT}$ ), amount of precipitated calcium (CaPrec),  $-pK_{SP}$  and Calcium Carbonate Crystallization Potential (CCCP) and rate of change of total calcium in the system ( $dCa_{TOT}/dt$ ).

To compare the kinetics for different experiments,  $dCa_{tot}/dt$  were plotted against Saturation ratio (SR) of calcite and two rates were found in each case with a point in saturation ratio at which the rate deviates. The graph is plotted on SR-1 to get an equation that goes to zero. Figure 17, the rate deviates at 40 (SR-1). By using linear regression equation of these graphs  $k_T * K_{SP} * SSA_W$  values were obtained. Ultimately the  $K_{SP}$  (temperature dependent) and  $SSA_W$  (knowing the  $d_{50}$  of pellets/Merck powder and porosity) for each experiment were known. So, the kinetic rate constant  $k_T$  was calculated. The intercept A is also taken from the high rate kinetics line.

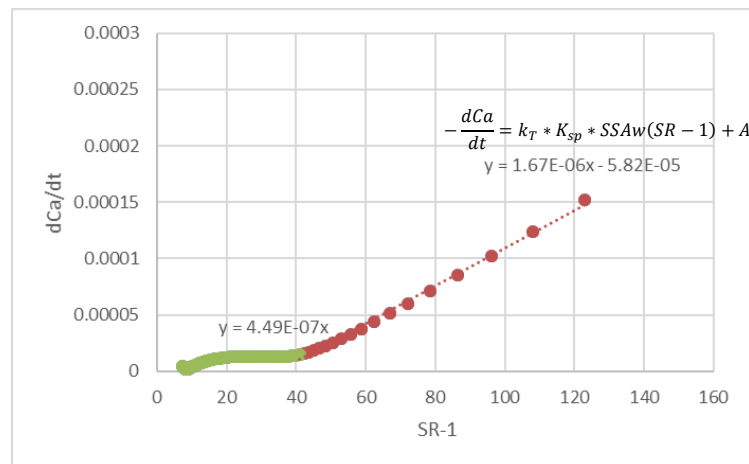


Figure 17  $dCa_{tot}/dt$  plotted against (SR-1) of calcite to calculate model parameters from experiment 1.1 (Table 1)

## 4.2 Calibration

The calibration of the layers model is done in different approaches. First, the model is calibrated with the experimental values from Seepma's research to witness if the same pH profile can be

recalculated (Seepma, 2018). Secondly, the model is calibrated with the experiments done by the previous researches (Schooten, 1985, Schetters, 2013) at different temperature. The final calibration is done with the full-scale plant data. In the following sections, the approaches of model calibration are explained.

## 4.2.1 Selection of experiments for calibration

Starting values for the parameters used in chemical model is based on Seepma's experiments (Seepma, 2018). The experiments were chosen based on temperature primarily. The source water is surface water and there exist temperature variations all around the year. Therefore, the model should be calibrated for a wide range of temperatures to predict the softening process. In addition, the full-scale plant has  $SSA_w$  ranging between 4000-6000  $m^2/m^3$ , so the selected experiments also have a  $SSA_w$  in that range. The list of selected experiments both in PFR and CSTR are listed in Table 1 and Table 2.

*Table 1 PFR experiments used for calibration*

No. of experiment	Temperature (°C)	NaOH dosing (mmolL <sup>-1</sup> )	$SSA_w$ (m <sup>2</sup> m <sup>-3</sup> )
<b>Experiment 1.1</b>	8.5	1.83	4284
<b>Experiment 1.5(LDN)</b>	22	1.50	4839

*Table 2 CSTR experiments used for calibration*

No. of experiment	Temperature (°C)	NaOH dosing (mmolL <sup>-1</sup> )	$SSA_w$ (m <sup>2</sup> m <sup>-3</sup> )
<b>Experiment 50</b>	5.6	1.82	2526
<b>Experiment 29</b>	20	1.82	5052

Three of four experiments were done with WPK raw water. Except for experiment 1.5, which is done with Leiduin (LDN)<sup>9</sup> ozonated raw water as there was a lack of representative PFR experiments with WPK water for higher temperature. The (dCa<sub>TOT</sub>/dt) vs SR-calcite graphs for these four experiments can be found in Appendix 6. Table 3 shows the model parameters obtained from these experiments by following the procedure mentioned in section 4.1.3.

*Table 3 Parameters obtained from the experiments (Seepma, 2018).*

Experiment No	T (°C)	$k_c$ molL <sup>-1</sup> *s <sup>-1</sup> m <sup>3</sup> /m <sup>2</sup>	$k_H$ molL <sup>-1</sup> *s <sup>-1</sup> m <sup>3</sup> /m <sup>2</sup>	$k_L$ molL <sup>-1</sup> *s <sup>-1</sup> m <sup>3</sup> /m <sup>2</sup>	$k_s$ molL <sup>-1</sup> *s <sup>-1</sup> m <sup>3</sup> /m <sup>2</sup>	CP (-)	SP (-)	A (molL <sup>-1</sup> *s <sup>-1</sup> )
<b>Experiment 1.1</b>	8.5	-	0.096	0.026	2.84E-05	40	10	-0.0582
<b>Experiment 1.5 (LDN)</b>	22	-	0.225	0.056	2.84E-05	10	3	-0.0207
<b>Experiment 50</b>	5.6	0.264	-	-	-	-	-	-
<b>Experiment 29</b>	20	0.287	-	-	-	-	-	-

<sup>9</sup> Leiduin (LDN) is another water treatment plant of Waternet. Seepma also did experiments using water taken from Leiduin plant water.

Therefore, the parameters used in the prediction model for two temperature range (Summer and winter) are given in the following table. In the following four calibrations, these parameters are used. When the experiments were conducted in lower temperature (0-12°C), the winter parameters used in the prediction model and when the experiments were conducted in higher temperatures (12-24°C), summer parameters are used in the prediction model.

Table 4 Initial kinetic parameters used in the prediction model.

Experiment No	$k_c$ $\text{molL}^{-1} \text{ *s}^{-1}$ $1 \cdot \text{m}^3 / \text{m}^2$	$k_H$ $\text{molL}^{-1} \text{ *s}^{-1}$ $1 \cdot \text{m}^3 / \text{m}^2$	$k_L$ $\text{molL}^{-1} \text{ *s}^{-1}$ $1 \cdot \text{m}^3 / \text{m}^2$	$k_s$ $\text{molL}^{-1} \text{ *s}^{-1}$ $1 \cdot \text{m}^3 / \text{m}^2$	CP (-)	SP (-)	A ( $\text{molL}^{-1} \text{ *s}^{-1}$ )
Summer	0.287	0.225	0.056	2.84E-05	10	3	-0.0207
Winter	0.264	0.096	0.026	2.84E-05	40	10	-0.0582

#### 4.2.2 Calibration with Seepma's experimental data

The first calibration of prediction model is done with the same experimental raw water quality, temperature, and NaOH dosing. At first the parameters from Table 3 used to get back the same pH profile. Table 5 shows the operational conditions of experiment 1.1 and 1.5.

Table 5 Experimental conditions for experiment no 1.1 and experiment no 1.5

Experiment No	T (°C)	$C_{in}$ (mmol/L)	$V_s$ (m/h)	Fluid bed height m	NaOH dose (mmol/L)
Experiment 1.1	8.5	1.94	80	3.15	1.83
Experiment 1.5	22	1.89	80	3.5	1.5

Figure 18 shows the experimental and model output of the pH profile for experiments 1.1 and 1.5 using the parameter from Table 4. The shape of the pH profiles over the height of the fluid bed of the reactor are almost same.

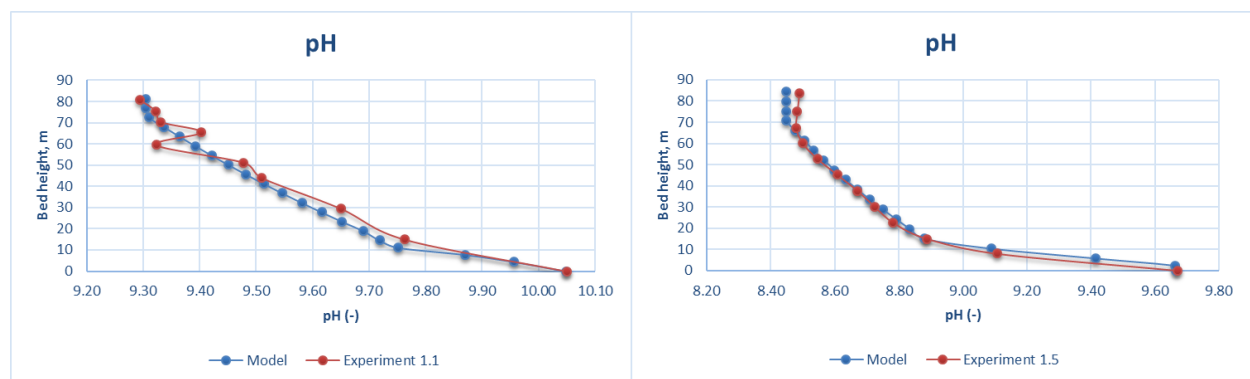


Figure 18 Experimental and model pH profile for experiment 1.1 (left) and experiment 1.5 (right).

The calibrated parameter used to recreate the experimental pH profiles of Seepma's experiments are given in Table 6.

Table 6 Parameters after first calibration

Experiment No	$k_c$ $\text{molL}^{-1} \cdot \text{s}^{-1}$ $1 \cdot \text{m}^3/\text{m}^2$	$k_H$ $\text{molL}^{-1} \cdot \text{s}^{-1}$ $1 \cdot \text{m}^3/\text{m}^2$	$k_L$ $\text{molL}^{-1} \cdot \text{s}^{-1}$ $1 \cdot \text{m}^3/\text{m}^2$	$k_s$ $\text{molL}^{-1} \cdot \text{s}^{-1}$ $1 \cdot \text{m}^3/\text{m}^2$	CP (-)	SP (-)	A ( $\text{molL}^{-1} \cdot \text{s}^{-1}$ )
Summer	0.287	0.225	0.028	2.84E-05	10	3	-0.0207
Winter	0.264	0.096	0.026	2.84E-05	40	10	-0.0582

In the Table 6 it can be seen that for summer, the  $k_L$  value is adjusted to make the pH profile analogous to the experimental pH profile.

### 4.2.3 Calibration with Schooten's experiments

For summer, prediction model is also calibrated with the with experiments done by Schooten (Schooten, 1985). Schooten measured the calcium profile over the height of the reactor (Schooten, 1985). The experimental data is given in the Appendix 7.

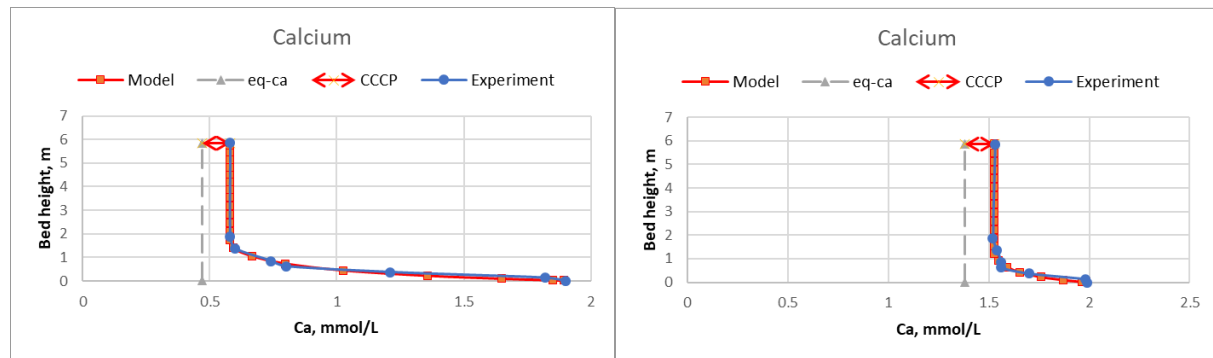


Figure 19 Experimental and modeled calcium content over fluid bed height. Operational conditions:  $c_{in} = 1.99 \text{ mmol/L}$ , temperature = 13.5-15.8°C, Flow = 20-25  $\text{m}^3/\text{h}$ , NaOH dosing = 1.55  $\text{mmol/L}$  (Left figure) and 0.57  $\text{mmol/L}$  (Right figure)

Figure 19 shows the modeled calcium content and the measured calcium content over the height of the fluid bed. To match experimental calcium content, the parameters for summer from Table 6 are adjusted. As these experiments were done in the range of summer temperature (13.5-15.8°C), thus only the parameters for higher temperature can be validated with these experiments. More graphs and experimental conditions are elaborated in Appendix 8. Additionally, it is discovered that the low rate constant ( $k_L$ ) is not pronounced in case of higher temperature. Therefore, the same value for  $k_H$  and  $k_L$  is used for higher temperature. The approximation is also buttressed by research where it has been shown that with the increase of temperature, bi-linear kinetics tends to diminish and a linear rate defines the crystallization (Seepma, 2018). Adjusted parameters are given in Table 7.

Table 7 Calibrated parameters for prediction model in summer

Experiment No	$k_c$ $\text{molL}^{-1} \cdot \text{s}^{-1}$ $1 \cdot \text{m}^3/\text{m}^2$	$k_H$ $\text{molL}^{-1} \cdot \text{s}^{-1}$ $1 \cdot \text{m}^3/\text{m}^2$	$k_L$ $\text{molL}^{-1} \cdot \text{s}^{-1}$ $1 \cdot \text{m}^3/\text{m}^2$	$k_s$ $\text{molL}^{-1} \cdot \text{s}^{-1}$ $1 \cdot \text{m}^3/\text{m}^2$	CP (-)	SP (-)	A ( $\text{molL}^{-1} \cdot \text{s}^{-1}$ )
Summer	0.287	0.089	0.089	2.84E-05	10	3	-0.0207

## 4.2.4 Calibration with Schetters's experiments

The pH measurements done by Schetters (Schetters, 2013) are recreated with the prediction model. In Schetters's research, the first point of pH measurements was erroneous as during the experiments the probe was held really closed to the dosing heads. So, the pH logged with probe gave a higher pH than expected with the amount of NaOH dose. Figure 20 shows the recreated pH profile with model and pH measurements.

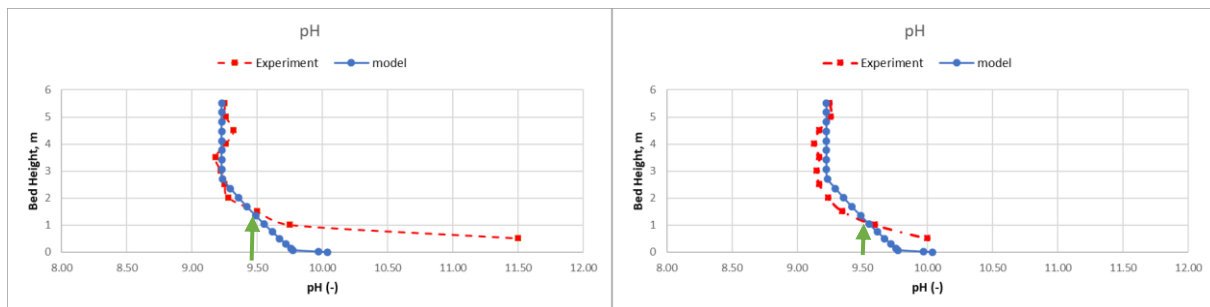


Figure 20 Experimental and modeled pH profile of Marc Schetters's experiments. Operational conditions:  $Ca_{in} = 1.94 \text{ mmol/L}$ , temperature =  $1.5\text{-}3^{\circ}\text{C}$ , Flow =  $5.7 \text{ m}^3/\text{h}$ , NaOH dosing =  $1.76 \text{ mmol/L}$  (Left figure) and  $1.75 \text{ mmol/L}$  (Right figure).

Despite that fact that the pH measurements at the bottom are erroneous, the shape of the pH profile matches modeled pH profile. It's noteworthy that within first one-meter, maximum pH reduction takes place and this shape is consistent with the model output that can be seen in Figure 20. Rest of the graphs along with experimental data can be found in the Appendix 9 and Appendix 10.

Only SP in winter parameters (Table 4) was adjusted to match the pH profile. Six experiments were chosen from Schetters experiment and a range of SP (8-10) could fit them better. Adjusted parameters are listed in Table 8.

Table 8 Calibrated parameters for prediction model in winter

Parameter	$K_c$ $\text{mOLL}^{-1} \text{ *s}^{-1}$ $1 \text{ *m}^3/\text{m}^2$	$K_H$ $\text{mOLL}^{-1} \text{ *s}^{-1}$ $1 \text{ *m}^3/\text{m}^2$	$K_L$ $\text{mOLL}^{-1} \text{ *s}^{-1}$ $1 \text{ *m}^3/\text{m}^2$	$K_s$ $\text{mOLL}^{-1} \text{ *s}^{-1}$ $1 \text{ *m}^3/\text{m}^2$	CP (-)	SP (-)	A (-)
Winter	0.268	0.096	0.026	2.84E-05	40	8-10	-5.82E-02

## 4.2.5 Re-calibration with full-scale for winter

As the winter parameter calibration was not entirely accurate due to the erroneous measurements of bottom pH of Schetters's experiments, therefore, the parameters for winter in Table 8 are recalibrated with full-scale plant measurements.

A month in severe winter in 2016 is chosen for calibration. As there are no direct measurements of CCCP available in the full-scale plant, therefore acid dosing for conditioning the softened water gives an estimation of overall CCCP from 8 reactors. As it is discovered in section 4.2.4 that for lower temperature, SP is more sensitive to the model outcomes than the rate constants ( $k_T$ ) and

CP. So, for re-calibration, only SP is adjusted to match the real-plant measurements. Figure 21 shows model output for 2 sets of CP and SP (CP=40,SP=10 and CP=40,SP=80), and evidently, CP=40, SP=10 gives closer value to average CCCP of 8 reactors. It is worth mentioning that the indicated HCl dose in the figure is the required amount of acidity to have a water of SI=0 for next treatment unit. Calcium and HCl react in equimolar basis. So, 1 mmol/L of calcium/CCCP is equivalent to 1 mmol/L HCl. In 2016, the conditioning of softened water was still done with HCl. In August 2017, it switched from HCl and CO<sub>2</sub>.

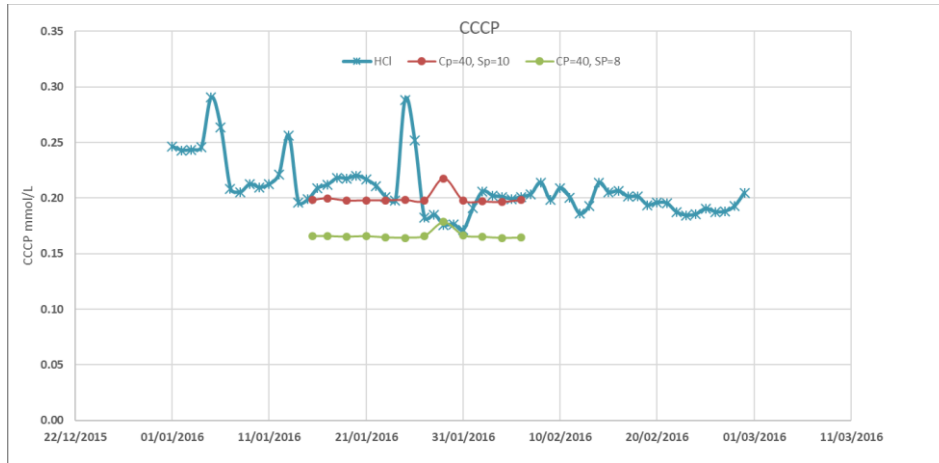


Figure 21 Average HCl dose from WebQuery for full-scale and modeled CCCP with different CP and SP value

In Table 9, final calibrated parameters are presented for layers model for two temperature range.

Table 9 Final calibrated parameters for prediction model of summer and winter.

Parameter	$K_C$ $\text{molL}^{-1} \cdot \text{s}^{-1} \cdot$ $1 \cdot \text{m}^3 / \text{m}^2$	$K_H$ $\text{molL}^{-1} \cdot \text{s}^{-1} \cdot$ $1 \cdot \text{m}^3 / \text{m}^2$	$K_L$ $\text{molL}^{-1} \cdot \text{s}^{-1} \cdot$ $1 \cdot \text{m}^3 / \text{m}^2$	$K_S$ $\text{molL}^{-1} \cdot \text{s}^{-1} \cdot$ $1 \cdot \text{m}^3 / \text{m}^2$	CP (-)	SP (-)	A (-)
<b>Summer</b>	0.284	0.089	0.089	2.84E-05	10	3	-2.07E-02
<b>Winter</b>	0.268	0.096	0.026	2.84E-05	40	10	-5.82E-02

Among the calibrated parameters, CP and SP are the most important ones as the model outcomes are highly dependent on these two. In summer  $k_H$  and  $k_L$  have same values indicate higher efficiency of the reactor. Whereas, in winter  $k_H$  is almost 4 times higher than  $k_L$ . Since in winter reactions are slower than summer a high rate constant region occurs for shorter time duration and it goes to the rate of 4 times lower faster. The  $k_C$  for both temperatures has similar value, as the temperature dependency is not that dominant when there is rapid mixing.

## 5 Validation

*This chapter represents the validation of the improved model for two separate range of temperature. The measurement data are obtained from web-queries<sup>10</sup>. The validation is done on Total Hardness (TH) and acidity(pH).*

The calibrated model is used for replicating the full-scale with the same raw water qualities obtained from web-queries. January and July in 2018 are chosen as the time period for validation of the prediction model. The kinetic parameters used in the model are described in Table 9. The diameter of average (operational) pellets at the bottom of the reactor are 1.0 mm and 0.5 mm ( $d_{50}$  of crushed calcite) at the top. The validation is done with 0% bypass, as only the value from reactors are compared to validate the model. From the web-queries, the data (TH, pH) for each reactor is available.

### 5.1 Method of validation

Validation of the model is done for two range of temperatures. For low-temperature range, the month of January in 2018 is chosen. For higher temperature range, July 2018 is chosen as the time period.

The validation is done on a single full-scale reactor. First, the model input parameters such as concentrations of Ca, Mg,  $\text{HCO}_3^-$ , NaOH dose, temperature, total water flow in reactor and pH of incoming water for a particular day in that one-month period are obtained from web-queries. Outputs (TH, pH) from the model are compared with the measurements from Web-queries. For validation, CCCP is not taken as a parameter since there is no direct measurement for it. The CCCP can be estimated from the  $\text{CO}_2$  dose for conditioning of softened water. But there are only two  $\text{CO}_2$  dose measurements for two streets (two streets contain the softened water from 8 reactors). Therefore, the model is only validated for TH and acidity (pH).

### 5.2 Validation on the total hardness

The total hardness measurements and modeled value shows a good fit (Figure 22 and Figure 23). The abrupt changes in some part of the graph in full-scale plant measurements both in winter and summer are due to erroneous data logging. A hardness of 3 mmol/L in winter is not possible as the incoming water has a hardness in the range of 1.8-2.2 mmol/L (Figure 22). So, these values can be considered as outliers.

---

<sup>10</sup> *Inline measurements of the Process, laboratory and manual data stored in the database called PIMS (process information management system)*

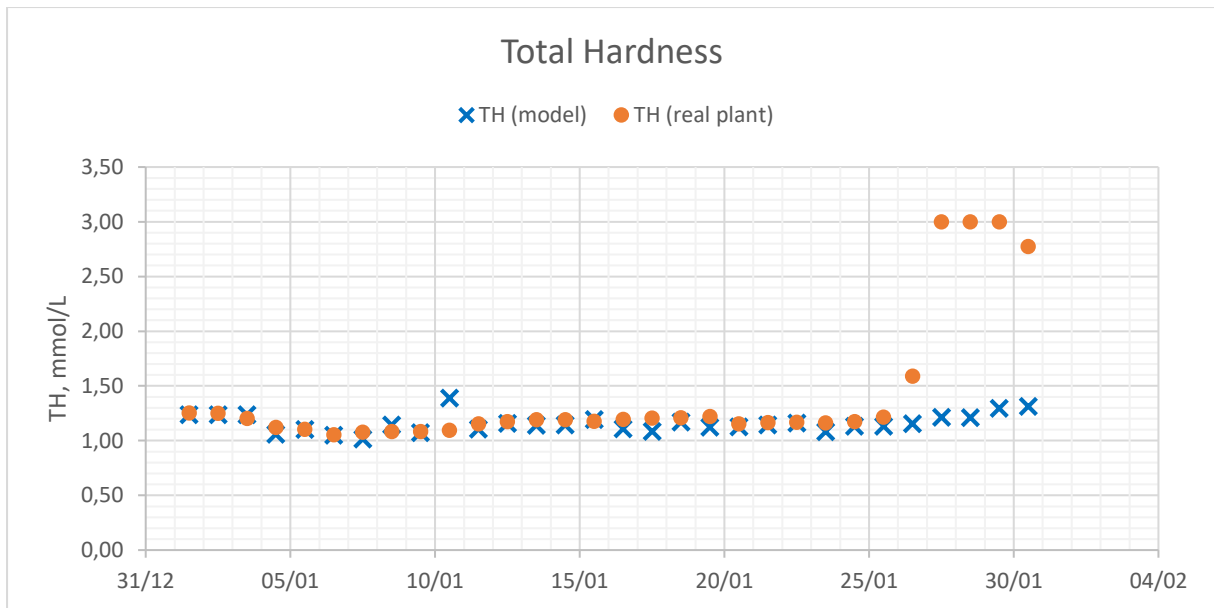


Figure 22 Modeled and full-scale total hardness measurements for the month of January in 2018. Temperature range 4-6°C.

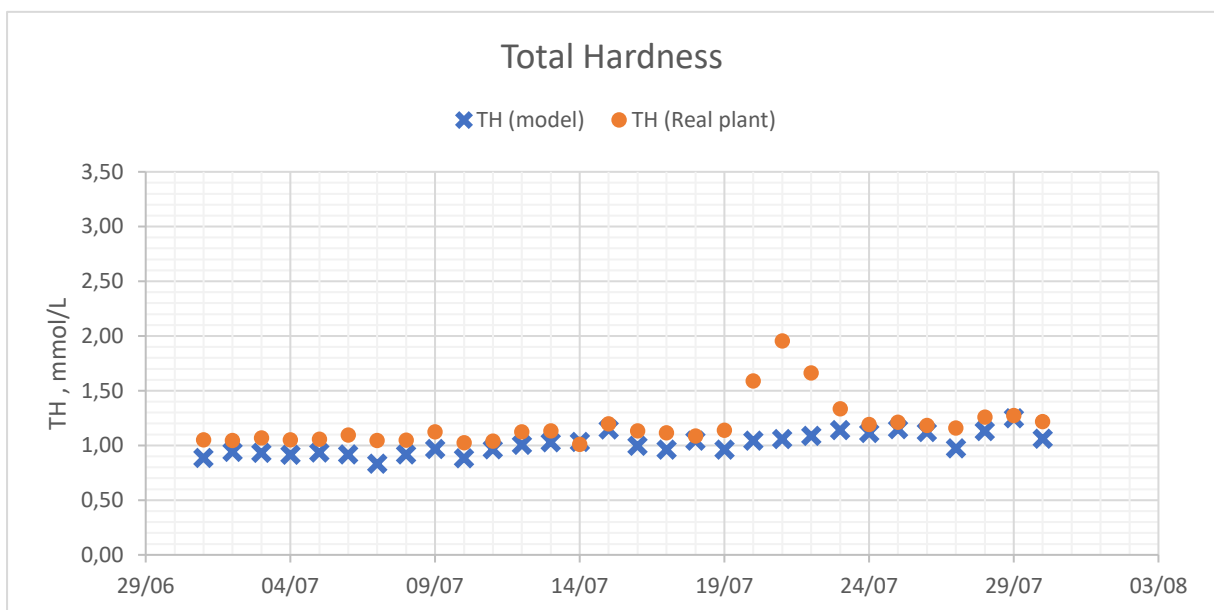


Figure 23 Modeled and full-scale total hardness measurements for the month of July in 2018. Temperature range at 18-23°C.

### 5.3 Validation on pH

The predicted pH with the model shows some deviation from the measurements. The pH on the top of the reactor is measured on a certain point. If NaOH is not mixed well in the reactor, it can cause a higher supersaturation in some part of the reactor. Which can cause an unrealistic pH measurement point. The variation in modeled and measured pH is more pronounced in summer (Figure 25) than in winter (Figure 24). Since in summer deeper softening is done with higher bypass, the dose in the reactors is higher and there are more chances of not well-mixed water

stream coming at the top of the reactor. In Appendix 11, the graph for caustic dosing in January and July is presented.

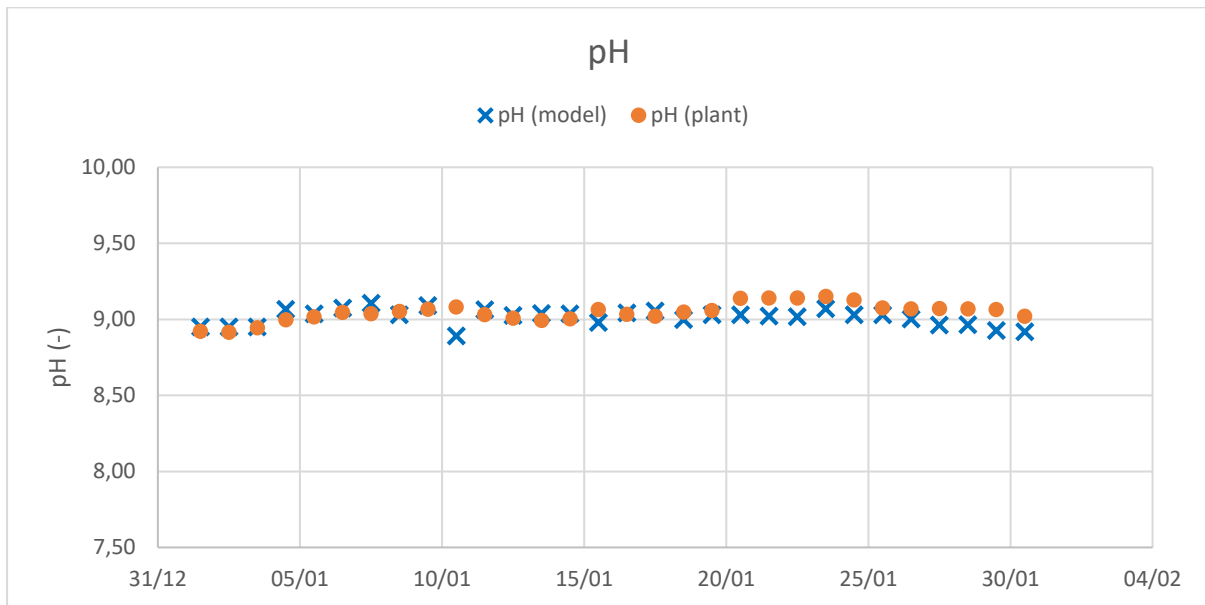


Figure 24 Modeled and full-scale pH measurements for the month of January in 2018. Temperature range at 4-6°C.

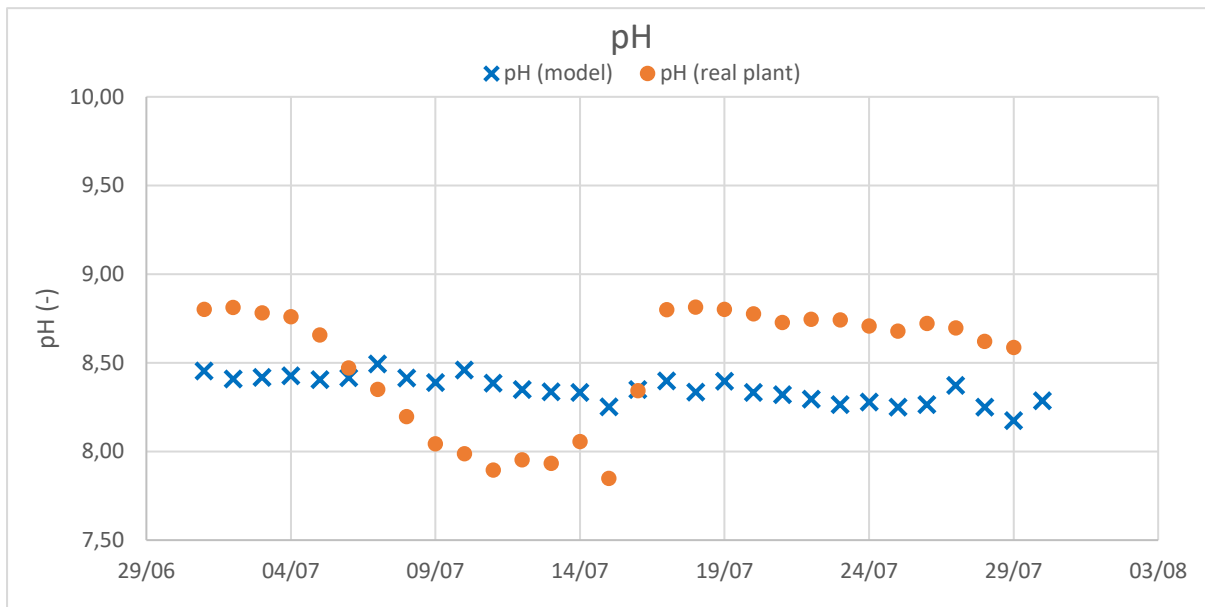


Figure 25 Modeled and full-scale pH measurements for the month of July in 2018. Temperature range at 18-23°C.

### 5.4 Absolute relative error in model predictions

To quantify the differences between the outcomes of improved prediction model and measurements, Absolute Relative Error (ARE) is used. The equation is as follows:

$$ARE = \frac{1}{n} \sum_{i=1}^n \left( \frac{y_{model,i} - y_{meas,i}}{y_{meas,i}} \right) \quad (51)$$

Here,  $y_{model}$  is the model predicted value and  $y_{meas}$  is measurement.  $n$  is the data point taken into account for validation. In this case,  $n$  is 30.

The following table shows the ARE of TH and pH measurements and modeled value.

*Table 10 Average Relative Error (ARE) of model results*

Model	Average Relative Error (ARE)	
	(TH)	(pH)
Winter (0-12°C)	12%	1%
Summer (12-24°C)	14%	4%

Observations showed that TH and pH measurements from full-scale can have a variation of  $\pm 0.1$ - $0.2$  depending on the regular lab analysis results. So, there is a window of 1-2% error in the pH measurements and 7-14% error in TH measurement. The predicted pH results in summer show a higher percentage of error. As mentioned before the deeper softening and not proper mixing of NaOH could lead to this higher percentage of error. In addition, by improving the inline measurements of pH or possibility to measure direct CCCP can provide a better validation of the model. Although the relative error in TH prediction with the model is within the range of possible error percentage from lab analyzing results.

*The validation results show that the improved model can predict the pH of the full-scale reactor with an error of 1-4%. In case of TH, the value ranges between 12-14%. Since pH is an important parameter as it determines the chemical dose ( $CO_2$ ) for conditioning softened water for the next treatment step, precise measurements are needed to validate model more accurately.*

## 6 Optimal operation for pellet softening process

*This chapter describes the scenario analysis executed by improved calibrated and validated prediction model. As a result of the scenario analysis, an optimal operational configuration for the full-scale plant is suggested based on CCCP, sustainability, reliability, and costs. Finally, a comparison between previous suggested optimal configurations with the new suggested configurations using prediction model is presented.*

Scenario analysis is a process of examining and evaluating possible future events by considering alternative possible outcomes. In this research scenario analysis are executed on different operational configurations on bypass water ratio, fluid bed height and flow velocity for summer and winter. The target of scenario analysis is to find out operational scheme which gives a lowest CCCP of the mixed effluent as it is the primary Key Performance Indicator (KPI) for quality check. The lowest CCCP will also give the lowest use of chemicals and lowest cost. Least amount of chemical use in the softening process will give the most sustainable scheme of operation.

CCCP is the concentration of excess calcium and carbonate ions in the water yet to crystallize in order to have a chemical equilibrium. As slightly higher super saturated reactor-effluent is mixed with bypass water aiming to obtain an chemical equilibrium. The CCCP of reactor-effluent depends on the efficiency of the reactor, which is a function of temperature,  $SSA_w$ , linear velocity and NaOH dosing. A bypass flow having a lower pH will decrease the overall CCCP of the mixed-effluent. So the degree of supersaturation or CCCP in the mixed-effluent depends on the efficiency of the reactor, bypass water quality and bypass ratio (Rietveld, 2005).

In addition, the fluidized bed and total amount of specific surface area plays an important role in achieving lowest CCCP from reactor. The specific surface area depends on the number and size of pellets in the reactor, water flow through the reactor and temperature of the water (Rietveld, 2005). The water flow velocity through the reactor depends on water demand, bypass ratio and the numbers of active reactors. If the bypass ratio is high, a deeper softening is possible by maintaining a lower flow velocity in the reactor.

After the scenario analysis, optimal operational configuration can be suggested by doing a multi criteria analysis. The optimal operational configuration which will lead to a sustainable operational approach for pellet softening reactors by exploiting fewer chemicals. Yet that can be accomplished when minimal supersaturation of mixed-effluent is achieved with existing infrastructure and minimizing NaOH doses. Therefore, the optimum operational configuration will be based on the criteria: quality (lowest CCCP), reliability, cost and sustainability (exploitation of less chemicals).

### 6.1 Choice of raw water quality

Two operational scenarios have been developed based on an average flow rate of 3000 m<sup>3</sup>/h with a lower (0-12°C) and higher (12-24°C) temperature range. In all the scenarios, mixed-effluent has a total hardness of 1.4 mmol/L. The flow velocity is maintained between 60-95 m/h depending on bypass ratio and numbers of active reactors. The raw water quality at WPK is consistent over time depending on temperature. Two raw water quality has been selected by taking average value for summer and winter period in the year 2016. Before 2016, there was still acid dosing in the pretreatment plant of LVN, so, the influent water quality is not representative of the present situation. In general, during summer, there is a presence of higher biological activities in the raw

water lake and rapid sand filtration step, which reduces the ammonium content and increases acidity in influent water. On the contrary, during winter, reduced biological activities results in higher pH in influent water (Table 11). Average pH of raw water during acid dosing period in winter was 7.62 where in summer it was 7.44. After stopping the acid dose, the average pH of raw water in winter and summer are increased to 7.8 and 7.6 respectively. Table 11 shows the influent water quality for summer and winter.

Table 11 Influent water quality used in scenario analysis for summer and winter

Parameters	Ca <sub>in</sub> mmol/L	Oxygen content (mmol/L)	Mg mmol/L	EC mS/m	Alkalinity (mmol/L)	pH (-)
Summer	1.77	0.26	0.28	47	3.35	7.6
Winter	1.90	0.36	0.28	49	3.46	7.8

## 6.2 Choice of operational parameters for scenario analysis

The scenario analysis is executed on 3000 m<sup>3</sup>/h as a total flow capacity of the plant. The maximum allowable bypass percentage is 40%. As going further higher in bypass percentage will cause deeper softening in the reactors which implies having a low calcium concentration in reactor-effluent. The optimal depth of softening in WPK reactor-effluent is calcium concentration of 0.5 mmol/L (Rietveld, 2005). In this research with 40% bypass has chosen to be maximum as having a higher bypass than that will cause dosing of NaOH more than 1.35 mmol/L. It can cause the overdose. More details of overdose and the restriction on NaOH dose can be found in section 6.3.1.2.

The softening plants at WPK are operated with a linear velocity between 60-95. To have a minimum fluidization of pellets, 60 m/h is the lower boundary. To avoid washout of the pellets, plants are not operated above 95 m/h. Table 12 shows the choices for bypass percentage and reactors in operation maintaining a velocity range between 60-95 m/h for a total capacity of 3000 m<sup>3</sup>/h.

Table 12 Choice of operation parameters for scenario analysis.

Bypass	Q <sub>tot</sub> (m <sup>3</sup> /h)	Area of reactor (m <sup>2</sup> )	v m/h (8 reactor active)	v m/h (7 reactor active)	v m/h (6 reactor active)	v m/h (5 reactor active)	v m/h (4 reactor active)	Q m <sup>3</sup> /h (8 reactors active)	Q m <sup>3</sup> /h (7 reactors active)	Q m <sup>3</sup> /h (6 reactors active)	Q m <sup>3</sup> /h (5 reactors active)	Q m <sup>3</sup> /h (4 reactors active)
0%	3000	5.3	71	81	94	113	141	375	429	500	600	750
15%	3000	5.3	60	69	80	96	120	375	429	500	600	750
25%	3000	5.3	53	61	71	85	106	375	429	500	600	750
40%	3000	5.3	42	48	57	68	85	375	429	500	600	750

In Table 12 the yellow boxes show the possible operational linear velocities for a certain number of active reactors with bypass percentage for scenario analysis. For example, with a 0% bypass 8, 7 or 6 reactors can be in operation as these falls within the allowable velocity range. That is designated by the yellow boxes in the first row and the red boxes represent the velocities those are not within the allowable range. Similarly, the possible operational schemes for 15%, 25% and 40% bypass showed in the table. The scenario analysis is conducted with these possible schemes with the prediction model.

## 6.3 Outcome of scenario analysis

The scenario analysis based on minimizing the criterium CCCP for both summer and winter are shown in Figure 26. The results show that the minimum CCCP is achieved by having a 40% bypass and operating 4-5 reactors with a linear velocity ranging 68-85 m/h gives the lowest CCCP in both cases<sup>11</sup>.

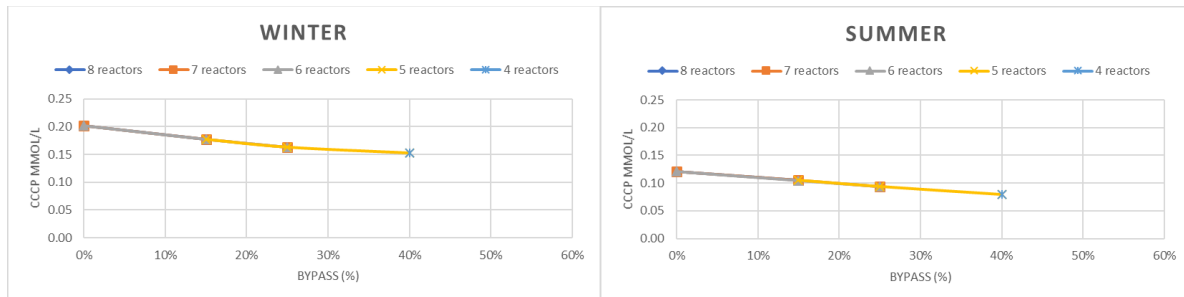


Figure 26 Outcome of scenario analysis with prediction model for softening at WPK in winter and summer.

A higher bypass will always lead to lower mixed-effluent CCCP. This can be explained with the carbonic equilibrium. The mixed-effluent always have lower pH and SI, in comparison with reactor-effluent. When the bypass water mixes with reactor-effluent, it lowers down the pH of mixed-effluent. The lower pH will shift the carbonic equilibrium towards left (5) and cause lowering of  $CO_3^{2-}$  ions in the water. Lower  $CO_3^{2-}$  ions will lower the supersaturation of  $CaCO_3$  and decrease the CCCP of the mixed-effluent. So, a higher bypass will always lead to lower CCCP in the mixed-effluent.

Nevertheless, the choices for operational configurations in the pellet softening process are not concluding as there are some operational windows that need to be taken into account. In the following sections, the operational windows and the narrowing down of choices for getting optimal operational configurations are explained.

### 6.3.1 Operational windows

The operational windows are the operational limits of the softening process in the water treatment plant at WPK, with 30 years of operational experiences.

#### 6.3.1.1 Reliability on number of the reactors in operation

The pellet softening process is less critical at higher temperature as it is possible to achieve deeper softening with higher bypass flow maintaining an average demand. That implies less reactors can be in operation. Therefore, the cleaning of reactors takes place preferably in summer. During summer, from each street, one reactor is taken out at a time for cleaning which resulted in operation of six reactors and other two inactive (Figure 3).

#### 6.3.1.2 Reliability on overdose

The influent Ca concentration at WPK is about 1.77-2.2 mmol/L. As NaOH and  $Ca^{2+}$  react with equimolar basis, in reactors the dosing of NaOH should not be more than incoming Ca

<sup>11</sup> Table 12 provides range for velocities for a certain bypass

concentration. A high dose of NaOH will remove all calcium ions from water and water will reach on the top of the reactor with still having high driving force

The NaOH dosing nozzles at the bottom of the reactors are 33% oversized. The reason of overdesigning is that within one year<sup>12</sup> of operational period, those nozzles may get clogged but still, the softening process can be reliable. The clogged nozzles cause uneven distribution of NaOH resulting overdose in some part of the reactor as the amount of dosing in reactor will be kept same. In addition, part of the reactor may not receive any caustic dosing and acts as “internal” bypass. For example, if 1/3 of the caustic soda nozzles are clogged, there will be an extra internal bypass of 1/3 of the flow. The real dose in the other part of reactor will then be 3/2 times higher than the original dose where there is no clogging of nozzles. The overdosed water will still have higher driving force and when it meets the internal bypassed water at the top of the reactor it starts crystallizing again. As there is no surface available (no seeding material available after 4 meters of fluidized bed), it starts crystallizing on the wall of the reactors where the water meets the surface (Figure 27, left).

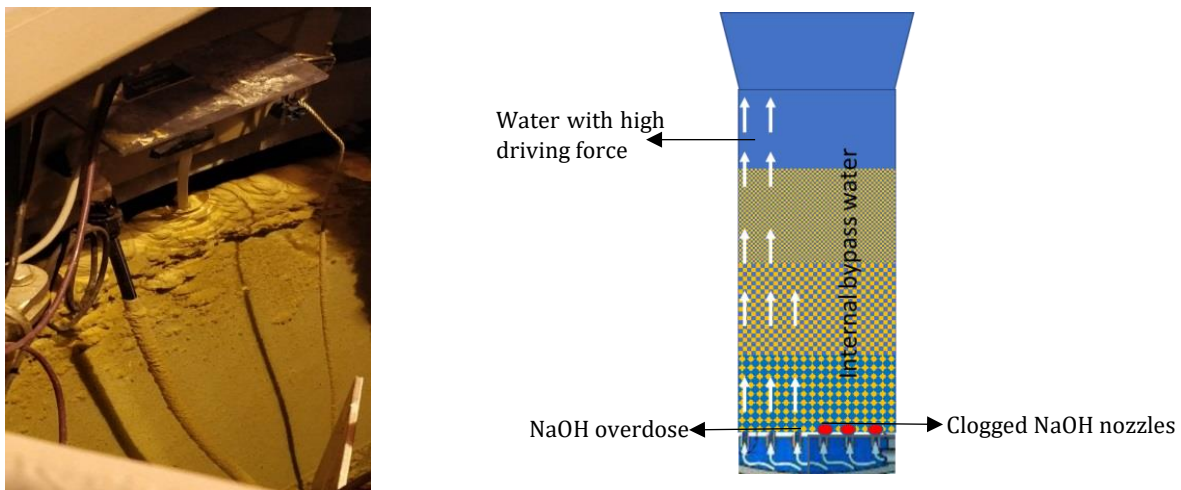


Figure 27 Sides of the reactor on the top where crystallization occurs due to uneven mixing of NaOH on the left and schematic of internal bypass on the right.

Figure 28 and Figure 29 show the operational windows for NaOH dosing in winter and summer for different bypass ratio. The orange lines in these two figures show the original NaOH dosing points with different bypass percentage. The blue dotted lines show the hypothetical NaOH dosing points when there exists 33% clogging of NaOH nozzles. Finally, the red lines show the calcium concentration in the influent water of WPK. When the blue dotted lines cross the red lines, that exhibits the critical point for dosing. For winter, the critical point is at 25% bypass and for summer the critical point lies on 40% bypass. In both the cases the dosing is 1.35 mmol/L NaOH. So, to avoid overdosing, the NaOH dosing should not exceed 1.35 mmol/L for both winter and summer. After that point, there will be more NaOH available than incoming  $\text{Ca}^{2+}$  ions and will result higher driving force in the softened water. As in summer the softening process is more efficient due to high temperature, therefore, the same amount of dosing allows higher bypass ratio with deeper softening. The green boxes in these two figures show the resulting operating possibilities in bypass after restrictions on overdosing of NaOH.

<sup>12</sup> Once a year the reactors are cleaned along with the NaOH dosing nozzles

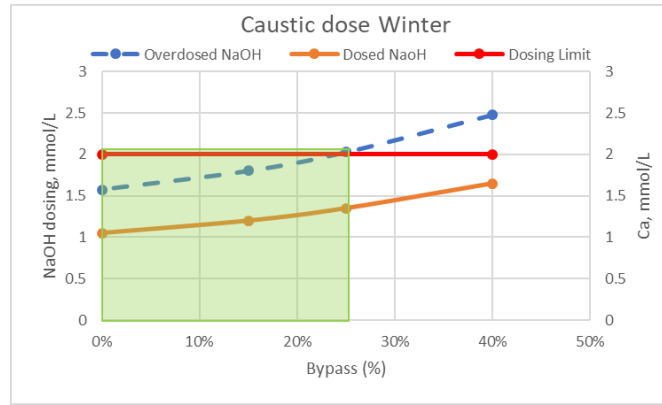


Figure 28 Operational window for dosing in winter after restrictions on the overdose of NaOH.

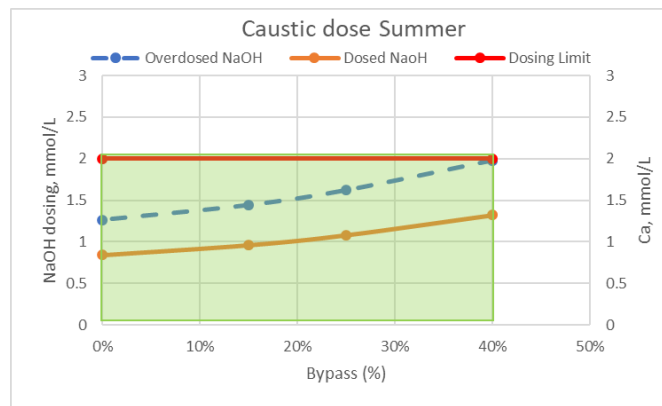


Figure 29 Operational window for dosing in summer after restrictions on the overdose of NaOH

### 6.3.1.3 Switching on and off reactors

The previous scenarios suggested (Rietveld, 2005) that the reactors can be switched on and off during average flow. Practical experiences from the experts at WTP Waternet claims that if reactors are switched on and off more than three times in a year, the clogging will be more than 33% and the softening process will not be reliable anymore. This phenomenon can lead to “internal bypass” (Figure 27) within the reactor and cause overdosing on the other part of the reactor. Therefore, switching on/off of the reactors is not permissible.

### 6.3.1.4 Reliability on minimal velocity

Previous research (Maduro, 2015) suggested a range of velocity ( $v_s$ ) and grain size ( $d_p$ ) to have the minimal porosity which makes it possible for seeding-material<sup>13</sup> to classify to the top of the reactor based on temperature (T). It is injected in the reactor at 1 meter of height and needs to get stratified to the top of the fluid bed as being the smallest diameter (0.5 mm). If the space between the pellets at 1 meter is not large enough, the seeding-material will be trapped between the pellets. Successively it will go down to the bottom of the reactor and will be taken out with the grown pellets (1 mm) from the bottom. So, the suggested range for porosity is 0.55-0.60 ( $m^3/m^3$ ) based on 1 mm of pellet at the bottom and diameter of seeding-material of 0.5 mm. The advised configuration is given in Table 13.

<sup>13</sup> crashed pellets of 0.5 mm diameter.

Table 13 Operational boundary proposed by (Maduro, 2015) on physical parameters

Season	T[°C]	$v_s$ [m/h]	Q [m <sup>3</sup> /h]	$d_p$ [mm]
Winter	0-5	65-70	350-370	1.0 – 1.1
Spring	5-10	70 - 85	370-450	1.1
Autumn	10-15	85-90	450-480	1.1
Summer	15-25	90 - 110	480-580	1.1-1.2

Therefore, in low temperature (0-10°C), the reactors should be operated between 65-85 m/h and at higher temperature (10 -25°) the boundary ranges from 85-110 m/h.

In Figure 30, the green window shows the operational schemes for winter based on proposed velocity boundary conditions with different number of reactors in operation. In winter, the lower achievable CCCP can be obtained by operating 4-7 reactors. The lowest CCCP of 0.15 mmol/L can be achieved by operating 4 reactors with a flow velocity of 85 m/h or operating 5 reactors with 67 m/h velocity. But these two schemes lead to bypass ratio of 40% and 25% respectively (Table 12). As mentioned in section 6.3.1.2, for winter the allowable maximum bypass percentage is 25%. Therefore, to stay in the conservative approach, operating 6-7 reactors with slightly higher CCCP (0.17-0.18 mmol/L) can lead to optimal configuration.

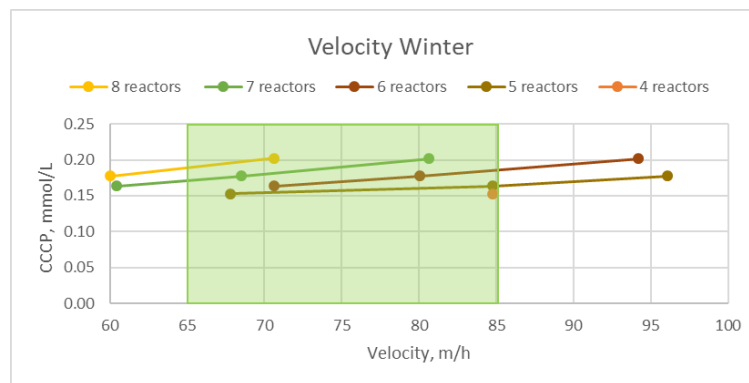


Figure 30 Operational window for velocity in winter after restrictions on porosity/velocity.

In contradiction to winter scenario, lowest CCCP can be achieved by operating 4 reactors in summer with lowest achievable CCCP of 0.08 mmol/L with a velocity of 85 m/h (Figure 31). But this scheme leads to a bypass percentage of 40% which is the critical value for overdose of NaOH. So, there are two other schemes of operating 5 -6 reactors with slightly high CCCP (0.09-0.12 mmol/L) can lead to an optimal configuration for pellet softening process by maintain the velocity

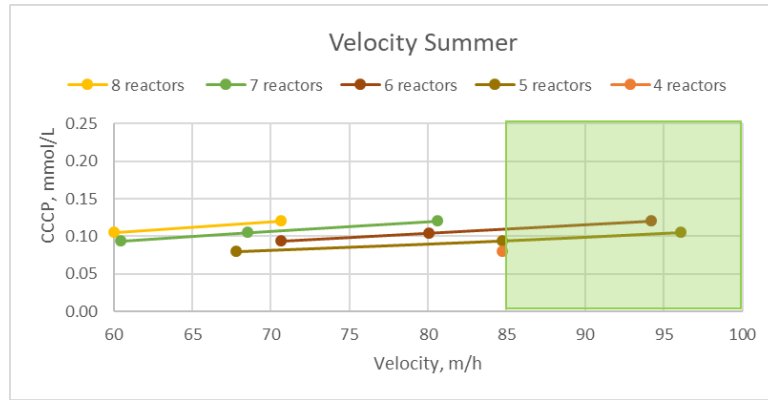


Figure 31 Operational window for velocity in summer after restrictions on porosity/velocity.

Therefore, based on optimal operational velocity to ensure minimum porosity, in winter the scheme should be running the full-scale plant with possible maximum number of reactors in actions and maintaining a lower velocity in the reactor. Although, the summer scenario suggests the opposite, running the full-scale plant on its full capacity by using a smaller number of reactors.

### 6.3.2 Optimum operation based on fluid bed height

In this section, the scenarios are based on fluid bed height. It shows that the first 1.0-1.5 meter is the most active region of the reactor. After that, the reactions go to a dead-end slow zone (Figure 35) since there is no change in calcium content for the rest of the fluid bed height.

In winter (Figure 32, left), within 1.5 m of bed height all the chemical reaction occur and after that, the crystallization process goes to region 4 (section 3.1.2). In summer (Figure 32, right), all the chemical reaction occurs even faster due to a higher temperature and within 0.5-0.75 m of the fluid bed, it goes to region 4.

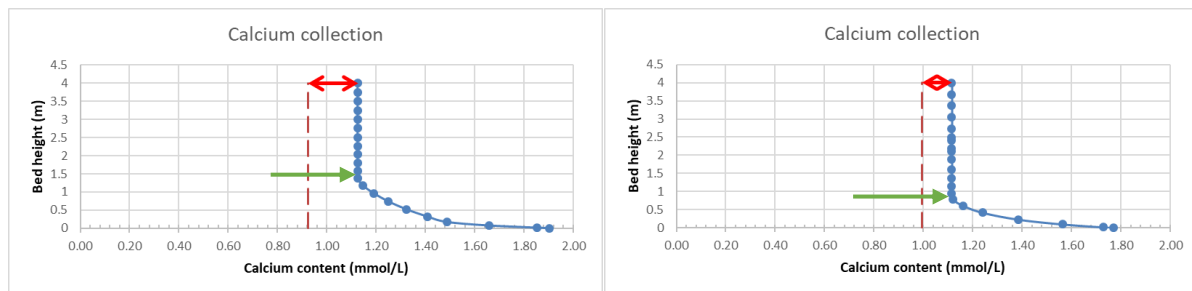


Figure 32 Calcium collection profile over the bed height. Winter scenario (left) and Summer scenario (right) operational conditions:  $Ca_{in} = 1.8-1.9$  mmol/L,  $v = 71$  m/h, caustic dose = 0.84 mmol/L, total flow per reactor = 375 m<sup>3</sup>/h, bypass = 0%, and particle diameter = 1 mm. The dosing in summer is 0.54 mmol/L and in winter 1.05 mmol/L

It is evident that 2 m of fluid bed height is sufficient for softening process. But in practice, it is not recommended for three reasons. First, after 1.5-2 m of fluid bed height, though there are no visible chemical reactions taking place, still the rest of the bed height acts as the polishing stage of water. The CCCP of the water at 1.5-2 m height is still high to form scaling. So, a higher bed height will provide the scope of reactor-effluent polishing. Secondly, the smaller fluid bed height does not give the flexibility of operation with higher flow, so, there is a possibility for washout of pellets.

Thus, conceiving future demand and process reliability, a higher fluid bed height is recommended. Finally, for crystallization, the availability of  $SSA_{H_2O}$  is one of the crucial parameters. So, a higher fluid bed height will provide more  $SSA_{H_2O}$  which will aid the crystallization process.

Therefore, for optimum operational configurations, maintaining a fluid bed height of  $4 \pm 0.5$  m is recommended.

## 6.4 Optimal configurations

The multi criteria analysis of the outcomes of the scenario analysis is performed in order to find the final optimal configurations for summer and winter. It is based on the quality (CCCP), chemical cost (caustic soda and  $CO_2$ ), sustainability and the limiting operational windows based on overdose, velocity, numbers of active reactors and switching on an off the reactors during operation of pellet softening process.

In Table 14 and Table 15, the results of multi criteria analysis for winter and summer are presented. In the left column the criteria are presented and a '+' signs represents the positive result for those criteria, '-' sign represents the negative results and '0' used in the reliability criterium which represents when the outcome falls on the edge boarder of the reliability windows. Highest number of '+' sign after the summation of '+' and '-' will give the preference for optimal bypass percentage in operating pellet softening reactors. Since avoiding the overdose of NaOH is the most important reliability criteria in plant operation, so a higher weight is assigned to it by incorporating more '-' signs when it does not fall in the overdose windows.

For example, '+++' for 40% bypass signs for quality represents that it has the lowest CCCP among all the scenarios. Again '----' signs for 40% bypass percentage in overdose represents it gives highest amount of NaOH overdose among all the scenarios. A '--' sign for 25% bypass in overdose represents that with this bypass ratio the overdose is just on the critical point. A '0' sign for the velocity represents that it falls on the boarder of the velocity window.

Table 14 Multi criteria analysis for optimal scenario in winter

Criteria		Winter			
		40%	25%	15%	0%
<b>Quality (CCCP)</b>		+++	++	+	-
<b>Cost</b>		+++	++	+	-
<b>Sustainability</b>		+++	++	+	-
<b>Reliability</b>	NaOH overdose	----	--	+++	+++
	velocity	++	++	++	-
	No of active reactor	-	++	+++	+++
	Switch on/off	+++	+++	+++	+++
<b>Total</b>		9 '+'	11 '+'	14 '+'	5 '+'

Table 15 Multi criteria analysis for optimal scenario in summer

		Summer			
Criteria		40%	25%	15%	0%
<b>Quality (CCCP)</b>		+++	++	+	-
<b>Cost</b>		+++	++	+	-
<b>Sustainability</b>		+++	++	+	-
<b>Reliability</b>	NaOH overdose	--	+++	+++	+++
	Velocity	0	0	+	+
	No of active reactor	-	++	+++	+++
	Switch on/off	+++	+++	+++	+++
<b>Total</b>		9 '+'	14 '+'	13 '+'	7 '+'

For winter, 15% and for summer 25% bypass water provides the highest amount of '+'. Therefore optimum configuration for winter would be operating the plant with 15% bypass and for summer with 25% bypass.

In winter, 15% bypass is possible to achieve by operating 6-7 reactors as mention in the section 6.3.1.4. As in winter chemical reactions are slower due to low temperature, operating more numbers of reactors will also provide more  $SSA_{H_2O}$ , which will make the overall softening process more efficient. So the choice for optimum operational configuration will be 7 reactors in operation. The choice is pointed out by circles in Figure 33. Here, in the left graph, chemical costs are shown for different bypass percentage with linear velocity. Also same cost is shown in terms of numbers of active reactors with linear velocity on the left graph.

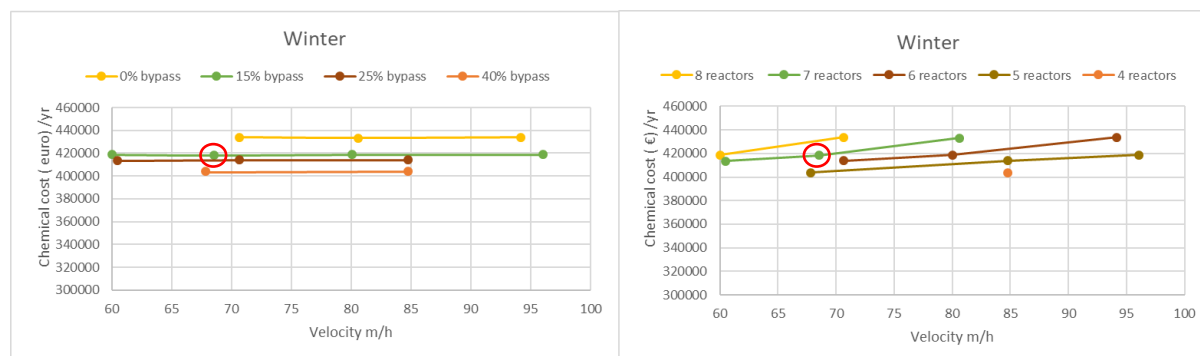


Figure 33 Optimal configuration for the operation of pellet softening in winter.

During summer, 25% bypass is possible to achieve by operating with 5-6 reactors in operation. Based on cost, 5 active reactors having a bypass of 25% with a linear velocity of 85 m/h gives the lowest chemical cost (Figure 34, circled points). Operating 5 reactors also gives the room for cleaning them in summer.

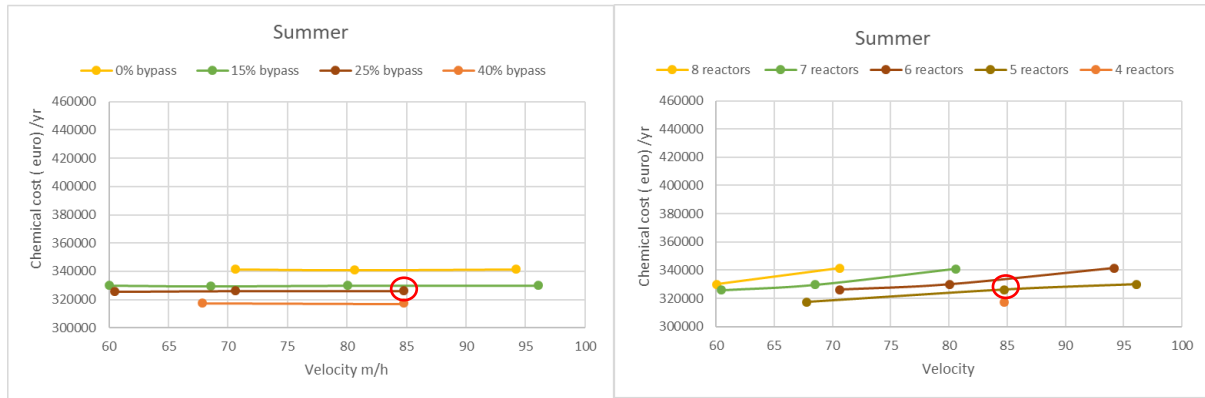


Figure 34 Optimal configuration for the operation of pellet softening in summer.

Therefore to conclude, the fluid bed height should be kept at its maximum ( $4 \pm 0.5$  m) to have a more classified bed and avoid flushing of pellets. In addition, the reactors will not be switch on and off on during non-operational phase rather it can work as a bypass reactor. Finally, the prediction model kinetics is based on the particle diameter of 1 mm at the bottom and 0.5 seeding material. The suggested configuration is based on this bed profile only.

In Table 16 the optimal operational configurations for summer and winter are presented.

Table 16 Optimal configurations for summer and winter

Parameter	Summer	Winter
Velocity (m/h)	85	67
Bypass	25%	15%
Reactors	5	7
Diameter of particle (calcite) $d_p$ , mm	1	1
Ent material (calcite) mm	0.5	0.5
Fluid bed height, m	4	4
Switch on /off	no	no

The chemical cost of these two scenarios are compared with the chemical cost of zero bypass percentage in winter and summer. In both the scenario, around 15000 € can be gained by operating the pellet softeners with 15% and 25% bypass for winter and summer (Table 17). The overall cost reduction is 3-4%.

Table 17 Cost reduction

Scenario	Chemical Cost (NaOH+CO <sub>2</sub> ) (€)/year			
	0% bypass	Optimal Bypass	Reduction of cost	Percentage Cost reduction
Summer	340,000	326,000	14,000	4%
Winter	434,000	419,000	15,000	3%

## 6.4.1 Comparison optimal configurations

In 2005, operational configurations were proposed for WPK based on lowest CCCP value and bypass (Rietveld, 2005). Later on, Schagen in 2008 also proposed a model for WPK (van Schagen et al., 2008a). Although in this research, a comparison of the model is done with the former one since the proposed scenario suggested is also based on CCCP and bypass.

The configuration suggested for the higher bypass as much as 50% with the flexibility of shutting down the reactors when it's not in operation (Rietveld, 2005). Figure 35 shows the CCCP for different bypass percentage scenario for two different temperature (10°C and 1.2°C). The low CCCP with higher bypass were possible because the raw water quality was different at that time due to the acid dosing at LVN. The acidic bypass water facilitated a high bypass ratio of 50% achieving a very low mixed-effluent CCCP (e.g. 0.02 mmol/L). In addition, garnet sand was used as a seeding material which has a higher  $SSA_{H_2O}$ . High  $SSA_{H_2O}$  helps better removal of calcium from water. Finally, the chemical model used for optimal configuration was based on mono-linear kinetics which makes the reactors more efficient and resulted in such a low CCCP value.

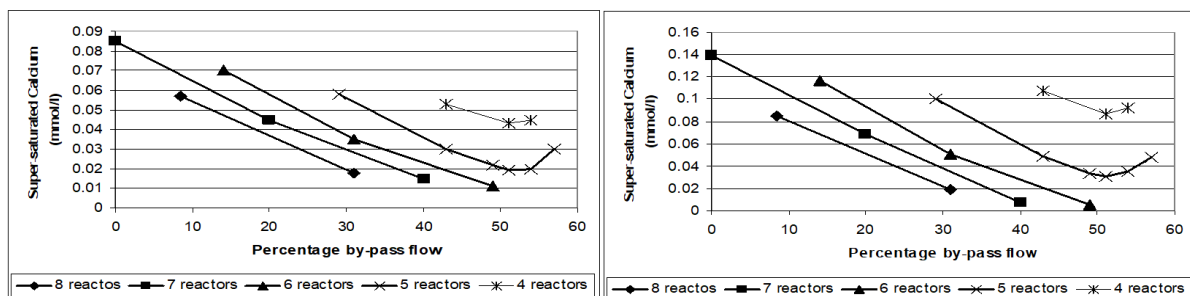


Figure 35 Operation scenarios for softening at WPK, flow 3500 m<sup>3</sup>/h, 10°C (left figure) and 1.2°C (right figure) ( $HCO_3^- = 204$  mg/L,  $Ca^{2+} = 80$  mg/L, pH=7.61, EC=53 mS/m,  $Mg^{2+} = 6.6$  mg/L) (Rietveld, 2005).

As the shift from garnet to calcite pellets as seeding material caused a vital change in the operational process of pellet softening. The scenario based on garnet sand needs to remodel for calcite pellets. Four scenarios presented in Figure 36 and Figure 37.

- (Figure 36, left) Raw water with a lower pH (7.6) replicating acid dose at pretreatment in winter (6°C).
- (Figure 36, right) Raw water with a higher pH (7.8) replicating existing situation in winter (6°C).
- (Figure 37 left) Raw water with a lower pH (7.44) replicating acid dose at pretreatment in summer (20°C).
- (Figure 37, right) Raw water with a higher pH (7.6) replicating existing situation in summer (20°C).

These scenarios are executed with the prediction model having improved kinetics in it and calcite pellets as seeding material. The observations are: First, high bypass provides lowest CCCP just like the former scenario, but minimum CCCP of mixed-effluent is higher in these scenarios than configuration suggested by (Rietveld, 2005) for both in summer and winter.

Secondly, the variation in CCCP depending on bypass is less pronounced since, with the new kinetics, the reactor is not as efficient as before. So, the reactor-effluent is having higher CCCP which makes the overall CCCP higher after bypass and a large amount of bypass could not help to get this value down.

Finally, in winter, for the non-acidified bypass water (Figure 36, right), the values show almost no difference with increasing bypass (25%-40% bypass). Though the lowest overall CCCP 0.13 mmol/L is achieved in acidified bypass flow water (Figure 36, left) among the winter scenarios. In summer, the CCCP gets the lowest value of 0.06 mmol/L in the acidified bypass flow scenario (Figure 37, left), whereas the lowest possible CCCP in non-acidified bypass scenario (Figure 37, right) is 0.08 mmol/L.

So, the acid dosing can indeed get the overall CCCP to the lowest value, but due to improved kinetics and using calcite pellets as seeding materials, the values is not as low as it was possible in Rietveld's scenario (0.02 mmol/L).

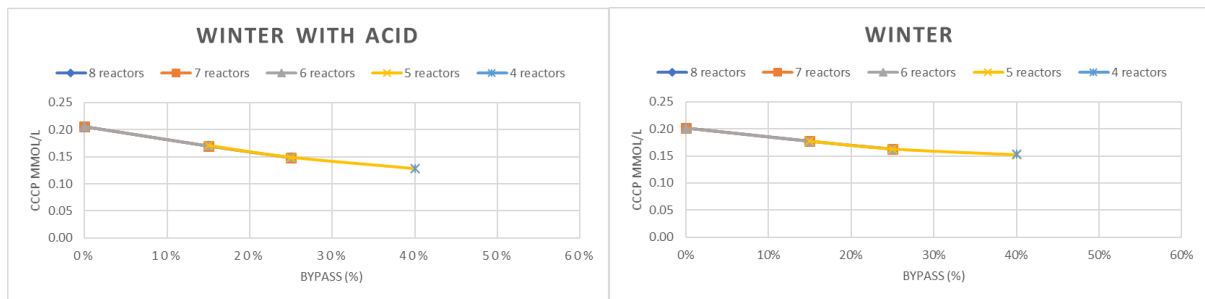


Figure 36 Operation scenarios for softening at WPK in winter, flow 3000 m<sup>3</sup>/h, 6°C (HCO<sub>3</sub><sup>-</sup> = 211 mg/L Ca<sup>2+</sup>=76 mg/L, pH=7.6 (left) and pH=7.8 (right), EC=47 mS/m, Mg<sup>2+</sup>=6.48 mg/L).

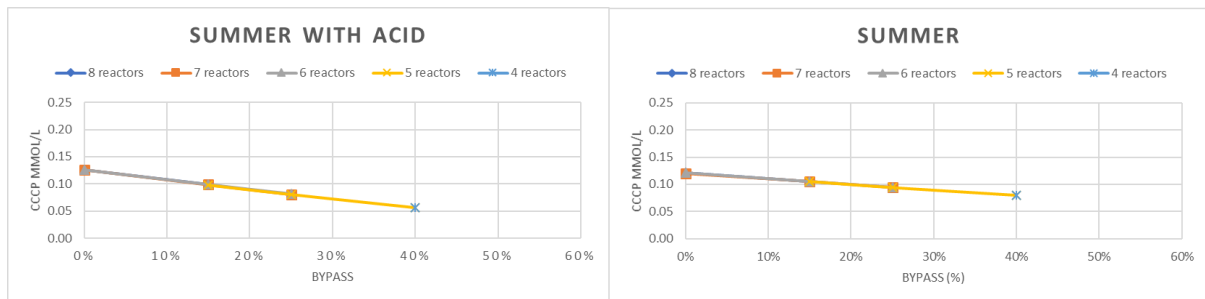


Figure 37 Operation scenarios for softening at WPK in summer, flow 3000 m<sup>3</sup>/h, 20°C (HCO<sub>3</sub><sup>-</sup> = 204 mg/L, Ca<sup>2+</sup>=71 mg/L, pH=7.44 (left) and pH=7.6 (right), EC=47 mS/m, Mg<sup>2+</sup>=6.48 mg/L)

Therefore, the process modifications and improvement of the chemical kinetics in the prediction model provided scenarios where the full-scale can be operated with higher bypass. Although based on CCCP, the choices can be applied to the other schemes (lower bypass and operating more reactors) as less pronounced variations in water quality (CCCP) are observed.

The cost reduction on optimal configuration suggested by Rietveld was 10%, whereas, with the new prediction model there is only 3-4% less cost reduction possible. The primary chemical cost is dependent on mixed-effluent CCCP. With the new prediction model and a non-acidified bypass water, the difference in CCCP with varying bypass percentage is not pronounced which makes the

cost reduction lower. Also the operational window will limit the high bypass percentage. These two phenomena causes lower cost reduction.

*The optimal configuration for pellet softening process is to run the reactors with 25% bypass flow in summer and going deeper in softening. Whereas, in winter pellet softeners should run with lower bypass flow of 15% with higher numbers of reactors in operation.*

## 7 Discussion

*This chapter includes an overall discussion on the improved prediction model and the optimal configurations for pellet softening process. Lastly, the limitations of the research are presented at the end of the chapter.*

### 7.1 Model

To simulate the pellet softeners more accurately and to have better control on the process operations an improved prediction model is established. A more realistic prediction model incorporating four-kinetics region provides a better interpretation of the real scenario. In addition, this research contains an overall description of the model development that will provide a better understanding of fundamental principles for chemical modeling of pellet softening and better scope for future improvement. The Hydraulic Fluidization Model (HFM) incorporated in the prediction model is based on the ongoing research on hydraulic modeling of liquid-solid fluidization (Kramer, 2016).

The prediction model has incorporated different reactor principle. It is a combination of CSTR and PFR. At the bottom of the reactor, due to rapid mixing of caustic soda and raw water, a zone of CSTR will be created. Above it, a zone of PFR will be established. Such a combination of reactor principles has changed the reactor efficiency and made the model more realistic.

The chemical model parameters ( $k_T$ , CP, SP, and A) were taken from experiments done with WPK and LDN water (Seepma, 2018). The model calibration was done using experiments done at WPK (Schooten, 1985, Schetters, 2013) and full-scale plant. The model could reproduce the experimental results by adjusting the parameters. CP (Changing point) and SP (sleeping point) are the most crucial parameters in the model. These two parameters have the largest influence on saturation ratio corresponding to the occurrence of the dead-end slow zone and CCCP coming out from the reactor.

The validation of the prediction model was done with the data from the full-scale plant. To have a comprehensive prediction model applicable for all temperature range (0-24°C), the model was validated with summer and winter temperature. For validation TH (total hardness) and pH (acidity) from the reactor were taken as the parameter to compare with modeled output. In the case of TH, the model predicted results have an error ranging between 12-14%. For pH measurements, the model has an error of 1-4%. Whereas the full-scale can have an error in TH measurements of 7-14% and in pH measurement 1-2%. These percentage errors are determined based on regular lab analysis at WPK. Although the pH measurement has an error more than expected, this mismatched can be accounted to a measurement error and the change in dosing style (dosing cross).

### 7.2 Operational configurations

The process modifications in the overall treatment scheme at WPK has made the raw water quality different and the shift from garnet to calcite pellet as a seeding material caused a change in reactor behavior. The previous operational configurations were based on mono-linear kinetics (Wiechers et al., 1975) using garnet sand as seeding material and acidified raw water (Rietveld, 2005). Later on, another scheme for operational mode was proposed by Liselotte (Hout, 2016) by proposing the change in seeding materials from garnet to calcite but with acidified raw water

and the same mono-linear kinetics. The model developed in this research has taken into account all the process modifications (calcite, no acid, and improved kinetics in four regions).

Scenario analysis has been executed based on bypass water ratio, fluid bed height and flow velocity for summer and winter. To get optimal operational configurations, a multi criteria analysis has been performed based on quality (CCCP), cost, sustainability and reliability. The optimal configuration will provide a sustainable operational scheme for pellet softeners, as it will lead to less use of chemicals. The optimum configuration suggested that for summer higher bypass (25%) is preferred and having a lower number of reactors (5 reactors) in operation. The flow velocity, in that case, is higher (85 m/h) to maintain the average water demand. For winter, the reactors should run with lower bypass flow and keep a higher number of reactors (7 reactors) in operation. The flow velocity should also be kept lower (69 m/h).

After that, a comparison has been made between model outcomes proposed by Rietveld (Rietveld, 2005) and the prediction model with calcite pellet as seeding material and having acidified raw water. Both the model outcomes suggested a higher bypass would make the softening process more optimal. Though the difference in CCCP depending on changing bypass was not dominant as in the scenarios suggested by Rietveld (Rietveld, 2005). Finally, a comparison was made between the model outcomes of acid and no acid raw water with the improved kinetic model on calcite. Both the model shows similar outcomes with a preference for a higher bypass for operational configuration. Though the trend gets less steep and the difference in CCCP with varying bypass is even less pronounced (Figure 36 and Figure 37).

### **7.3 Critical thoughts on the research**

This section describes the limitations of the research.

As mentioned before, SP and CP are the most critical parameter for the improved kinetic model. The model calibrations were done on the experiments. The experiments have a very small range of varying parameters. For example, the PFR experiments are done on 80 m/h linear velocity. Whereas the full-scale plant runs on a velocity ranging from 60-90 m/h. Therefore, the change in CP and SP depending on different flow velocity is not investigated.

Moreover, the model is not based on the dosing level of NaOH but on CCCP. Therefore, the depth of softening is not investigated. The threshold of NaOH dosing which can provide the lowest CCCP and subsequently causes the dissolution of  $\text{CaCO}_3$  needs to be investigated and incorporated into the model for making it more robust and widely applicable.

In the model, the threshold point for CCCP in reactor-effluent is set by defining SP which is based on a small range of experimental data. So more in-depth research is needed on this threshold CCCP for different operational conditions (velocity, temperature, the dose of NaOH, etc.)

Furthermore, pH smoothing function is used in the experimental data (CSTR) to estimate the first couple of pH points. The smoothing function gives the most desirable outcome yet, what actually is the condition in the first few seconds after dosing is the most important to determine the kinetics. The actual change of pH with time is important for the model to predict the rate constant precisely.

The optimal configuration suggested in this research is based on an average production of 3000 m<sup>3</sup>/h. It is recommended to investigate the model outcome on a wide range of production capacity between 2500-4800 m<sup>3</sup>/h.

## 8 Conclusions and recommendations

*The goal of the thesis was to determine the optimum scenario due to the process modifications for pellet softening reactors with improved chemical kinetics. In this chapter, the final conclusions and recommendations for future works are given.*

### 8.1 Conclusions

The new improved kinetics implemented in prediction model gives a more evident process that goes in the reactors. Defining the four regions (section 3.1.2) in the chemical modeling gives better control to predict the crystallization process depending on temperature. The model could predict pH and TH from the reactor with an error ranging from 1-4% and 12.0-14% respectively.

The choice of criteria for scenario analysis was based primarily on optimizing CCCP and bypass ratio. An optimal combination between bypass ratio and CCCP would give the maximum profit for process operation.

Due to the process modifications (switch to calcite from garnet sand as seeding material and shutting off acid dose in the pretreatment process at LVN) a lower bypass both in winter and summer is suggested. The previous operational configurations proposed a higher bypass percentage as the acidified bypass flow could result in a lower overall CCCP after mixing. In addition, garnet sand having a higher specific surface area aided to a more efficient softening process. Recognizing the circular economy and sustainability, the process modification induced different sets of operational criteria for optimum outcome in the pellet softening process at WPK.

The optimal configuration of the softening process at Waternet will be:

Parameter	Summer	Winter
Velocity (m/h)	85	69
Bypass	25%	15%
Reactors	5	7
Diameter of particle (calcite) dp, mm	1	1
Seeding material (calcite) mm	0.5	0.5
Fluid bed height, m	4	4
Switch on /off	no	no

The cost reduction in with these two optimal configurations is about 3-4% in summer and winter. Whereas in the previous suggested optimal configuration could lead to 10% reduction ((Rietveld, 2005). With the new prediction model and non-acidified bypass, the difference in CCCP with varying bypass percentage is not that pronounce which makes a lower cost reduction.

## 8.2 Recommendations

CCCP is the most important KPI for the softening process. CCCP is a soft sensor and is calculated from a set of measured parameters ( $\text{CO}_3^{2-}$ , TH, pH, temperature and EC). Control of CCCP at each reactor is necessary for constant quality check. CCCP is correlated to  $\text{CO}_2$  dosing for conditioning softened water. The conditioning is done until water achieve a saturation index of zero. Estimating CCCP from  $\text{CO}_2$  is subjected to raw water quality. It has been seen in practices that, 1 mmol/L CCCP = 1.15-1.3 mmol/L  $\text{CO}_2$ . In case of WPK, roughly 1.3 mmol/L  $\text{CO}_2$  is needed for 1 mmol/L of CCCP. Figure 38 left, shows this relation between CCCP and  $\text{CO}_2$  with increasing bypass. The figure on right shows the correlation of CCCP and  $\text{CO}_2$ .

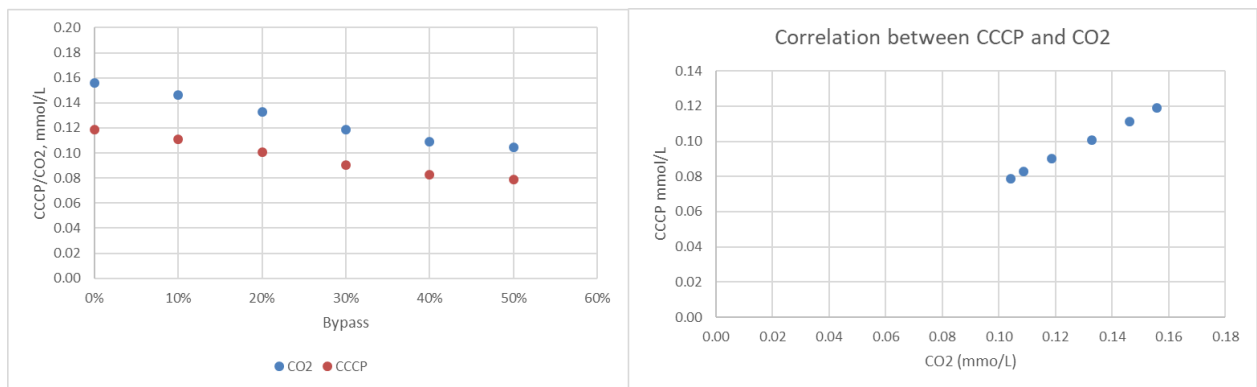


Figure 38 Relation of  $\text{CO}_2$  dose and CCCP with bypass and Correlation of CCCP and  $\text{CO}_2$  for WPK water quality.

Therefore, an online CCCP soft sensor (online calibrated measurements of water flow and NaOH flow for the input of the CCCP model calculations) can be incorporated in the dashboard for the softening process at Waternet. This advancement can highly aid the quality control of the process. The  $\text{CO}_2$  dosing can also be used as control of the total softening process for constant quality check.

The kinetic rate constant obtained from CSTR experiments based on Merck powder. The  $SSA_{H_2O}$  of Merck powder is not correctly quantified as the diameter of the powder varies from 13-26.5 micron. Therefore, accurate measurement of the surface area was not possible. A more sophisticated measurement of  $SSA_{H_2O}$  is recommended as the kinetic rate constants ( $k_T$ ) are highly depended on this.

To simulate a full-scale plant, a more representative pilot plant experiment should be carried out. In the PFR experiments, caustic soda was mixed with raw water before and then pumped to the column reactor. This set up could be more similar to the full-scale plant by proving a continuous mixing at the bottom.

It is recommended to investigate in more details if the model can give the same optimal configurations on different operational conditions (e.g. velocity, NaOH dose, depth of softening).

If the CCCP of mixed-effluent in the full-scale plant exceeds the predicted CCCP from the model, and if the  $\text{CO}_2$  dosing also exceeds, then the upstream system (bypass ratio, dosing of NaOH and fluid bed height) needs further investigations to identify the mismatch.

The kinetics of crystallization models are based on PFR experiments (Seepma, 2018) in a small 10-centimeter diameter with 2-meter high reactor with no variation in velocity and limited variation in particle size. So, for further research, a wide range of velocity can be incorporated to see if the model predicts the same result.

In the pilot, plant two 40 centimeters diameter and 6 meters high reactors can be used to compare the model suggested by Rietveld (Rietveld, 2005) and the improved prediction model developed in this research. This would give a more reliable comparison of model outputs.

## Bibliography

- BIRD, R. B., LIGHTFOOT, E. N. & STEWART, W. E. 1960. *Notes on Transport Phenomena. Transport Phenomena. By RB Bird, Warren E. Stewart, Edwin N. Lightfoot. A Rewritten and Enlarged Edition of "Notes on Transport Phenomena"*, New York, London.
- CHIOU, E. 2018. *An improved model of calcium carbonate crystallization: An improved kinetics-model for the calcium carbonate crystallization in the fluidized bed softening reactors at the Weesperkarspel drinking water treatment plant*. Master of Science master thesis, Delft University of Technology.
- DE MOEL, P., VAN DIJK, J. & VAN DER MEER, W. 2013. *Aquatic chemistry for engineers–Volume 1–Starting with PHREEQC 3. Delft University of Technology, Delft, the Netherlands*, 20.
- ERGUN, S. 1952. Fluid flow through packed columns. *Chem. Eng. Prog.*, 48, 89-94.
- HARMS JR, W. D. & ROBINSON, R. B. Characterization of fluidized bed crystallizers used for softening in South Florida. 1990. 717-724.
- HOUT, L. V. D. 2016. *"Modelling van de hardheidsreductie, Optimalisatie van het hardheidsreductieproces door het ontwikkelen van een laagjesmodel waarbij de koppeling is gemaakt tussen de waterchemie en hydraulica"*. Master in Science, Hogeschool Utrecht.
- JOBSE, M. 2013. *Modeling fluidization at grain reactors*. Master Master's thesis, University of Utrecht, Institute of Life Science and Chemistry.
- KRAMER, O. 1991. *Fluid bed (theorie en praktijk)*. Master Master Thesis, University of Amsterdam.
- KRAMER, O. 2016. Hydraulic modelling of liquid-solid fluidisation in drinking water treatment processes. Delft University of Technology.
- MADURO, A. F. E. 2015. *Optimalisatie van de ontharding. Een optimaal werkgebied voor de bedrijfsvoering van het hardheidsreductieproces met calcië als entmateriaal gebaseerd op een optimale porositeit, specifiek oppervlakte, en contactoppervlakte*. Master.
- MAENG, S. K., RODRIGUEZ, C. N. A. S., CHOI, J., KIM, S. H., YU, Y., KIM, B. S. & HONG, S. W. 2016. Organic micropollutant removal from groundwater: Comparison of pellet softening and nanofiltration. *Journal of Water Supply: Research and Technology - AQUA*, 65, 453-464.
- PARKHURST, D. L. & APPELO, C. 2013. Description of input and examples for PHREEQC version 3: a computer program for speciation, batch-reaction, one-dimensional transport, and inverse geochemical calculations. US Geological Survey.
- PLUMMER, L. N. & BUSENBERG, E. 1982. The solubilities of calcite, aragonite and vaterite in CO<sub>2</sub>-H<sub>2</sub>O solutions between 0 and 90°C, and an evaluation of the aqueous model for the system CaCO<sub>3</sub>-CO<sub>2</sub>-H<sub>2</sub>O. *Geochimica et Cosmochimica Acta*, 46, 1011-1040.
- RHODES, M. J. & RHODES, M. 2008. *Introduction to particle technology*, Wiley Online Library.
- RICHARDSON, J., DAVIDSON, J. & HARRISON, D. 1971. Fluidization. *edited by Davidson, JF and D. Harrison*, 25-64.

- RICHARDSON, J. & ZAKI, W. 1954. The sedimentation of a suspension of uniform spheres under conditions of viscous flow. *Chemical Engineering Science*, 3, 65-73.
- RIETVELD, L. C. 2005. *Improving operation of drinking water treatment through modelling*. Ph.D. Pd-Thesis, Delft University of Technology.
- RIETVELD, L. C., MEIJER, L., SMEETS, P. W. M. H. & VAN DER HOEK, J. P. 2009. Assessment of cryptosporidium in wastewater reuse for drinking water purposes: A case study for the city of Amsterdam, The Netherlands. *Water SA*, 35, 211-215.
- SCHETTERS, M. J., VAN DER HOEK, J. P., KRAMER, O. J., KORS, L. J., PALMEN, L. J., HOF, B. & KOPPERS, H. 2015. Circular economy in drinking water treatment: reuse of ground pellets as seeding material in the pellet softening process. *Water Sci Technol*, 71, 479-86.
- SCHETTERS, M. J. A. 2013. *Grinded Dutch calcite as seeding material in the pellet softening process*. Master of Science Master, Delft University of Technology.
- SCHILLER, L. & NAUMANN, A. 1933. Fundamental calculations in gravitational processing. *Zeitschrift Des Vereines Deutscher Ingenieure*, 77, 318-320.
- SCHOCK, M. R. 1984. TEMPERATURE AND IONIC STRENGTH CORRECTIONS TO THE LANGELIER INDEX - REVISITED. *Journal / American Water Works Association*, 76, 72-76.
- SCHOOTEN, A. V. 1985. Bepaling van de onthardings-orde en de invloed van de stroomsnelheid, de vaste bedhoogte en de zuurwaarde op de kristallisatie snelheids constante.
- SEEPMA, S. Y. M. H. 2018. *Revision of CaCO<sub>3</sub> Crystallisation Kinetics in Drinking Water Softening*. Master of Science, University of Utrecht.
- STUMM, W. & MORGAN, J. J. 2012. *Aquatic chemistry: chemical equilibria and rates in natural waters*, John Wiley & Sons.
- VAN DER BRUGGEN, B., GOOSSENS, H., EVERARD, P. A., STEMGÉE, K. & ROGGE, W. 2009. Cost-benefit analysis of central softening for production of drinking water. *Journal of Environmental Management*, 91, 541-549.
- VAN DER HELM, A., KRAMER, O., HOOFT, J. & DE MOEL, P. Plant wide chemical water stability modelling with PHREEQC for drinking water treatment. IWC 2nd International Water Conference: New Developments in IT & Water, Rotterdam, The Netherlands, 8-10 February 2015; Authors version, 2015. IWC.
- VAN DER HOEK, J. P. 2012. Towards a climate neutral water cycle. *Journal of Water and Climate Change*, 3, 163-170.
- VAN DIJK HANS, J., QJC, V. J. & DE MOEL PETER, J. 2006. *Drinking water: principles and practices*, World Scientific.
- VAN DIJK, J. C. & WILMS, D. A. 1991. Water treatment without waste material. Fundamentals and state of the art of pellet softening. *Aqua London*, 40, 263-280.
- VAN SCHAGEN, K., RIETVELD, L., BABUŠKA, R. & BAARS, E. 2008a. Control of the fluidised bed in the pellet softening process. *Chemical Engineering Science*, 63, 1390-1400.

- VAN SCHAGEN, K. M., RIETVELD, L. C. & BABUŠKA, R. 2008b. Dynamic modelling for optimisation of pellet softening. *Journal of Water Supply: Research and Technology - AQUA*, 57, 45-56.
- VAN SCHAGEN, K. M., RIETVELD, L. C., BABUŠKA, R. & KRAMER, O. J. I. 2008c. Model-based operational constraints for fluidised bed crystallisation. *Water Research*, 42, 327-337.
- WIECHERS, H. N. S., STURROCK, P. & MARAIS, G. V. R. 1975. Calcium carbonate crystallization kinetics. *Water Research*, 9, 835-845.

## Appendix 1 Relative number for each layer in particle bed model

No. of Layers	Relative number (-)
1	0.010
2	0.050
3	0.100
4	0.200
5	0.300
6	0.400
7	0.500
8	0.600
9	0.700
10	0.800
11	0.900
12	0.920
13	0.940
14	0.960
15	0.980
16	1.000
17	1.000
18	1.000
19	1.000
20	1.000

Appendix 2 Adopted initial diameter profile and profile after 60 iterations.

No of layers	Adopted profile (mm)	Profile after 60 iterations (mm)	Profile from mass balance (mm)
1	1.00	1.00	1.00
2	0.91	0.97	0.97
3	0.80	0.88	0.88
4	0.67	0.83	0.83
5	0.63	0.76	0.76
6	0.60	0.67	0.67
7	0.57	0.58	0.58
8	0.56	0.50	0.50
9	0.54	0.50	0.50
10	0.53	0.50	0.50
11	0.52	0.50	0.50
12	0.52	0.50	0.50
13	0.51	0.50	0.50
14	0.51	0.50	0.50
15	0.51	0.50	0.50
16	0.51	0.50	0.50
17	0.51	0.50	0.50
18	0.50	0.50	0.50
19	0.50	0.50	0.50
20	0.50	0.50	0.50

### Appendix 3 Hydraulic model used for porosity estimation

The hydraulic model used in this research is data driven model. It is based on the expansion tests at eight different sieve fractions. This hydraulic model is adopted from the previous research (Hout, 2016). The following table shows the sieve fractions:

<b>Sieve fractions (mm)</b>
<b>0.41-0.50</b>
<b>0.50-0.61</b>
<b>0.60-0.71</b>
<b>0.71-0.80</b>
<b>0.80-0.90</b>
<b>0.90-1.12</b>
<b>1.12-1.40</b>
<b>1.40-1.70</b>
<b>1.70-2.00</b>

The average diameter of each fraction is determined by taking the square root of upper and lower boundary. It is assumed that particle has a spherical shape with a shape factor 1. The mean diameter is:

$$d_p = \sqrt{d_{\text{Below}} * d_{\text{Top}}} \quad (52)$$

For each sieve fraction, experiments on four different temperatures were carried out with a water flow rate varying from 0 to 400 l/h in more or less 30 steps. So, for 9 sieve classes, there are 1080 points of measurements and for each of them bed height and pressure drop are determined. The measurements are used to calculate porosity at known particle diameter and linear velocity. For each sieve fraction, the linear velocity is plotted against porosity (Figure 39 Porosity as a function of linear velocity and temperature for sieve fraction 0.8-0.9 mm).

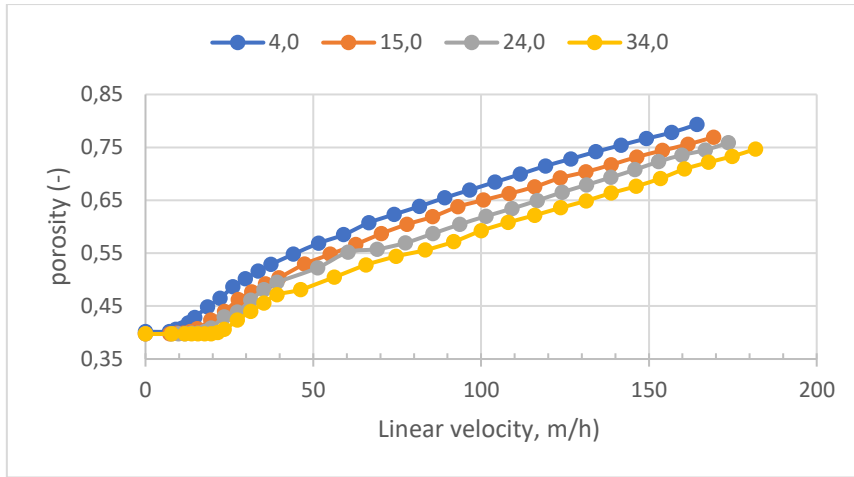


Figure 39 Porosity as a function of linear velocity and temperature for sieve fraction 0.8-0.9 mm.

Trend line for every line is established (Figure 40). So, the porosity can be determined at any random velocities at the four temperatures. In order to determine the porosity in other temperature, the porosity is plotted against kinematic viscosity as this parameter has a direct influence on porosity. A lower viscosity indicates lower porosity (Figure 41).

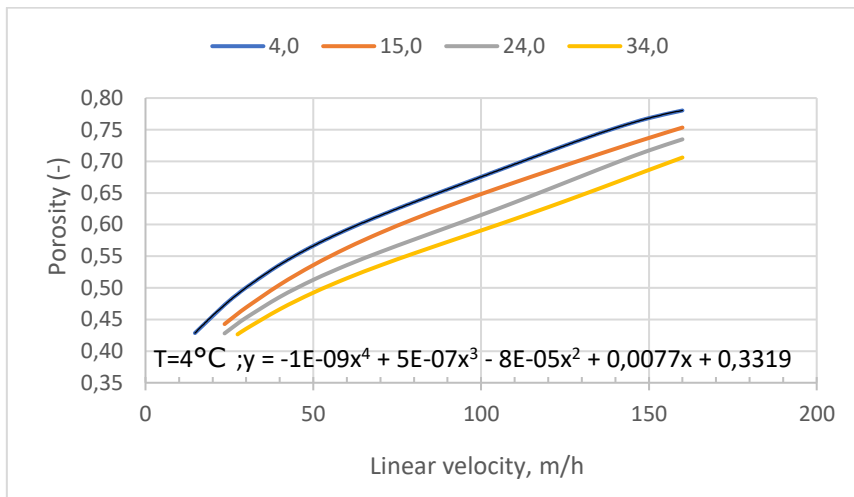


Figure 40 Fourth-order polynomials of the measured points on the sieve fraction 0.8-0.9 mm

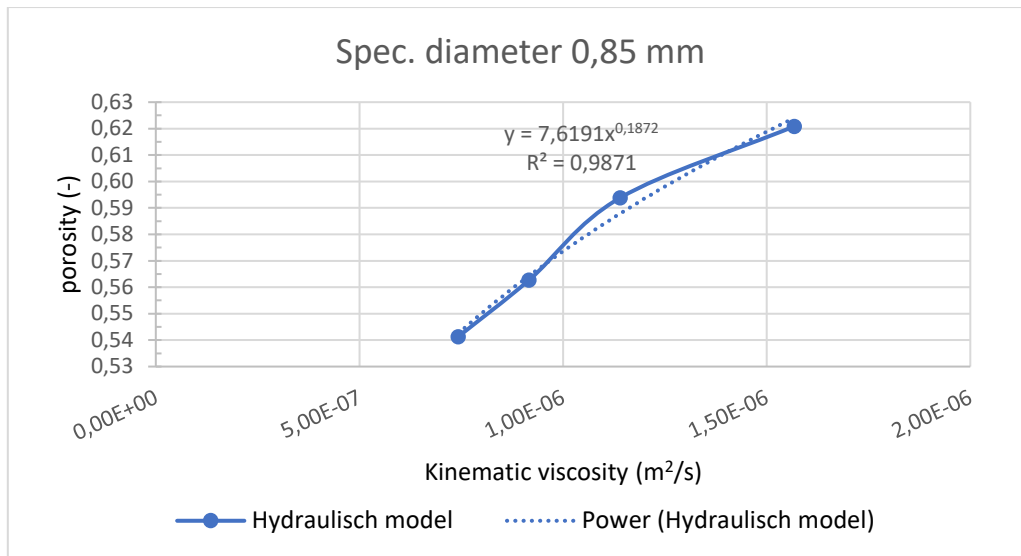


Figure 41 Kinematic viscosity against the porosity, with the trend line function for sieve fraction 0.8-0.9 mm

Therefore, for each sieve fraction the porosity can be calculated by using five equations, the four fourth degree equations at different temperature and the power function of kinematic viscosity plotted against porosity. This results a relationship between porosity and particle diameter shown in Figure 42.

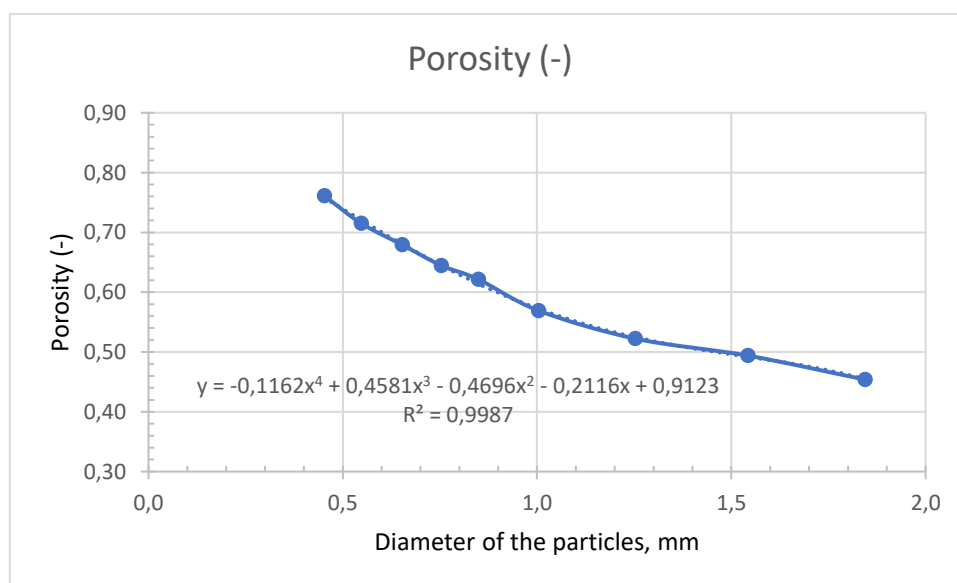


Figure 42 Particle diameter is against the porosity with a fourth-degree polynomial at  $T = 4.6^{\circ}\text{C}$  and  $v = 73 \text{ m/h}$

With this fourth-order polynomial can be determined, the porosity at a given temperature and linear velocity. The hydraulic model is coupled to the layer model, which is at any temperature and linear velocity, the porosity can be determine.

## Appendix 4 Relationship between the Merck powder and $SSA_w$ (Seepma, 2018)

Amount of Merck powder [g/L]	Amount of $SSA_{H_2O}$ [ $m^2 m^{-3} H_2O$ ]
<b>~0 (0.01)</b>	~0 (0 -1)
<b>1</b>	40 - 80
<b>5</b>	200 - 400
<b>10</b>	400 - 800
<b>30</b>	1250 - 2500
<b>60</b>	2500 - 5000

## Appendix 5 Coding for chemical model

### Raw water quality input

SOLUTION	1		
-units		mg/kgs	
-redox		0 (-2)/0 (0)	
-density		1	
-water		1	
-pe		4.00	
temp		19.5727	
O (0)		8.4500	
pH		7.6000	
[C-4]		0.0000	as CH4
[S-2]		0	as H2S
Ca		70.9717	
Mg		6.8650	
Na		23.1700	
K		2.6150	
Fe		0.0410	
Mn		0.0245	
[N-3]		0.00	as NH4
# N (-3)		0.00	as NH4
Al		0.00	ug/kgs
Ba		0.00	ug/kgs
Cd		0.00	ug/kgs
Cu		0.00	ug/kgs
Pb		0.00	ug/kgs
Li		0.00	ug/kgs
Sr		0.00	ug/kgs
Zn		0.00	ug/kgs
Alkalinity		204.2107	as HCO3
Cl		57.2745	
N (+5)		3.2788	as NO3
S (+6)		5.4745	as SO4
F		0.0000	
Br		0.0000	
P		0.0245	as PO4
[N+3]		0.0014	as NO2
# N (0)		1	N2(g) -0,1079
# Ntg		1	Ntg(g) -0,1079
Si		10.4045	as SiO2
B		0.00	ug/kgs as B

## Calcite kinetics coding

```
CalciteCR
-start
10      d = PARM (1)/1000
20      p = PARM (2)
30      kC = PARM (3)
40      kH = PARM (4)
50      kL= PARM (5)
60      CP = PARM (6)
70      A1 = PARM (7)
100     H = PARM (10) *100
101     kS = PARM (11)
101     SP = PARM (12)
110     SSA = 6*(1-p)/d/p
130     SRc = SR("Calcite")
140     rateC = kC * SSA * (SRc - 1)
150     rateH = kH * SSA * (SRc - 1) + A1
160     rateL = kL * SSA * (SRc - 1)
161     rateS = kS * SSA * (SRc - 1)
170     IF H < 10 THEN rate = rateC
180     IF H > 10 THEN rate = rateH
190     IF SRc < CP THEN rate = rateL
200     IF SRc < SP THEN rate = rateS
210     mmoles = rate * TIME
220     moles = mmoles/1000
230     SAVE moles
-end
```

```
TITLE Simulation for calculating pe (redox equilibrium)
```

```
USE solution 1
```

```
EQUILIBRIUM_PHASE
```

```
SAVE SOLUTION 1
```

```
END # Simulation 2
```

```
TITLE Simulation for calculating Calcium Carbonate Precipitation Potential
```

```
USE solution 1
```

```
EQUILIBRIUM_PHASE
```

```
Calcite
```

```
END # Simulation 3
```

```
TITLE Simulation for temperature correction
```

```
Use solution 1
```

```
REACTION_TEMPERATURE 1
```

```
20.000
```

Save Solution 2  
END # Simulation 4

TITLE Simulation for calculating chemical dosing  
USE solution 2  
REACTION  
NaOH  
1.30000 millimoles  
SAVE SOLUTION 3  
END # Simulation 5

TITLE Simulation for calculating Calcium Carbonate Precipitation Potential  
USE solution 4  
EQUILIBRIUM\_PHASE  
Calcite  
END # Simulation 26

TITLE Simulation for mixing raw and softened water  
MIX  
1 0.15  
4 0.85  
SAVE solution 5  
END # Simulation 27

TITLE Simulation for calculating Calcium Carbonate Precipitation Potential  
USE solution 5  
EQUILIBRIUM\_PHASE  
Calcite  
END # Simulation 28

Appendix 6 dCa/dt vs (SR-1) plot of the selected experiment

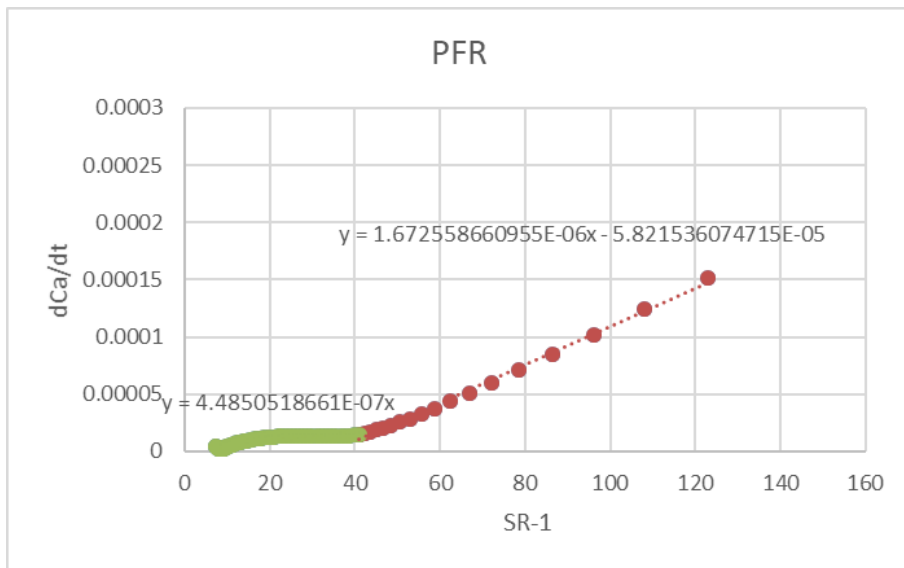


Figure 43 Experiment no 1.1, temperature 8.5°C

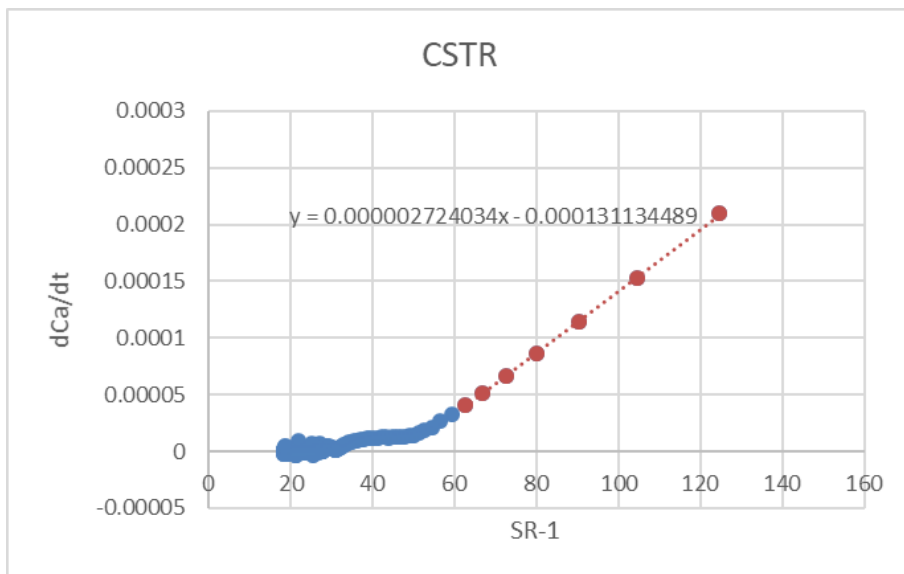


Figure 44 Experiment no 50, temperature 5.6°C

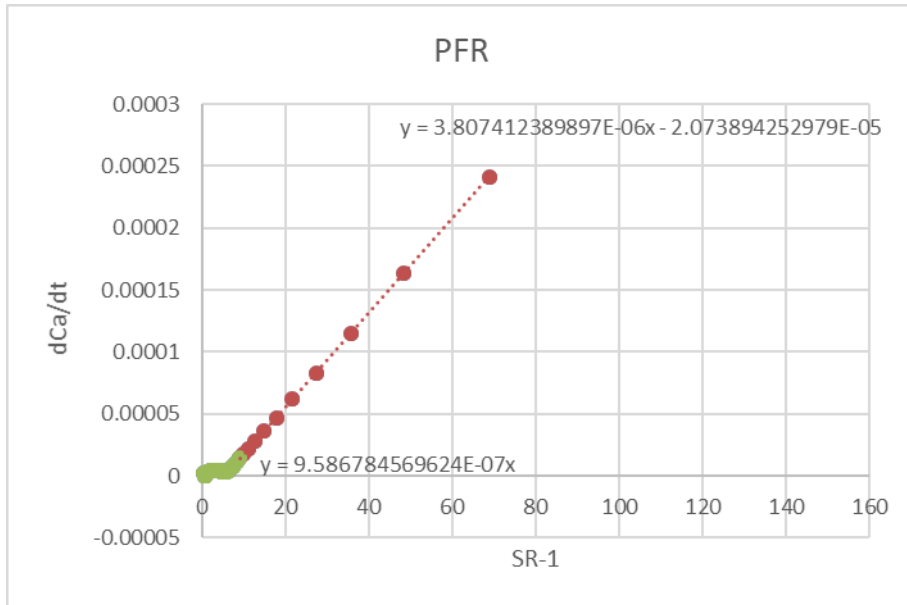


Figure 45 Experiment no 1.5, temperature 22°C

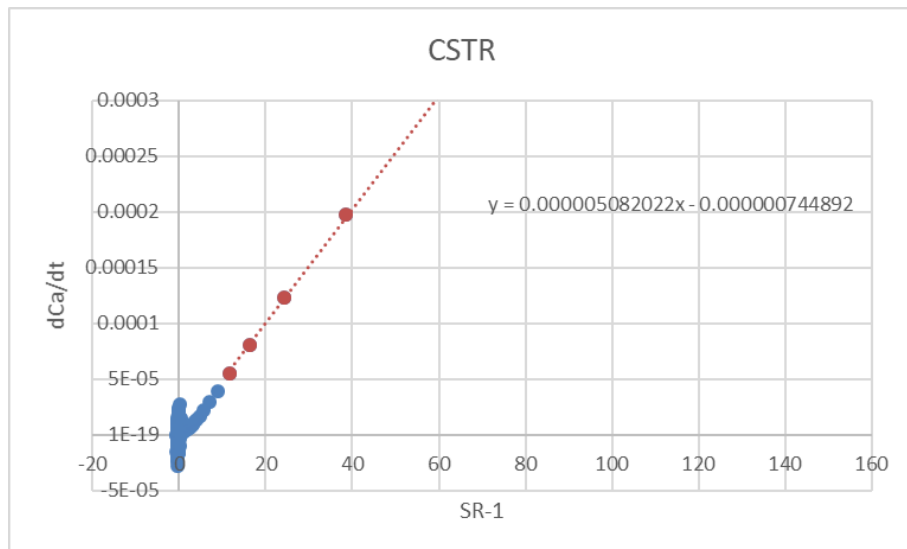


Figure 46 Experiment no 29, temperature 20°C

## Appendix 7 Experimental details (Schooten, 1985)

<b>Experiment dates</b>	<b>Ca (in), mmol/L</b>	<b>Temperature °C</b>	<b>NaOH, mmol/L</b>	<b>Flow, m3/h</b>
09/09/1985	2	13.5	0.88	20
10/09/1985	1.99	13.8	0.76	20
12/09/1985	1.99	14.8	0.56	20
17/09/1985	1.87	14.3	1.09	35
20/09/1985	1.88	15.3	1.43	15
24/09/1985	1.88	15.8	0.7	25
24/09/1985 (v2)	1.91	15.8	1.19	25
25/09/1985	1.91	15.8	1.55	25

## Appendix 8 Calibration graphs (Schooten, 1985)

The experiment date and caustic dose is entitled in the chart title.

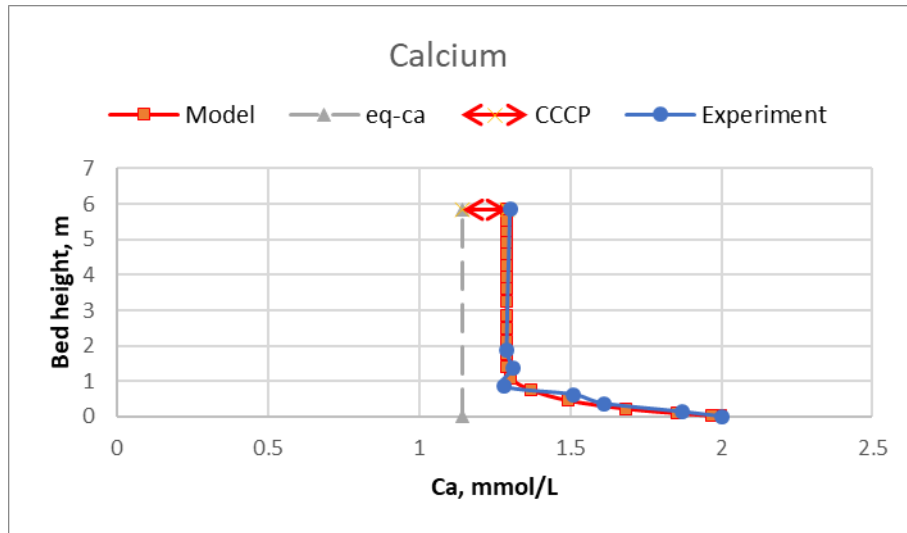


Figure 47 Experimental and modeled calcium content over bed height. Operational conditions:  $C_{in} = 1.99$  mmol/L, temperature = 13.5°C, Flow= 20 m<sup>3</sup>/h, NaOH dosing =0.88 mmol/L

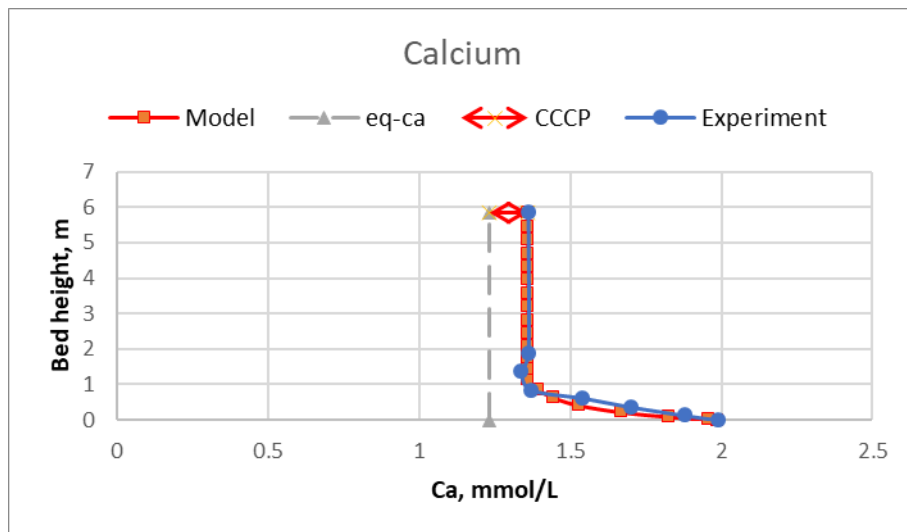


Figure 48 Experimental and modeled calcium content over bed height. Operational conditions:  $C_{in} = 1.99$  mmol/L, temperature = 13.8°C, Flow= 20 m<sup>3</sup>/h, NaOH dosing =0.76 mmol/L

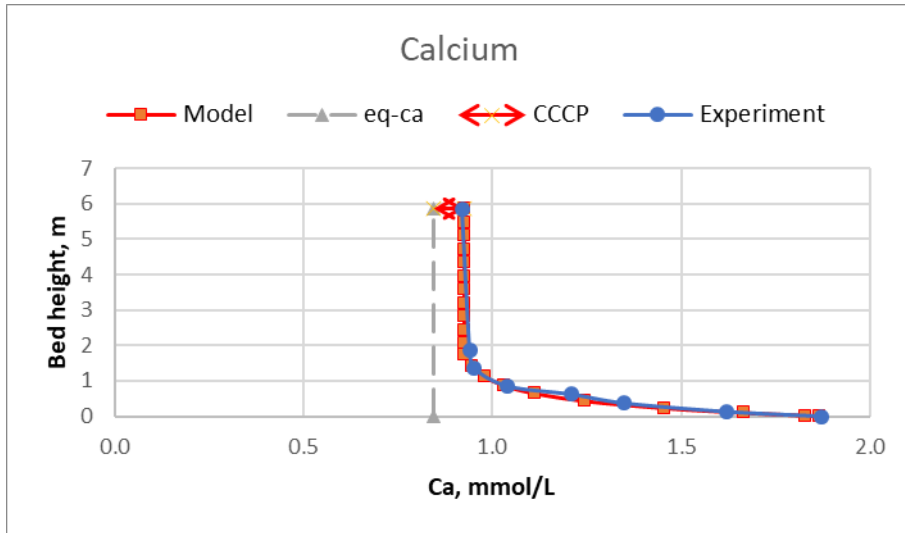


Figure 49 Experimental and modeled calcium content over bed height. Operational conditions:  $C_{ain} = 1.87 \text{ mmol/L}$ , temperature =  $14.3^\circ\text{C}$ , Flow =  $35 \text{ m}^3/\text{h}$ , NaOH dosing =  $1.09 \text{ mmol/L}$

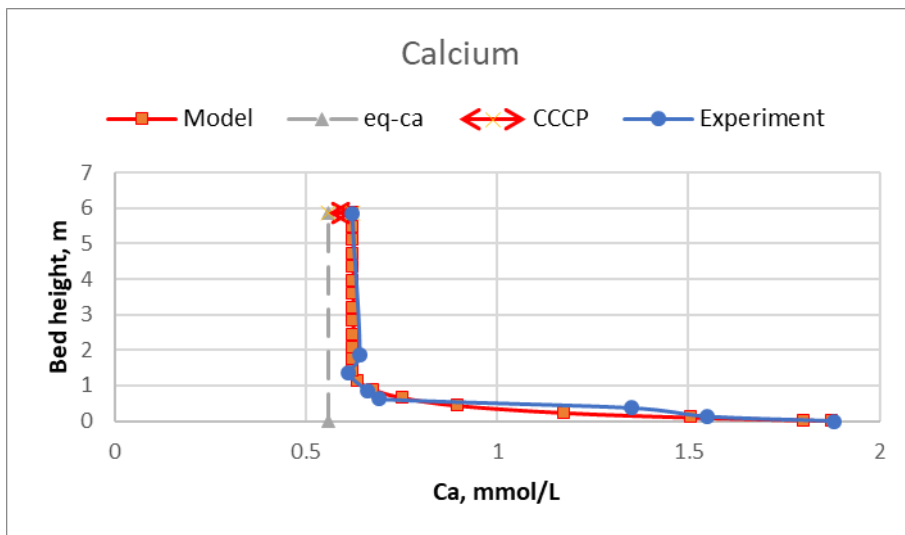


Figure 50 Experimental and modeled calcium content over bed height. Operational conditions:  $C_{ain} = 1.88 \text{ mmol/L}$ , temperature =  $15.3^\circ\text{C}$ , Flow =  $15 \text{ m}^3/\text{h}$ , NaOH dosing =  $1.43 \text{ mmol/L}$

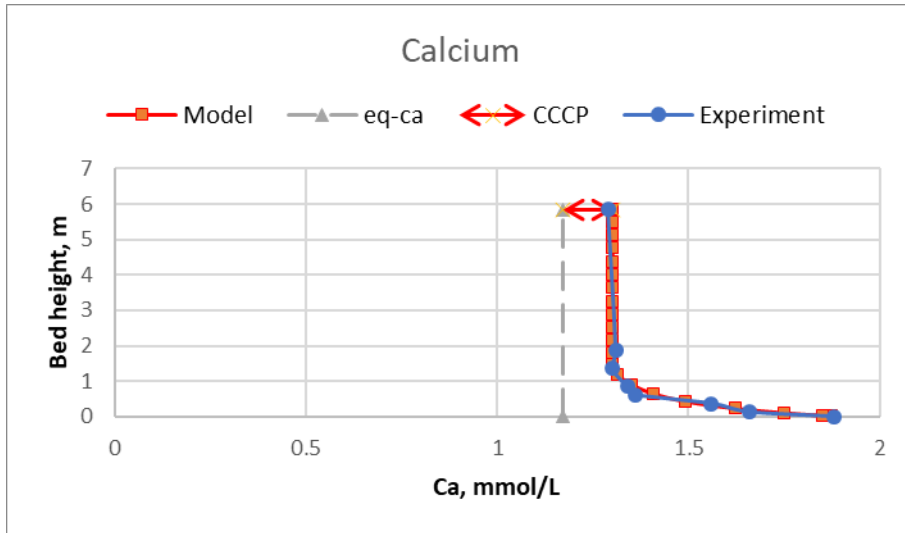


Figure 51 Experimental and modeled calcium content over bed height. Operational conditions:  $C_{in} = 1.88 \text{ mmol/L}$ , temperature =  $15.8^\circ\text{C}$ , Flow =  $25 \text{ m}^3/\text{h}$ , NaOH dosing =  $0.7 \text{ mmol/L}$

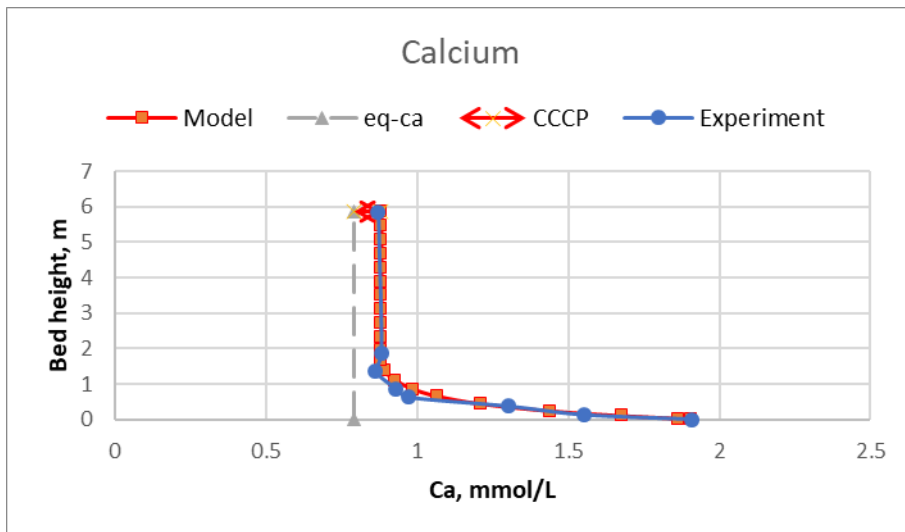


Figure 52 Experimental and modeled calcium content over bed height. Operational conditions:  $C_{in} = 1.91 \text{ mmol/L}$ , temperature =  $15.8^\circ\text{C}$ , Flow =  $25 \text{ m}^3/\text{h}$ , NaOH dosing =  $1.19 \text{ mmol/L}$

Appendix 9 Experimental Data (Schetters, 2013)

Datum	20-20-2013	Temperature (°C)		2.2
Time	2.2			
L (m)	pH	Cond. (µS/cm)	P	
0.5	9.25	397	29	
1.0	9.26	399	78	
1.5	9.32	360	130	
2.0	9.26	355	197	
2.5	9.18	343	265	
3.0	9.22	341	337	
3.5	9.25	326	410	
4.0	9.28	328	482	
4.5	9.5	336	553	
5.0	9.75	352	625	
5.5	11.5	386	703	
6.0			744	

Datum	21/02/2013	Temperature (°C)		1.5
Time	12			
L (m)	pH	Cond. (µS/cm)	P	
0.5	9.25	466	29	
1.0	9.26	466	79	
1.5	9.17	463	132	
2.0	9.13	464	197	
2.5	9.17	463	264	
3.0	9.15	463	337	
3.5	9.17	463	408	
4.0	9.24	466	478	
4.5	9.35	470	551	
5.0	9.6	502	621	
5.5	10	550	679	
6.0			746	

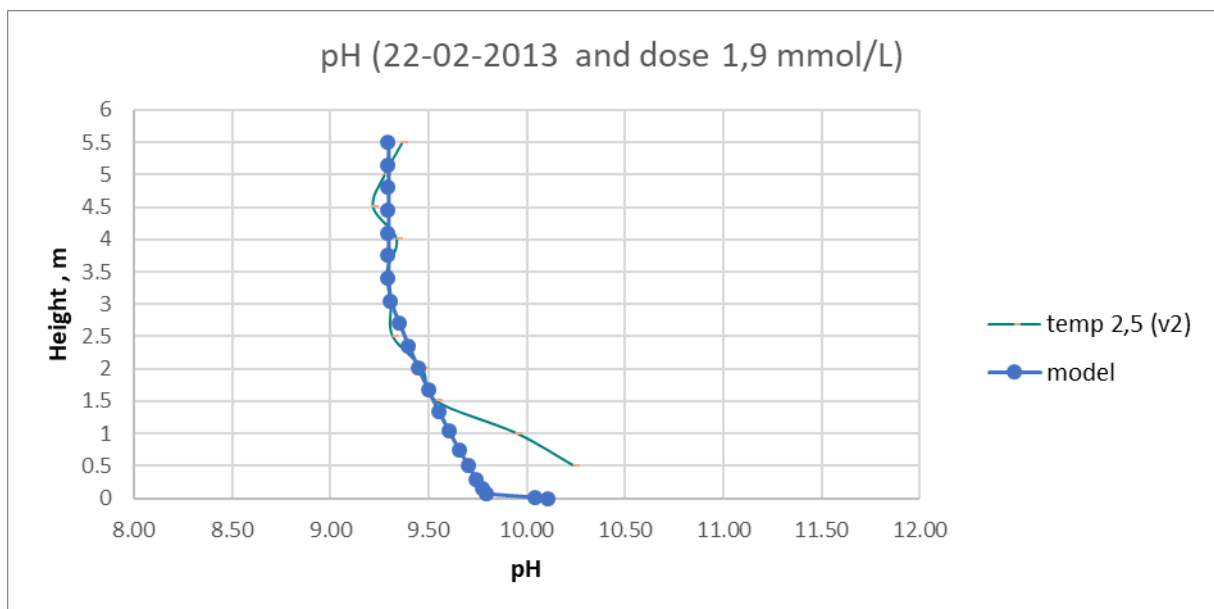
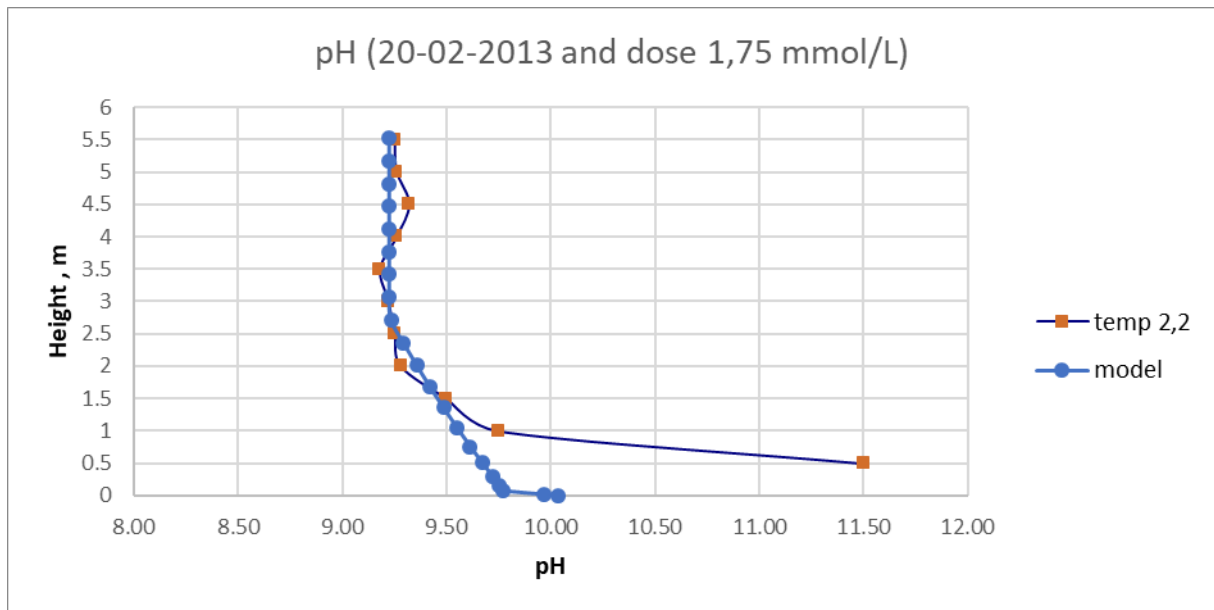
Datum Time	22/Feb 10.15	Temperature (°C)	2.5
L (m)	pH	Cond. (µS/cm)	P
0.5	9.02	478	29
1.0	9	474	78
1.5	9.04	470	129
2.0	9.06	471	193
2.5	9.14	468	259
3.0	9.11	468	331
3.5	9.11	468	402
4.0	9.23	469	471
4.5	9.35	475	544
5.0	9.71	507	615
5.5	10.5	527	691
6.0			745

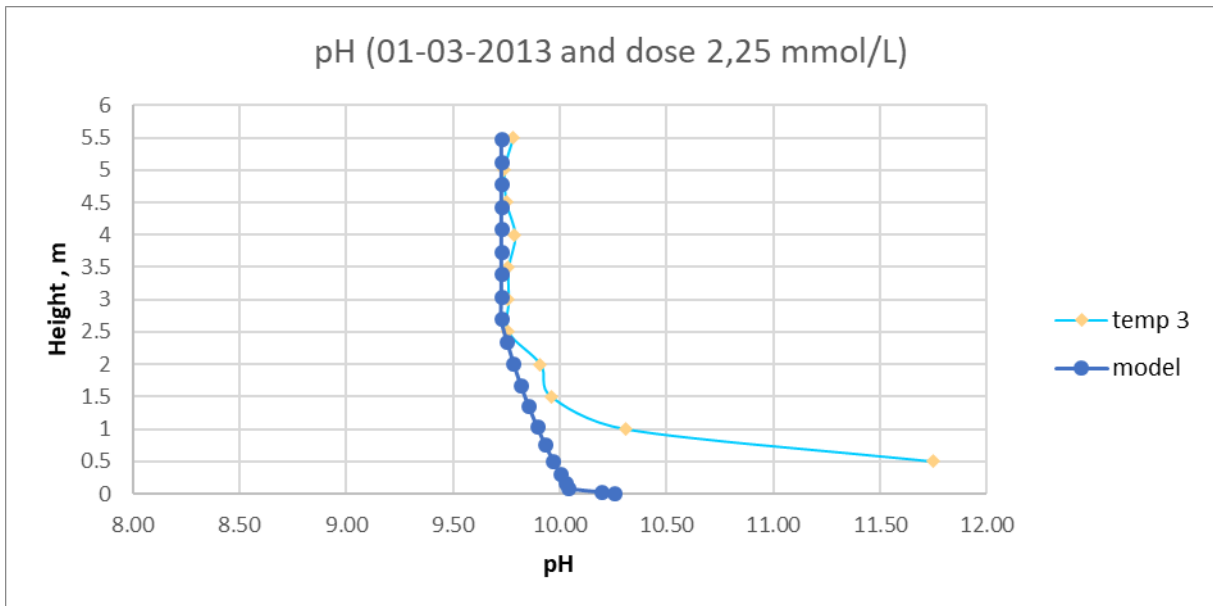
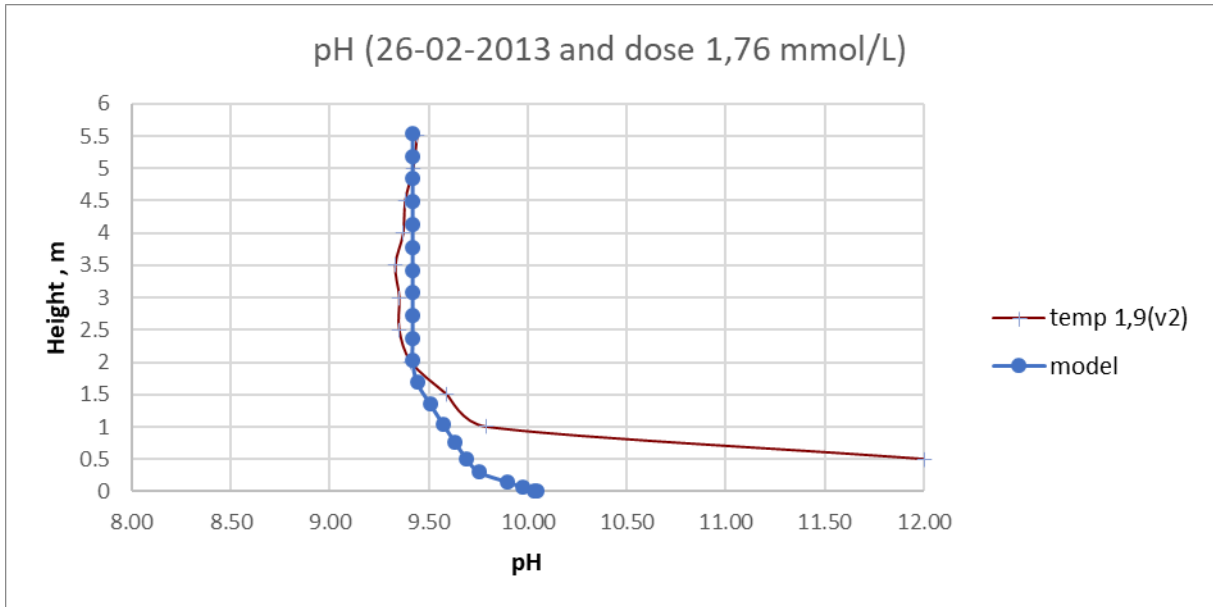
Datum Time	25/Feb 15.45	Temperature (°C)	1.9
L (m)	pH	Cond. (µS/cm)	P
0.5	9.38	477	29
1.0	9.36	478	79
1.5	9.33	467	133
2.0	9.31	475	197
2.5	9.27	475	263
3.0	9.27	474	334
3.5	9.27	473	404
4.0	9.34	4721	473
4.5	9.48	483	545
5.0	9.81	507	617
5.5	10	580	693
6.0			744

Datum Time	26/Feb 11	Temperature (°C)	1.9
L (m)	pH	Cond. (µS/cm)	P
0.5	9.44	477	29
1.0	9.42	484	78
1.5	9.38	477	130
2.0	9.37	473	193
2.5	9.33	475	259
3.0	9.35	472	330
3.5	9.35	472	401
4.0	9.41	472	470
4.5	9.59	475	541
5.0	9.79	493	614
5.5	12	1064	689
6.0			741

Datum Time	01/Mar	Temperature (°C)	2.5
L (m)	pH	Cond. (µS/cm)	P
0.5	9.37	407	29
1.0	9.28	420	78
1.5	9.22	425	140
2.0	9.34	408	208
2.5	9.29	423	276
3.0	9.31	419	350
3.5	9.32	408	422
4.0	9.47	404	493
4.5	9.54	406	568
5.0	9.95	421	643
5.5	10.24	409	719
6.0			777

Appendix 10 Calibration graphs (Schetters, 2013)





Appendix 11 Dosing of NaOH in January and July, 2018

